Title
Role of Retinal Pigment Epithelium in Myopia Development and Control

Author
Zhang, Yan

Publication Date
2013

Peer reviewed|Thesis/dissertation

Role of Retinal Pigment Epithelium in Myopia Development and Control

By

Yan Zhang

A dissertation submitted in partial satisfaction of the

requirement for the degree of

Doctor of Philosophy

in

Vision Science

in the

Graduate Division

of the

University of California, Berkeley

Committee in charge:

Professor Christine F. Wildsoet, Chair
Professor Marla Feller
Professor Kunxin Luo

Spring 2013

Role of Retinal Pigment Epithelium in Myopia Development and Control

By

Yan Zhang

University of California, Berkeley

Abstract

Role of Retinal Pigment Epithelium in Myopia Development and Control

by

Yan Zhang

Doctor of Philosophy in Vision Science

University of California, Berkeley

Professor Christine F. Wildsoet, Chair

Myopia (near-sightedness) is one of the most common ocular disorders in humans. Due to the dramatic increases in prevalence of myopia worldwide, especially in children and young adults, myopia has also become a significant public health problem, both socially and economically. While the prevalence and severity of myopia continue to increase, effective therapeutic interventions for myopia remain limited. Currently, management of myopia is largely limited to traditional optical corrections - spectacles, contact lenses, and refractive surgery - which correct distance vision but have no effect on myopia progression. While slowed myopia progression has been reported in clinical studies using the contact lens-based, corneal reshaping therapy and atropine, a pharmaceutical agent, these approaches come with limitations and in the latter case, significant ocular side-effects. Uncontrolled progression may lead to high "degenerative" myopia, for which posterior scleral reinforcement surgery remains the only treatment option and a last resort directed at preserving vision. Thus there is a clear need for new myopia control treatments. Understanding more about the molecular and cellular mechanisms underlying myopic eye growth has the potential to uncover novel treatment options.

This dissertation presents results from three investigations into the role of the retinal pigment epithelium (RPE) in eye growth regulation, focusing on molecular and cellular mechanisms, and using both *in vivo* animal models and *in vitro* cell culture models. In the first *in vivo* study (Chapter 2), we investigated expression of candidate genes in chick RPE of imposing short-term optical defocus. Specifically, gene expression levels of the three bone morphogenetic proteins (BMP-2, 4 & 7) were examined after 2 and 48 h of treatment, with negative and positive lenses used to impose defocus of opposite sign. These growth factors were observed to be differentially and bidirectionally expressed in RPE, expression generally increasing with imposed myopia, which is associated with ocular growth inhibition. Because eyes had little chance to change their dimensions with such short-term lens treatments, these genes are assumed to play important roles in the onset and early phase of defocus-induced ocular growth changes. For this reason, these genes represent potential targets for molecular-based myopia treatments. In the second study (Chapter 3), high-through gene expression profiling was employed to examine changes in gene

expression in chick RPE with long-term imposed hyperopic defocus, which resulted in eyes being longer than normal and highly myopic. This DNA microarray screening revealed changes in the expression of many genes, including BMPs, noggin (NOG), dopamine receptor D4 (DRD4), retinoic acid receptor, beta (RARB), and retinal pigment epithelium-derived rhodopsin homolog (RRH). Some of these genes showed increased expression while others showed decreased expression. It is plausible that some may be linked the ocular pathological complications seen in myopia, while others may be linked to ocular growth regulation, the imposed visual conditions resulting in sustained, increased ocular growth. The third and final study (Chapter 4), addressed the possibility of an RPE site for the anti-myopia action of apomorphine (APO), a dopamine receptor agonist, observed in animal studies. We further investigated the possibility that TGF-β secretion from RPE mediates this inhibitory growth effect. APO applied to cultured human fetal RPE cells was found to alter the secretion of both TGFβ1 and TGFβ2, which was biased towards the basal (choroidal) side. These growth factors also exhibited constitutive polarized secretion, albeit biased in the opposite direction to APO-induced paracrine secretion. The results for APO are consistent with its observed inhibitory (anti-myopia) effects *in vivo* and offer the RPE as a possible site of action.

In summary, the research reported in this dissertation provides evidence that RPE plays an important role in postnatal eye growth regulation, (including myopic growth), as a conduit for relaying growth modulatory retinal signals to choroid/sclera. Genes and molecules identified in these studies offer potential directions for novel anti-myopia treatments, with the RPE being a potential target for the same.

TABLE OF CONTENTS

LIST OF FIGURES

LIST OF TABLES

LIST OF ABBREVIATIONS

aa	amino acid
ACh	acetylcholine
ADRA2C	adrenoceptor alpha 2C
AHD2	aldehyde dehydrogenase-2
AL	axial length
ANOVA	analysis of variance
APO	apomorphine
AQP4	aquaporin 4
bFGF	basic fibroblast growth factor
BMP	bone morphogenetic protein
BMPR	bone morphogenetic protein receptor
bp	base pairs
BSA	bovine serum albumin
CACNA1G	calcium channel, voltage-dependent, T type, alpha 1G subunit
cDNA	complementary deoxyribonucleic acid
CGAC	conventional glucagon-expressing amacrine cell
Ch	choline
ChAT	choline acetyltransferase
CHO	choroid
ChT	choroid thinkness
CLCN	chloride channel, voltage-sensitive
CNS	central nervous system
CRABP	retinoic acid binding protein
cRNA	complementary RNA
ct	threshold cycle
CT	choroidal thickness
CTGF	connective tissue growth factor
D	diopters
DA	dopamine
DAPI	4',6-diamidino-2-phenylindole
DAVID	database for annotation, visualization and integrated discovery
DOPAC	3,4-dihydroxyphenylacetic acid
DRD	dopamine receptor D
DMEM	Dulbecco's modified Eagle medium
DNA	deoxyribonucleic acid
dNTP	deoxyribonucleotide triphosphate
DTT	dithiothreitol
E	efficiency of primer amplification
EB	ethidium bromide
ECM	extracellular matrix
ECMA	ethylcholine mustard aziridinium ion
EGR1	early growth response 1
EDNRB	endothelin receptor type B
FGFR2	fibroblast growth factor receptor 2
FIGF	c-fos induced growth factor (vascular endothelial growth factor D)
FN1	fibronectin 1
GAC	glucagon-expressing amacrine cell
GAG	glycosaminoglycan

GPCRs	G protein-coupled receptors
GACs	glucagon-expressing amacrine cells
GAPDH	glyceraldehyde-3-phosphate dehydrogenase
GCL	ganglion cell layer
h	hour
hf	human fetal
HH	Hamburger and Hamilton
HPRT1	hypoxanthine phosphoribosyltransferase 1
HRP	horseradish peroxidase
IGF-1	insulin-like growth factor-1
IL	interleukin
INHBA	inhibin, beta A
INL	inner nuclear layer
IPL	inner plexiform layer
IOP	intraocular pressure
IVT	*in vitro* transcription
KDR	kinase insert domain receptor (a type III receptor tyrosine kinase)
LGEN	large glucagon-expressing neuron
mAChRs	muscarinic acetylcholine receptors
mm	millimetre
MMP	matrix metalloproteinase
MNE	mean normalized expression
mRNA	messenger ribonucleic acid
NOG	noggin
NTS	neurotensin
NUSE	normalized unscaled standard error
OCT	optimal cutting temperature
OD	optical density
ONL	outer nuclear layer
OPL	outer plexiform layer
ortho-k	orthokeratology
PBS	phosphate buffered saline
PCR	polymerase chain reaction
PDGFA	platelet-derived growth factor alpha polypeptide
PDGFRA	platelet-derived growth factor receptor, alpha polypeptide
PDGF	platelet-derived growth factor
PM	perfect match
PNS	peripheral nervous system
QC	quality control
qPCR	quantitative polymerase chain reaction
RA	retinoic acid
RALDH2	retinaldehyde dehydrogenase 2
RAR	retinoic acid receptor
RARB	retinoic acid receptor, beta
RMA	robust multiarray averaging
RE	refractive error
RIN	RNA integrity number
RLE	relative log expression
RNA	ribonucleic acid
RRH	retinal pigment epithelium-derived rhodopsin homolog

RXR	Retinoid X receptor
RPE	retinal pigment epithelium
SCL-C	sclera cartilaginous layer
SCL-F	sclera fibrous layer
SEM	standard error of mean
SFM	serum-free medium
SP	signal peptide
SPARC	osteonectin
SPP1	osteopontin
SNP	single-nucleotide polymorphism
SST	somatostatin
TBP	TATA box binding protein
TGF-β	transforming growth factor, beta
TGFBI	transforming growth factor-beta-induced protein ig-h3
TGFBR	transforming growth factor receptor
TH	tyrosine hydroxylase
THBS1	thrombospondin 1
TIMP	tissue inhibitor of matrix metalloprotease
TNC	tenascin
t-PA	tissue plasminogen activator
VCD	vitreous chamber depth
VIP	vasoactive intestinal polypeptide
ZENK	zinc finger protein

ACKNOWLEDGEMENTS

I would like to thank my mentor, Professor Wildsoet for her guidance that leads me into this interesting and exciting myopia research, and for her continuous and strong support for my dissertation research and career development over the past six years. I am grateful for my Ph.D. dissertation committee members, Professors Christine F. Wildsoet, Professor Marla Feller, and Professor Kunxin Luo for their advice, guidance and long-lasting support. I would like to thank my qualifying committee members, Professor Xiaohua Gong and Lu Chen for their guidance and inspiring suggestions for research projects. I would also like to thank all of my research collaborators, Dr. Sheldon S. Miller (NIH), Arvydas A. Maminishkis (NIH), Rong Li (NIH), Don Yuen (UC Berkeley), and Tan Truong (UC Berkeley), for providing research insights, advice, assistance, research materials and sharing experimental instruments. I would like to thank all members of the Wildsoet Lab for working together as a team and creating an invaluable training experience throughout my graduate studies. I would like to thank for the Vision Science Program at School of Optometry, which has provided me with unique learning experiences through courses, seminars, and teaching experience. The mentoring and teaching experience with Optometry students and undergraduate students filled my life with surprises and left me with lovely memories. Finally, I would like to thank my whole family for their unconditional love and support.

Chapter 1

Introduction
Myopia Development and Control

Abstract

Myopia, or near-sightedness, is one of the most common ocular disorders in human. Due to the increased prevalence and severity of myopia worldwide, especially in children and young adults, myopia has become a significant public health problem, both socially and economically. The ocular change underlying myopia is accelerated eye growth, which results in a mismatch between the axial length of eye and its refractive power, and in turn, blurred retinal images without optical correction. In high myopia, generally categorized as -6.0 D or higher, the associated stretching of internal ocular structures with the increase in axial length may lead to blinding complications such as retinal degeneration, retinal detachment, myopic maculopathy, choroidal neovascularization and glaucoma. Both genetic and environmental factors are thought to play roles in the development of human myopia. Studies using animal models have provided convincing evidence for the role of visual environmental factors, with manipulations of the visual input, either with optical defocusing lenses or diffusers, producing consistent abnormalities in the emmetropization process. Since localized manipulation of retinal images induce localized eye elongation, and optic nerve section does not prevent the development of myopia, it has been concluded that postnatal eye growth is controlled locally within the eye itself. The RPE is a monolayer of cells positioned between the neuronal retina and the choroid. It is a component of the blood-retina barrier, with already established roles in maintaining normal retinal function. However, based on its location, it is placed to also play a critical role in the regulation of eye growth. Identification of genes showing differential regulation in RPE during altered eye growth would provide indirect evidence for such a role and could also provide new insights into the molecular and cellular mechanisms underlying myopia development. Furthermore, evidence linking specific genes with growth modulation would open up the possibility of developing novel anti-myopia treatments targeting such genes in the RPE, for which there is precedence in the form of RPE-targeted treatments of some retinal diseases.

1.1 Myopia and Eye Growth Regulation

1.1.1 Prevalence and significance

Myopia, or near-sightedness, describes the condition in which images of distant objects are focused in front of the retina, resulting in blurred vision. Myopia reflects the mismatches between the refracting power of the eye, to which the cornea and crystalline lens contribute, and its optical axial length, which composes anterior chamber depth, lens thickness, and vitreal chamber depth. Most myopia is axial rather than refractive in nature, the product of excessive elongation of the vitreous chamber (Figure 1-1).[1, 2] Babies are typically born with refractive errors, which are corrected during early development through a process of coordinated ocular growth known as emmetropization.[3, 4] However, myopia more commonly occurs in childhood as a failure of emmetropization, when the eye continues to elongate after emmetropia is achieved. Excessive ocular elongation results in high myopia (classically defined as spherical equivalent refractive errors equal to or greater than - 6.0 D), which carries a high risk of sight-threatening complications such as retinal degeneration, retinal detachment, choroidal neovascularization, myopic maculopathy, cataract, and glaucoma.[5-7]

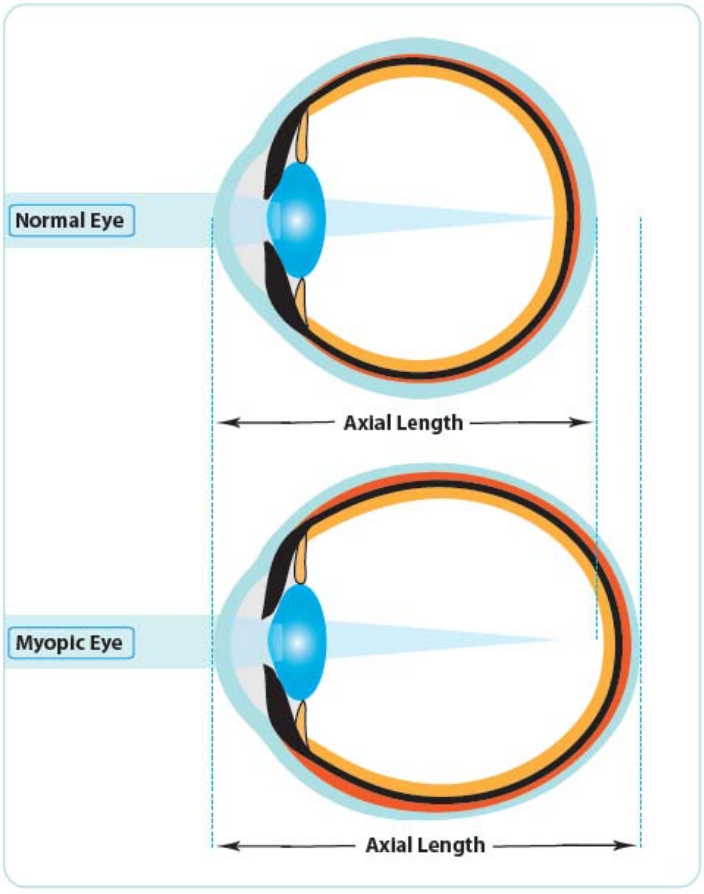

Figure 1-1. Schematic diagram illustrating the principal anatomical difference between a normal emmetropic human eye and a myopic eye, which typical has a longer axial length, largely attributable to a longer vitreous chamber.

Myopia is one of the most common refractive errors, which are one of the world's leading causes of functional blindness due to lack of access to optical corrections; they are also significant contributors to the global burden of eye disease.[8] In a recent published study, the overall prevalence of myopia in the US was given as 41.6% for persons aged 12 to 54 years.[9] However, in many Asia countries and populations, myopia has now reached epidemic levels.[10, 11] Due to the increased prevalence and severity of myopia worldwide, especially in children and young adults, myopia has become a significant public health problem, both socially and economically.[8, 9, 12-15] The increasing prevalence and severity of myopia has stimulated increased research into the underlying mechanisms, an essential step in developing effective therapies.

1.1.2 Aetiology of myopia

It is now generally accepted that both genetic and environmental factors play roles in the development of myopia.[7, 16-18] Genetic studies of myopia using linkage and genome-wide association approaches have identified many loci (MYP1–MYP17) and genes although no unique gene for the most common form of juvenile myopia has emerged.[19-21]

Human epidemiological studies and studies using animal models have provided strong evidence for the environmental contributions to myopia development. Near work,[22] educational levels,[23] life-styles,[24] and outdoor activities[11, 25] are among the factors identified to influence refractive errors in human clinical studies. Animal studies using chickens, guinea pigs, tree shrews, and monkeys have provided the most convincing evidence for visual environmental influences on postnatal eye growth regulation and thus myopia development.[16, 26-30] Currently there are two different experimental paradigms for inducing myopia in animal studies, utilizing form depriving diffusers and negative defocusing lenses, respectively. Both paradigms have been shown to elicit robust responses in most animal models. In all cases, the induced myopia is characterized by an increased rate of axial elongation, attributable to expansion of the posterior vitreous chamber of the eye, and reflecting altered growth of the outer choroidal and scleral support layers.

In the case of human myopia, myopia likely reflects interactions between genetic and environmental factors; how each factor contributes to the development and progress of myopia is the subject of much on-going debate.[16, 17] It is also possible that a large number of genes, each contributing a small effect, may prove important in determining the development of myopia, which is aetiologically heterogeneous in human populations.[31-33]

1.1.3 Local eye growth regulation

Myopia development is characterized by accelerated eye growth, which can be induced experimentally by visual manipulations such as form-deprivation and optical defocus, as already noted. The preservation of these altered growth patterns in eyes isolated from the brain by optic nerve section points to local ocular growth regulation.[34-36] That localized manipulation of retinal images induces localized ocular changes, confined to the area underlying the affected retina, is interpreted as further evidence that postnatal eye growth

is controlled locally.[37, 38] Such local regulatory mechanisms must necessarily involve the retina, choroid, and sclera (retino-sclera signal cascades, Figure 1-2). Identifying genes showing differential regulation in retina, choroid and sclera during altered eye growth has been one commonly used approach to investigate the ocular growth modulatory pathways.[16, 26, 39-41] In the research described in this dissertation, we have targeted the RPE for similar studies on the basis of its critical location between the retina and choroid.

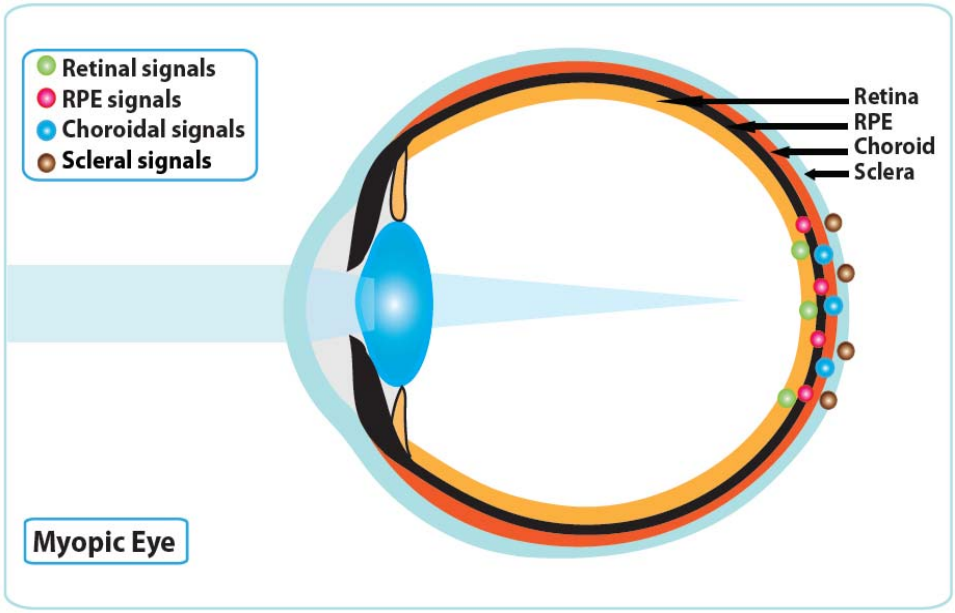

Figure 1-2. Schematic diagram illustrating a possible local retino-scleral signal pathway mediating myopic growth changes; in the model shown, the signal is initiated in the retina and transduced in turn into an RPE signal, choroidal signal and scleral signal.

1.1.4 Retino-scleral signal cascades

1.1.4.1 Retina

The experimental animal models of myopia induced by retinal image degradation (form-deprivation and optical defocus), combined with evidence of local control point to the retina as a source of myopia-generating signals.[16] Apart from input from the central retina, recent research points to an important role for the peripheral retina in regulating postnatal eye growth. For example, studies in monkey have shown that the fovea is not essential for either normal refractive development (emmetropization), or the development of form-deprivation-induced myopia,[42] and in chicks, myopic defocus imposed on peripheral retina using 2-zone lenses results in slowed axial myopia progression.[43, 44] Interestingly, a recent study of retinal function in myopic human eyes using multifocal electroretinography (ERG) documented impaired function in the paracentral and peripheral retina and not in the central retina.[45] At least for inducing myopia experimentally in chicks, high visual acuity does not appear to be essential, as Ritchey *et al.*, have shown recently that excessive ocular elongation can be induced by both form-deprivation and imposed hyperopic defocus using

genetically mutant chickens with poor visual acuity.[46] Nonetheless, changes in the responses to such experimental manipulations have been reported with retinal neurotoxins, providing further evidence for the role of the retina as the source of ocular growth regulating signals.[47, 48]

Since emmetropization and eye growth regulation is visually guided and thus the retina must necessarily play a key role, it has also been extensively investigated using visual manipulations combined with molecular and cellular approaches. The following section focuses on what is known about the role of retinal amacrine cells, neurotransmitters and other molecules, and gene and protein expression in myopia development.

As a part of the central nervous system, the retina primarily consists of three layers of nerve cell bodies (outer nuclear layer [ONL], inner nuclear layer [INL], and ganglion cell layer [GCL]) and two layers of synapses (inner plexiform layer [IPL] and outer plexiform layer [OPL]; Figure 1-3). The outer nuclear layer contains cell bodies of the rods and cones (the photoreceptors), the inner nuclear layer contains cell bodies of the bipolar, horizontal and amacrine cells, and the ganglion cell layer contains cell bodies of ganglion cells and displaced amacrine cells. The outer segments of the photoreceptors lie outermost in the retina, against the retinal pigment epithelium (RPE). The retina contains numerous neurotransmitters, including glutamate, dopamine, acetylcholine, and serotonin, which mediate normal retinal functions and may also have roles in postnatal eye growth regulation (Table 1-1).

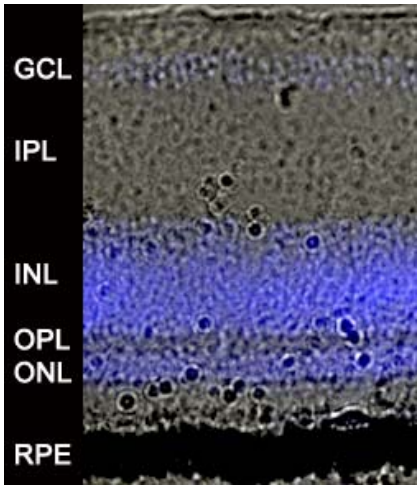

Figure 1-3. Chick retina. Layers of retina are shown and labeled as GCL, IPL, INL, OPL, and ONL. The outer segments of the photoreceptors lie outermost in the retina, against the RPE.

Table 1-1. Retinal cells, neurotransmitters and other molecules and genes implicated in either or both eye growth regulation and myopia

Cells	Neurotransmitters and Molecules	Gene and Proteins Expression
Conventional glucagon-expressing amacrine cells (CGACs)	Acetylcholine	AHD2
	bFGF	BMP2
	Dopamine	CTGF
	Glucagon	EDNRB
Large glucagon-expressing neurons (LGENs): bullwhip and mini-bullwhip	Insulin and IGF-1	IL-18
	Retinoic acid	NOG
	TGF-β	NTS
Photoreceptors	VIP	TGF-β
		VIP
		ZENK

1.1.4.1.1 Amacrine cells, bullwhip cells, and mini-bullwhip cells

Amacrine cells are a highly varied retinal cell class, which includes at least 24 different cell types in the monkey and human retina.[49, 50] They are classified into different types based on morphological characteristics of dendritic tree size (small-, medium-, and large-field) and the stratification of their dendrites in the IPL. They may also be classified according to their neurotransmitter and protein-expression profiles; thus many cell types have been described, including glucagon-expressing amacrine cells (GACs), and amacrine cells showing immunoreactivity to retinoic acid binding protein (CRABP), choline acetyltransferase (CHAT), somatostatin (SST), tyrosine hydroxylase (TH), and vasoactive intestinal polypeptide (VIP), etc.[51] Although the roles of many amacrine cells in retinal physiology remain poorly understood, of relevance to this dissertation research are studies suggesting their involvement in the retinal processing of contrast information and growth-modulating visual stimuli.[47, 52]

Conventional glucagon-expressing amacrine cells (CGACs) have been most extensively studied in the context of eye growth regulation. These cells are reported to show changes in the transcription factor zinc finger protein, ZENK (otherwise known as early growth response 1, EGR1), in response to form-deprivation and lens-induced defocus in young chicks.[51] Specifically, Fischer *et al*., reported that two hours of form-deprivation significantly reduced ZENK protein expression in glucagon-expressing amacrine cells. With lens treatments that imposed optical defocus, the number of ZENK-positive glucagon amacrine cells was found to be increased with positive lenses, after as little as 30 minutes of wear, and decreased after 2 hours of negative lens wear. Bitzer and Schaeffel later undertook a closely related study, and found the number of ZENK-expressing cells to be increased with positive lenses and reduced with negative lenses, after as little as 40 minutes of exposure to the lenses, with the changes lasting at least 2 hours.[53] The same trends in terms of the total number of glucagon amacrine cells expressing ZENK in eyes treated with positive and negative lenses were observed under reduced illuminance and monochromatic light.[53] A related immunohistochemistry study showed the CGACs to be asymmetrically distributed across the retina, with highest density in a central zone between the nasal and temporal edges of the retina.[54] Other follow-up studies have further investigated the role of glucagon in myopia development and related changes ZENK gene expression using pharmacological manipulations. We will discuss these studies in a separate section under the neurotransmitter subheading, glucagon.

Another two types of amacrine cells in the avian retina, labeled bullwhip and mini-bullwhip cells, are also glucagon-expressing neurons (LGENs). Their roles in ocular growth regulation have been the subject of more recent investigations.[54] Bullwhip cells share phenotypic features with both amacrine and ganglion cells, including morphological features and protein expression. In the chick retina, bullwhip cells are found only in ventral and mid-peripheral regions while mini-bullwhip cells are found only in dorsal and far-peripheral regions. Both bullwhip and mini-bullwhip cells has been implicated in the regulation of eye size and shape in chick studies.[55] For example, while eliminating the majority of bullwhip and mini-bullwhip cells by intravitreal injection of colchicine into the vitreous chambers of young chick eyes did not change the axial length, it resulted in

expansion of equatorial diameter, and the latter effect could be prevented by intravitreal injections of glucagon. Visual manipulation with form-deprivation for 24 hours also caused a significant reduction in the percentage of bullwhip cells expressing ZENK (Egr1), while 2 hours of unrestricted vision following 5 days of form-deprivation lead to an increase in the number of ZENK-positive bullwhip cells as compared to control eyes. Together these results suggest that bullwhip and mini-bullwhip cells may play important roles in regulating the equatorial dimensions of eyes, with the peptide, glucagon, playing a key role as a growth inhibitor.

1.1.4.1.2 Neurotransmitter: glucagon

Glucagon, which is a 29-amino-acid long peptide, is one of the neuropeptides released from ZENK-expressing retina amacrine cells in the chick and so likely represents a key messenger for ocular growth modulation although the downstream elements of this ZENK pathway are still not very well understood.[53, 56]

In studies aimed at understanding the role of glucagon in eye growth regulation, Feldkaemper *et al*., using Northern blot analysis, reported that proglucagon mRNA was increased in chick retina after treatment with positive lenses.[57] The retinal gene expression levels of glucagon and its receptor have also been investigated using semi-quantitative real-time PCR using the chick model, for form-deprivation as well as lens-induced myopia and hyperopia paradigms.[58, 59] Form-deprivation and negative lenses induced a significant down-regulation of glucagon mRNA expression comparing to contralateral control eyes, while positive lens resulted in up-regulation of glucagon mRNA expression, although the latter change did not reach statistical significance. Glucagon receptor mRNA expression was also not different between lens-treated and contralateral control eyes, although a transient increase in glucagon receptor mRNA expression was observed in lens-treated eyes. A follow-up study from Feldkaemper and Schaeffel showed retinal glucagon protein levels to be decreased with negative lenses, while positive lenses had no effect on retinal glucagon protein levels, even though the latter treatment reliably inhibits eye growth.[60] Currently, there is no direct evidence linking the changes of glucagon mRNA gene expression with protein levels in retina. The only small population of retinal neurons that synthesize and release glucagon, the possibility that there are other sources of glucagon synthesis and secretion (e.g. RPE), and the complicated metabolism of glucagon, all represent obstacles to designing conclusive studies.[54, 58, 60, 61]

Pharmacological studies using glucagon analogs represent a more direct approach to studying its role in eye growth regulation. In one such study, both glucagon or glucagon receptor agonists were observed to inhibit myopia development, induced by either form-deprivation or negative lenses.[60, 62, 63] Certain concentrations of intravitreally-injected glucagon also slowed the growth of otherwise untreated eyes.[63] Surprisingly, for eyes treated with positive lens, both glucagon and a glucagon antagonist inhibited hyperopia development.[60, 62, 63] These apparently paradoxical results for glucagon injected, positive lens-treated eyes may reflect interactions between endogenous glucagon levels, the injected glucagon concentrations, and/or the number and sensitivity of glucagon receptors. These studies also focused on changes in axial ocular dimensions and refractive errors.

Thus it is perhaps also of relevance that in a later study, Fischer *et al*., found that exogenous glucagon primarily decreased equatorial eye growth, and conversely, glucagon receptor antagonists caused excessive equatorial growth. In summary, based on reported experimental evidence, glucagon appears to serve as a stop signal for eye growth, although the underlying signal pathway and mechanisms appear complicated.

1.1.4.1.3 Neurotransmitter: dopamine

Dopamine (DA) is a monoamine neurotransmitter, which is synthesized from L-tyrosine by a subset of amacrine cells. One of its principal metabolites is 3,4-dihydroxyphenylacetic acid (DOPAC). DA receptors have been identified on both neural cells within the retina[64] and RPE.[65-68] There are five subtypes of DA receptors (D1-D5), and based on their biochemical and pharmacological properties they have been categorized into D1-like (D1, D5), and D2-like (D2-D4) subfamilies.[69, 70]

In the retina, dopamine plays major roles in light adaptive processes and contrast sensitivity.[71] In myopia-related research, retinal dopamine has also been shown to be associated with eye growth regulation. Specifically, animal studies have demonstrated that retinal DA concentration, retinal DA synthesis rate, and concentrations of retinal and vitreal DOPAC, the latter serving as indices of retinal dopamine release, show changes related to altered eye growth, induced with form-deprivation, negative or positive lens treatments or even changes in the illuminance used in rearing.[72-77] Nonetheless, in one of few studies to challenge the role of DA in eye growth regulation, Luft *et al.*, reported changes in the retinal dopaminergic system in response to altered light intensity, but not spatial frequency, with short-term (2 hours) treatment.[78]

Direct evidence for a role of DA in eye growth regulation is provided by observations that ocular administration of apomorphine, a nonselective DA receptor agonist, inhibits both form-deprivation and lens-induced myopia, in both chick and monkey models.[74, 79-84] Furthermore, co-administration of a DA receptor selective antagonist along with apomorphine, prevents the latter inhibitory effects on eye elongation in chicks,[74, 79] and D2-selective antagonists alone enhance form-deprivation myopia in chicks.[85] These data together provide convincing evidence for a role of retinal dopamine in eye growth regulation.

1.1.4.1.4 Neurotransmitter: acetylcholine

Acetylcholine (Ach), another classic neurotransmitter, is widely distributed throughout both the peripheral nervous system (PNS) and central nervous system (CNS).[86] In the retina, cholinergic amacrine cells have been identified in both INL and GCL.[87-91] Ach activates two types of integral membrane receptors, ionotropic nicotinic acetylcholine receptors (nAChR) and metabotropic muscarinic acetylcholine receptors (mAChRs).[92-97] There are at least five subtypes of mAChRs (M1-M5), which are widely distributed through out ocular tissues; thus in chicks and tree shrews, mAChR subtypes have been localized to retina, RPE, choroid, and ciliary body.[98-102] Retinal cholinergic mechanisms have been

implicated in many important aspects of visual processing, including motion detection and light adaptation.[86, 103]

The observed potent inhibitory effects on eye elongation of muscarinic receptor antagonists such as atropine are among evidence implicating acetylcholine in the control of ocular growth.[104-106] Intravtireal administration of selective mAChR antagonists further suggest that such anti-myopia effects are mediated by M1 and/or M4 receptor subtypes. However, the exact ocular site of action of mAChR antagonists remains unresolved due to the wide distribution of mAChRs and the variable effects of different muscarinic receptor antagonists on myopia development.[105, 107-109] Arguing against a retinal site of action are results from investigations of form-deprived chick and tree shrew eyes, which did not reveal any treatment-related differences in the retinal content of Ach or choline, its metabolite, or choline acetyltransferase (ChAT), the Ach synthesizing enzyme.[110, 111] Furthermore, the depletion of the majority of cholinergic amacrine cells in the chick retina using ECMA, a neurotoxin, did not prevent the development of myopia in response to form-deprivation.[112] These results thus call into question the role of retinal Ach and retinal cholinergic cells in myopia development and raise the possibility that mAChR antagonists may act through other ocular tissue sites such as RPE, choroid, and sclera rather than retina or that other noncholinergic mechanisms may be involved.[40, 98, 101, 113, 114]

1.1.4.1.5 Other molecules and gene expression regulation

Retinoic acid (RA) is known to be a potent regulator of cell growth and differentiation, acting via nuclear receptors (RARs and RXRs), to activate or repress the expression of genes.[115, 116] RA also has been put forward as a potential eye growth regulator.[117, 118] There are extensive data linking RA with ocular growth regulation in a number of different species, although there are also subtle species-related differences. In chicks, RA levels in both retina and choroid exhibit bidirectional changes with altered eye growth. In the case of both form-deprivation or negative lens treatment, retinal RA levels are increased.[117, 119-122] In addition, negative lens treatments up-regulate retinal mRNA expression of aldehyde dehydrogenase-2 (AHD2), one of the enzymes involved in RA synthesis.[123] In monkey, the rate of retinal RA synthesis was found to be positively correlated with eye elonagetion.[124]

Other neurotransmitters or molecules that have been suggested to play roles in eye growth regulation and/or myopia development include vasoactive intestinal polypeptide,[125-127] somatostatin, insulin,[63, 128, 129] insulin-like growth factor-1 (IGF-1),[63] basic fibroblast growth factor (bFGF),[130] transforming growth factor-β (TGF-β).[130]

ZENK is one of the most extensively studied genes in the context of myopia. As already noted (section on retinal amacrine cells), early studies found ZENK protein expression in chick retina to be altered by visual manipulations known to affect eye growth.[51, 53, 131] Interestingly, more recent studies have reported for two drugs known to inhibit myopia, a muscarinic cholinergic antagonist and a dopamine agonist, rapid increases in ZENK mRNA expression in the retinas of form-deprived chicks, although previously identified ZENK expression glucagonergic amacrine cells only comprised a small portion of retinal cells

affected,[132] and another researcher reported disparate results in relation to the effects of muscarinic antagonists on ZENK expression in the chick retina.[132]

Recent studies combining high-throughput microarray and semi-quantitative PCR have identified a number of retinal or retina/RPE genes with potentially important roles in eye growth regulation.[127, 133, 134] Listed genes include BMP2, endothelin receptor type B (EDNRB), interleukin-18 (IL-18), connective tissue growth factor (CTGF), neurotensin (NTS), and noggin (NOG). Theses results provide additional insight into possible molecules involved in the regulation of ocular growth, and also reinforce the complex nature of ocular growth regulation.

1.1.4.2 RPE

The retinal pigment epithelium (RPE) is a unique tissue, located between the neuroretina and choroid/sclera. Arrayed in a monolayer of cells, linked by tight junctions, the RPE represents a critical component of the retina-blood barrier, preventing the free exchange of molecules and ions between the retina and choroid. Thus, the RPE serves to protect the health and integrity of the neural retina and maintain of physiological homoestasis.[135-137] By virtue of its anatomical location, the RPE is also ideally suited to relay presumed growth modulatory signals that originate in the retina, to the choroid and sclera, where remodeling and other growth processes occur to achieve changes in eye size.[16, 40] The RPE possesses a rich array of receptors, including ones for neurotransmitters already implicated in eye growth regulation.[40, 98, 138, 139] The RPE is also known to be an important source of growth factors that may have autocrine and/or paracrine functions.[135, 140] Of relevance to the research reported in this dissertation, differential gene expression as well as morphological changes in RPE has been documented during the development of myopia and hyperopia.[141-145]

1.1.4.2.1 Neurotransmitter receptors and retinoic acid receptors

Glucagon receptors: Glucagon receptors belong to the G protein-coupled family of receptors (GPCRs).[146] Stimulation of the GPCR results in activation of adenylate cyclase and the regulation of intracellular cAMP levels.[147] RPE is both a possible source of glucagon and a tissue site of action as it also expresses glucagon receptors.[58] Studies have shown the application of glucagon to embryonic chick RPE to increase intracellular cyclic AMP and adenylate cyclase activity.[148]

Dopamine receptors: There is evidence linking D2 receptors to inhibitory eye growth effects of dopamine,[74, 79] and in chicks, dopamine D2/3 receptors have been identified on the basal side of the RPE, with their presence on the apical surface of RPE cells being left unresolved due to the heavy pigmentation in this region.[65] mRNA expression also has been detected for both D2 and D4 receptors in chick RPE.[65, 143] D2 receptors have also been demonstrated on the RPE of mammals, including cat and cow,[67, 68] while their presence on human RPE is controversial.[149, 150] Nonetheless, cultured human fetal RPE (hfRPE) are reported to posses D2 receptors.[151] *In vitro* electrophysiological studies using chick retina-RPE-choroid tissue preparations suggest the presence of DA receptors on both apical and basolateral

membranes, which result in altered RPE membrane potentials when pharmacologically manipulated.[152] At least some of these DA effects on RPE can be abolished using a Cl^- channel blocker, suggested that DA may act through a signaling pathway involving basal membrane Cl^- channels. Intriguingly, application of dopamine to an *in vitro* co-culture of RPE with scleral chondrocytes showed an effect on the proliferation of scleral chondrocytes that was not seen when dopamine was applied to chondrocytes cultured in isolation.[153]

Muscarinic acetylcholine receptors (mAChRs): Since mAChR antagonists such as atropine and pirenzepine have been shown to be among the most potent anti-myopia agents, much research efforts have been focused on the characterization of mAChR in different ocular tissues.[154] However, as noted previously, the target tissues for the above mAChR antagonists remain unresolved, at least in part due to the wide expression of mAChR in the eye.[98, 102] Expression of mAChR has been demonstrated in the RPE of a number of different species, including chick, for which M2, M3, and M4 proteins have been identified in RPE.[98] Activation of mACh receptors in cultured human RPE leads to increased phosphoinositide turnover and increases in intracellular calcium.[155] Other pharmacological studies have implicated mAChRs in RPE metabolism in humans and rats.[156, 157]

Retinoic acid receptor: Retinal and choroidal RA concentrations show bidirectional changes under conditions corresponding to accelerated or slowed eye growth respectively.[117, 118, 120] Since RPE is interposed between the retina and choroid, it may potentially be affected by either or both changes in retinal RA and choroidal RA, making interpretation of studies into the role of the RPE in these events very difficult.[135, 158, 159] Nonetheless, the RPE does possess RA receptors and down-regulation of RAR-β mRNA in RPE has been reported with lens-induced myopia.[143]

In addition to the neurotransmitters and receptors already discussed above, RPE is also reported to possess a number of other types of receptors including those for insulin, IGF-I,[160, 161] and VIP,[148] with application of VIP to cultured RPE cells reported to stimulate polarized secretion of macromolecules.[162]

1.1.4.2.2 Ion channels and fluid transport

As noted above, RPE cells are interconnected by tight junctions, which prevent the free, transepithelial movement of ions and water between the retina and choroid. Thus ion and water channels on RPE play important roles in fluid transport across RPE and maintaining homeostasis for adjacent tissues, the retina and choroid.[40] The RPE is also polarized, reflecting the asymmetric arrangements of these channels on the apical and basal membranes of RPE cells.

In the context of myopia research, the roles of RPE on ion and fluid channels are not well understood. Potassium and chloride channels are known to regulate transepithelial fluid transport while voltage-dependent calcium channels act as regulators of secretory activity. It is possible that some neurotransmitters, including dopamine, modulate eye growth through effects on these ion channels.[40, 136] The observed rapid thickness changes in the

choroid of the chick in response to myopia- and hyperoia-inducing stimuli may also reflect, at least in part, transepithelial fluid transport between the subretinal space and choroid.[16, 35] The volume and thickness changes in the choroid are discussed in more detail in the next section.

1.1.4.2.3 Growth factors and cytokines

The RPE represents a major source of growth factors and cytokines, including IGF-I,[163, 164] TGF-βs,[165, 166] FGFs,[167, 168] MMPs,[169] and TIMP.[170] Synthesized locally and subsequently secreted, they have been attributed roles in the maintenances of the structure and homeostasis of retina and choroid,[135] and some have also been implicated in postnatal eye growth regulation. Depending on the direction of their secretion, i.e., towards the retina and/or choroid, the growth factors synthesized by RPE have potential to affect the morphological and functional changes of retina and/or choroid and sclera.

Excepting the research reported in this dissertation, to-date, there has been only limited study of the roles of RPE and RPE-derived growth factors in postnatal eye growth regulation,[140, 141, 143, 151, 171] and in studies involving the chick model, gene expression studies have been limited to retina/RPE combined tissues rather than RPE in isolation.[133, 134] This dissertation research was dedicated to the investigation of role of RPE itself in myopia development, with studies into the roles of RPE-derived growth factors and cytokines in the retino-scleral signaling cascades, using both *in vivo* chick animal models and *in vitro* human fetal RPE culture models. A schematic diagram showing potential mechanisms by which the RPE might be involved in the eye growth regulation is provided in Figure 1-4.

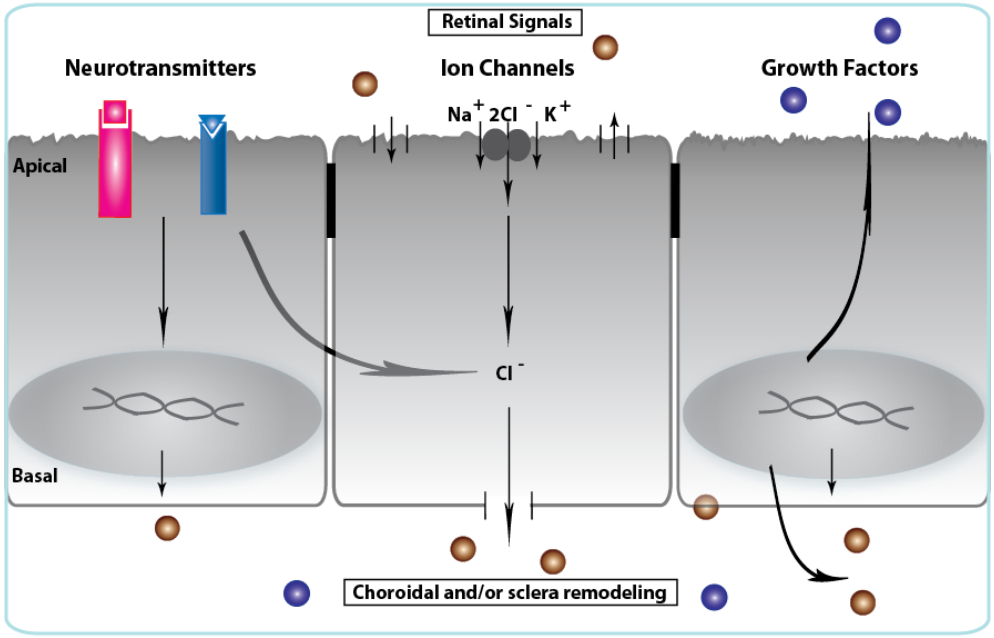

Figure 1-4. Schematic diagram showing potential mechanisms by which RPE may be involved in eye growth regulation.
(Modified based on Rymer and Wildsoet. *Vis Neurosci.* 2005. 22; 251–261.)

1.1.4.3 Choroid

Between the RPE and sclera lies the choroid, which is a richly vascular structure, with resident melanocytes, fibroblasts and immunocompetent cells, supported by collagenous and elastic elements.[41] Its major functions include supplying oxygen and nutrients to the outer retina, light absorption (pigmented choroid), thermoregulation, and modulation of intraocular pressure (IOP). More recently, it has also been recognized that the choroid plays a critical role in emmetropization, through early postnatal eye growth regulation.[41]

Histoloigcally, the choroid is divided into five layers starting from the inner retinal side: Bruch's membrane, choroicapillaris, two vascular layers (Haller's and Sattler's), and the suprachoroidea.[41] In birds, the suprachoroid contains large, endothelium-lined spaces (lacunae), which resemble lymphatic vessels.[172, 173]

In experimental myopia studies involving the chick myopia, it has been shown that the protein content of the suprachoroidal fluid decreases in form-deprived eyes and increases after vision is restored.[174] Bidirectional changes in the permeability of the choroidal vasculature also have been reported with form-deprivation and recovery from form-deprivation myopia in the chick.[174-176] These changes are linked to thickness changes of chick choroid – thinning in eyes with form-deprivation and lens-induced myopia, and thickening in eyes recovering from form-deprivation myopia and with lens-induced hyperopia.[16, 35, 140, 177] These changes in thickness can be very dramatic. For example, under normal visual conditions, the choroid of young chicks is about 250 μm thick in the central, axial region and 100 μm in the periphery.[177] With imposed myopic defocus, the choroid can increase its thickness by as much as 1 mm (>17 D), the effect being to push the retina towards the altered image plane, thereby compensating for the imposed focusing error.[177] In contrast, with imposed hyperopic defocus, the choroid thins to pull the retina backwards in the direction of the sclera towards the altered image plane. Likewise, form-deprivation also induces choroidal thinning. These changes in choroidal thickness occur very rapidly, being detectible with high frequency ultrasonography a matter of 1-2 hours.[178-180]

In addition to serving as a focusing mechanism as accomplished by moving the retina forward and backward to match the image focal plane, the choroid may also play an important role in regulating scleral growth and remodelling.[41] Of potential relevance here are observations that the choroid expresses and synthesizes a variety of growth factors and enzymes, including bFGF,[181] MMPs,[182] tissue plasminogen activator (t-PA),[183] and TGF-β. [131, 184, 185] For example, during the development of myopia, TGF-β gene expression has been shown differentially expressed in the choroid.[131, 185] The choroid also expresses glucagon and its receptor,[58] and choroidal glucagon content is reported to increase with positive lens treatments, although is not affected by negative lens treatments, at least up to one day.[60] Exogenous glucagon as well as insulin also affects the thickness of choroid.[63] There is also strong evidence for a role of choroidal retinoic acid (RA) in ocular growth regulation - RA shows bidirectional changes in response to visual manipulations that slow (positive lens and removal of diffusers) or accelerate (negative lens or diffuser) eye growth.[118] Choroidal expression of the RA-synthesizing enzyme, retinaldehyde dehydrogenase 2 (RALDH2) is also increased after 12 and 24 hours of recovery from form-deprivation.[186]

Finally, dopamine also has been linked to choroidal thickness changes in myopia development and inhibition in a number of animal models, although it is not clear whether the site of action is local to the retina in these cases.[41, 187, 188]

1.1.4.4 Sclera

The sclera represents the outer supportive coat of the eye, ultimately determining the shape and size of the globe. The sclera is constantly undergoing remodeling and/or growth changes, especially during early development, and responds rapidly to visual manipulations with changes in remodeling, with effects on both eye size and refractions.

In mammals and primates, the sclera comprises a dense fibrous connective tissue, which is primarily composed of extracellular matrix (ECM) and fibroblasts.[26] In the ECM, collagen, proteoglycans, and elastic fibers are major components. In mammals, the scleral tissue contains approximately 90% collagen (type I, III, IV, V, VI, VIII, XII and XIII) by weight. The relative proportions of these various subtypes of collagen determine the size of collagen fibrils, which are irregularly organized into lamellae. Located between the collagen lamellae are scleral fibroblasts, whose functions include the production and turnover of ECM; thus they play an important role in the regulating eye elongation. Proteoglycans including glycosaminoglycan (GAGs) are one of the most important non-collagenous components of the ECM (approximately 0.7–0.9% of the total dry weight of the sclera). Known functions of proteoglycans include the modulation of collagen fibril assembly and arrangement.[26] The sclera also includes elastic fibers, which account for approximately 2% of the dry weight of the ECM,[189] are also synthesized by scleral fibroblasts and are distributed homogenously throughout the sclera stroma.

During the development of myopia, morphological and histological changes of sclera has been documented, including overall enlargement of the sclera surface, sclera thinning, reduced diameter and derangement of collagen fibrils, with these changes becoming more exaggerated with time.[190, 191] With short term myopia inducing treatments, collagen fibril diameters may remain normal but scleral dry weight decreased.[192] Changes in ECM synthesis and degradation, and related molecules have also been observed during the development of myopia and recovery in mammalian models.[190, 193, 194] Specifically, decreases in the amount and/or gene expression of type I collagen,[195] GAGs,[194] MMP2,[196] MMP4,[197] TIMP3, TGFB1, TGFB2, thrombospondin 1 (THBS1), tenascin (TNC), osteonectin (SPARC), and osteopontin (SPP1)[198] in sclera have been reported during the development of myopia, while mRNA expression is reported to be up-regulated for TGFBR3, TGFBI, MMP14, FGFR-1.[198, 199] These molecular changes go

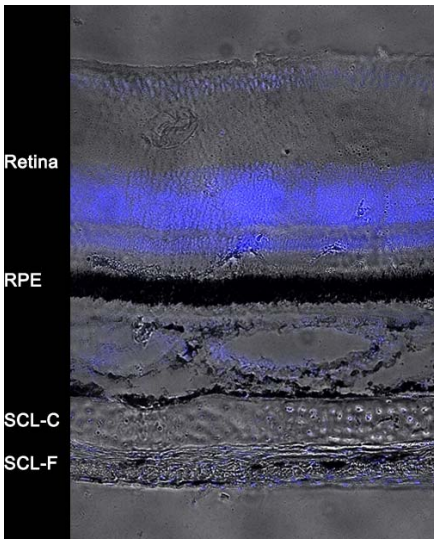

Figure 1-5. Histological cross-section of the posterior eye wall of the chick; SCL-C & SCL-F indicate scleral cartilage and fibrous layers respectively.

hand-in-hand with changes in the biomechanical properties of sclera, which shows an increase in "creep rate" during the development of myopia.[200, 201]

The above discussion is relevant to mammalian and primate sclera. There are important differences between these scleras and the sclera of chicks, which is one of the most common used myopia models in research. Specifically, in addition to a fibrous layer, the avian sclera has an additional inner layer of cartilage (Figure 1-5), and in myopic eyes, the cartilage layer becomes thicker than normal while the fibrous layer thins.[202, 203] Both the scleral dry weight and protein synthesis are also increased in the myopic eyes of chicks.[204, 205]

Growth factors likely play important roles in regulating scleral remodeling during the development of myopia, a possibility supported by results of pharmacological studies. For example, in chicks subconjunctival and intravitreal delivery of bFGF and TGF-β1 are reported to influence the development of form-deprivation myopia, and bFGF, TGF-β, and BMPs have also been shown to stimulate the proliferation of both scleral chondrocytes and fibroblasts *in vitro*.[130, 206-208] As retinoic acid (RA), is known to regulate ECM remodeling in a variety of connective tissues, it is plausible that it may also regulate sclera ECM remodeling, given that it also shows bidirectional regulation in the nearby choroid.[118, 120, 209] Finally, the presence of mAChRs on scleral cells opens up the possibility of cholinergic regulation of scleral growth, although the source of cholinergic input is yet to be resolved. Nonetheless, the sclera is considered a plausible site of action for the anti-myopia effects of mAChR antagonists, such as atropine.[98, 104, 113, 210]

1.1.5 Anti-Myopia Treatments

While the prevalence and severity of myopia continues to increase, effective therapeutic interventions for myopia remain limited.[211] Most myopia develops during the early to middle childhood years, extending into late teenage years and early adulthood in susceptible individuals.[11] As already indicated, most myopia results from excessive lengthening of the vitreous chamber such that images of distant objects are focused in front of the retina and thus blurred in the absence of correcting lenses.[212]

Human-based epidemiological research points to a role of prolonged near work, particularly excessive reading, in the development of myopia.[213, 214] Interestingly, recent studies point to outdoor activity as being protective against the development of myopia.[25, 215] Among the factors likely to be contributing to the latter outdoor effect are the reduction in near work activities and the properties of the outdoor visual environment, which includes higher light levels compared to indoor environments.[25] In terms of anti-myopia treatments, these observations argue for changes in life style, to reduce the time spent in intensive, continuous near work, and to increase the outdoor activities and duration.

Currently, the management of myopia remains largely limited to traditional optical corrections – single vision spectacles and contact lenses, and refractive surgery. These traditional corrections are intended to correct the mismatch between the optical power of

the eye and its length and so to correct distance vision, with no effect on myopia progression. However, novel soft contact lens designs intended to impose myopic defocus on periphery retina are currently under trial with early results showing promising evidence of slowed myopia progression.[43, 216-218] Studies of orthokeratology (ortho-k), which uses rigid contact lenses to reshape and so reduce the power of the central cornea, have also reported promising results of slowed myopia progression,[219] with imposed peripheral myopic defocus resulting from corneal reshaping being proposed as the underlying mechanism.

Clinically tested, pharmacological interventions for slowing or preventing the development of myopia are limited in most countries to two mAChR antagonists, atropine and pirenzapine, which have both been shown to retard myopia progression, although the mechanisms underlying their inhibitory effects remain poorly well understood, as already noted.[220, 221] Most studies involving atropine have used concentrations intended for ophthalmic diagnostic applications, with their use accompanied by many visually debilitating ocular side-effects, including glare and loss of accommodation, and the efficacy of such atropine treatments is also reported to attenuate over time. These findings underlie the only limited use of atropine for myopia control in the US. However, this picture may change with a recent report showing significant reductions of myopia progression with much lower concentrations (100-fold less), with far fewer ocular side-effects.[222]

For high, sometime referred to as “degenerative” myopia, posterior scleral reinforcement surgery is currently the only clinical treatment option, a last resort aimed at preserving vision in an eye that has become excessively large and mechanically unstable.[223] However, recent and still on-going studies investigating the application of biomaterials and slow release drug delivery systems to reinforce the sclera and/or manipulate the sclera remodeling have shown interesting results.[224] Apart from such treatments aimed at stabilizing the myopic eye, specific pathological complications of high myopia are targets of other treatments, including for choroidal neovascularization, intravitreal injections of anti-VEGF-A, which have yielded effective and sustained benefits.[225]

In summary, current treatment options for controlling myopia progression and its complications are limited. For the development of new effective clinical interventions, it is important to better understand the molecular mechanisms underlying the development of myopia and associated complications. The research reported in this dissertation searched for the molecular and cellular signaling pathways and mechanisms involving the RPE that could potentially be exploited for myopia control.

1.2 General Experimental Approaches and Methods

The following sections summarize the general experimental approaches and methods used in the studies reported in this dissertation, including animal models (chick) and visual manipulations used to perturb eye growth (defocusing lens treatments), ocular biometry (for measurement of axial ocular dimensions), RPE gene expression assessments (ocular tissue collection, RNA purification and quantification, reverse transcription, real-time PCR), and protein assays (western blot and immunohistochemistry). Details of materials and methods that are specific to individual studies are presented in relevant chapters.

1.2.1 Animal model

Chicks were used as the animal model for this dissertation research. A White-Leghorn strain was used, also for consistency with that used mostly commonly in myopia research. The chick is the most widely used animal model of myopia and also the most practical and reliable model. Young chicks respond very rapidly to form-deprivation and imposed optical defocus. The refractive error and axial length changes in response to various visual manipulations have been characterized in detail for the chick.[35, 59, 226, 227] For example, form-deprivation, achieved by covering eyes with diffusers, induces refractive errors up to -30 diopters (D), within ~10 days in young chicks, and increased ocular elongation results in almost complete compensation for the optical defocus imposed by -10 D lenses after ~7 days.[59] These axial growth changes occur more slowly in older birds.[227] Apart from changes to the overall axial ocular dimensions, changes in the thickness of the choroid are also observed with both form-deprivation and imposed optical defocus.[35, 179, 180] Choroidal thickening is detectable with just 10 minutes of positive lens treatments, and significant thinning of the choroid is detectible after an 1 h of negative lens wear.[16, 179]

1.2.2 Lens treatment

To manipulate ocular growth, monocular defocusing lenses were used, negative lenses (imposed hyperopia) to induce accelerated eye growth and so myopia and positive lenses (imposed myopia) to induce slowed eye growth and hyperopia. The magnitude of the ocular growth changes directly reflect the power of the defocusing lens and duration of the treatment period, being only small for very short treatment durations, irrespective of lens power. Three treatment durations, 2 h, 48 h, and 38 days, were employed in this research, to investigate the gene and protein expression at different stages of altered eye growth (Figure 1-6). Specifically, to identify genes important for initiating changes in eye growth, short-term (2 h) treatment was used to minimize ocular growth changes and potentially confounding effects of the latter. Genes showing differential expression after 48 h of treatment are assumed to be critical for maintaining induced altered growth patterns, as by this time altered growth is detectable. The longer-term negative lens treatment (38 days) was employed to investigate the genes involved in maintaining already established myopia and ocular (retinal) complications of the same.

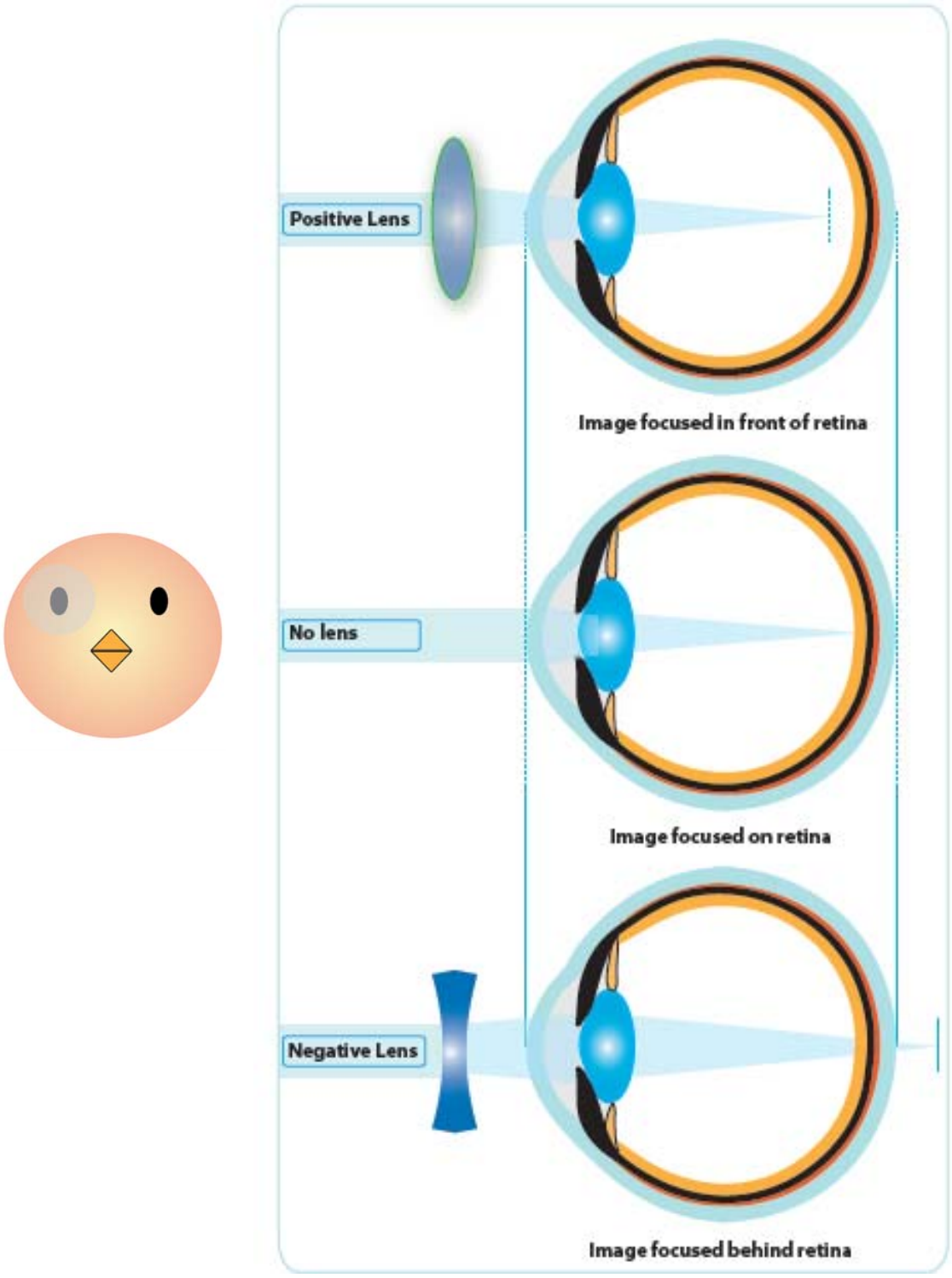

Figure 1-6. Monocular lens treatments used in dissertation research and the patterns of optical defocus imposed on normal (emmetropic) chick eyes. For distant objects, positive lenses move the image plane in front the retina, imposing myopic defocus while negative lenses move the image plane backwards, imposing hyperopic defocus.

1.2.3 Ocular biometry measurement

High frequency A-scan ultrasonography was used to measure, both before and after lens treatments, axial ocular dimensions, including anterior chamber depth, vitreous chamber depth, and choroidal thickness. A typical A-scan ultrasonography trace is shown in Figure 1-7. The resolution of our customized A-scan ultrasonography set-up is 10 μm. Axial length is represented by the sum of anterior chamber depth (F to peak 1), lens thickness (peak 1 to 2), vitreous chamber depth (peak 2 to 3), retinal thickness (peak 3 to 4), choroidal thickness (peak 4 to 5), and scleral thickness (peak 5 to 6).

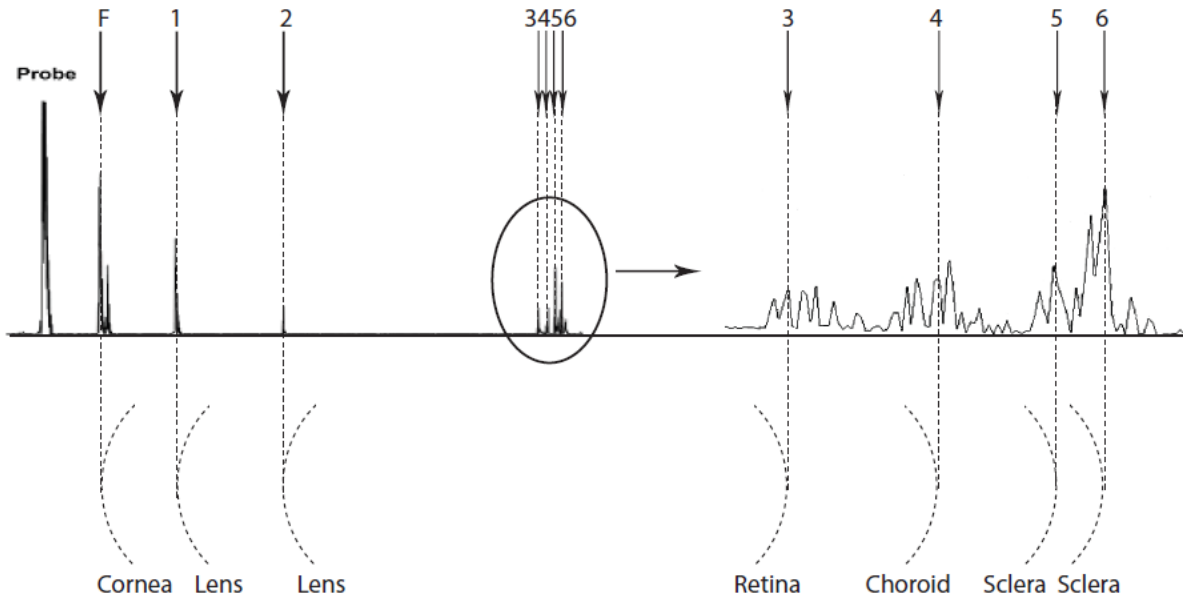

Figure 1-7. A-scan ultrasonography of chick eye.

1.2.4 Ocular tissue collection

In all experiments, chicks were sacrificed, eyes quickly enucleated, and tissues separately collected over ice for molecular and/or biochemical analysis. First, the anterior segment of the eye is cut away; the remaining posterior eye cup is immersed in cold Ringer's buffer, the retina peeled off from the RPE with forceps, and then the RPE collected by gently rinsing cells off the choroid with buffer. In experiments requiring retina, pieces contaminated with RPE were discarded. Choroid was collected last, by peeling away it from the adjacent sclera. For RNA samples, all ocular tissues were lysed with RLT buffer from RNeasy Mini kits (Qiagen, Valencia, CA). Ocular protein samples were lysed with RIPA buffer (Sigma-Aldrich, St. Louis, MO) containing a protease inhibitor cocktail (Sigma-Aldrich). All samples were stored at -80 °C immediately for later use.

1.2.5 RNA purification and quantification

Total RNA from retina and RPE samples was purified using RNeasy Mini kits, while total RNA from choroid was purified using RNeasy Fibrous Tissue Mini Kits (Qiagen, Valencia, CA), with on-column DNase digestion, according to the manufacturer's protocol. RNA concentration and A_{260}/A_{280} optical density ratios were measured for quantification and quality control with a spectrophotometer (NanoDrop 2000, NanoDrop Technologies, Inc., Wilmington, DE). RNA quality was also examined by gel electrophoresis, using a 1.2 % agarose gel, with ethidium bromide staining.

1.2.6 Reverse transcription

Total RNA was reverse transcribed to cDNA using SuperScript III First-Strand Synthesis System for RT-PCR (Invitrogen, Carlsbad, CA). The amount of cDNA used in each real-time PCR reaction varied across tissues and between genes, reflecting an adjustment for differences in expression levels. The possibility of genomic DNA contamination was examined using RNA samples without RT enzymes.

1.2.7 Real-time PCR

Primers for these studies were designed using Primer Express 3.0 (Applied Biosystems, Foster City, CA). Ten-fold serial dilutions of cDNA were used for generating standard curves for each pair of primers. Melt curves were performed for all genes examined to detect potential non-specific amplification of primers. The efficiency (E) of each primer was calculated using equation (1) in Table 1-2.

QuantiTect SYBR Green PCR Kits (Qiagen, Valencia, CA) and a StepOnePlus Real-Time PCR System (Applied Biosystems, Foster City, CA) were used for gene expression quantification. The equations using in analyzing these data are given in Table 1-2. Mean normalized expression (MNE) values were used to compare gene expression levels in RPE from lens-treated eyes, their fellow (control) eyes, and normal eyes from untreated birds. MNE values were derived as equation (2). Mean mRNA expression levels were calculated using equations (3). Lens treatment-induced changes were expressed as Fold-changes, calculated using equation (4).

1.2.8 Western blot

Protein expression profiles were established for chick ocular tissues using Western blots and samples from untreated birds. Total protein concentration was measured using a BCA assay (Pierce Biotechnology, Rockford, IL). For Western blots, protein samples were prepared in NuPAGE LDS sample buffer (Invitrogen), with or without DTT as a reducing agent, and heated at 95 °C for 5 minutes. Protein samples were then electrophoresed under non-reducing and reducing conditions on 4% - 12% gradient gels (NuPAGE 4-12% Bis-Tris Gel, Invitrogen), before being transferred to nitrocellulose membranes (iBlot Gel Transfer Stacks, Invitrogen). Membranes were blocked (StartingBlock T20 [TBS]; Pierce Biotechnology), then incubated with primary antibodies, and finally labeled with HRP-

conjugated secondary antibodies. Immunoreactive bands were detected with chemiluminescence (Supersignal Pico ECL; Pierce Biotechnology), and images developed using a bioimaging system (FluorChem Q, Alpha Innotech; San Leandro, CA). The choice of antibody was based on results of database searches. Both positive and negative controls were included. All assays involved three independent biological samples and triplicate repeats.

1.2.9 Immunohistochemistry

Posterior eyecups were prepared from enucleated eyes, immersed in Optimal Cutting Temperature (OCT) compound and stored at - 80 °C immediately for later use. Seven-micron cryostat sections were cut and dried at room temperature, fixed with acetone, washed with PBS, and then blocked with 10% normal serum in PBS containing 2% bovine serum albumin (BSA). Immunostaining made use of a primary antibody and fluorescence conjugated secondary antibody; as a negative control, some sections were incubated in isotype IgG. After labeling, sections were mounted on glass slides with medium containing the nuclear stain, DAPI (Vector Labs, Burlingame, CA), and photodocumented with a Zeiss Axioplan 2 microscope (Carl Zeiss, Inc., Germany).

Table 1-2. Equations used in semi-quantitative estimates of gene expression

Equations	Number
$E = 10^{(-1/\text{slope})}$	(1)
$MNE = \frac{(E_{\text{reference}})^{CT_{\text{reference, mean}}}}{(E_{\text{target}})^{CT_{\text{target, mean}}}}$	(2)
$\text{mRNA levels} = \frac{1}{N}\sum_{i=1}^{N} MNE_i$	(3)
$\text{Fold} = \frac{1}{N}\sum_{i=1}^{N}\frac{\text{Treatment}_i}{\text{Fellow}_i}$ or $\text{Fold} = -1 \Big/ \left(\frac{1}{N}\sum_{i=1}^{N}\frac{\text{Treatment}_i}{\text{Fellow}_i}\right)$	(4)

1.3 Dissertation Outline

This dissertation describes investigations into the role of RPE in myopia development, focusing on the molecular and cellular mechanisms such as differential gene expression in RPE underlying the altered eye growth. The ultimate goal of these studies is to develop novel approaches for myopia control targeting RPE and these signaling pathways.

Chapters 2, 3, and 4 of this dissertation are divided and organized according to the specific aims in the following order:

1. To investigate the differential gene expression of bone morphogenetic protein (BMP) 2, BMP4, and BMP7 in chick RPE with short-term (2 and 48 hours) imposed optical defocus. As part of this study, the expression of related proteins, as well as the localization of BMPs in chick posterior ocular tissues, was also investigated. Our interest was in whether the expression of one of more of these genes, which have been linked to growth modulation in other tissues, might be modulated by optical defocus, consistent with roles in initiation and maintaining early stage of altered eye growth. The results of this study were published in the journals of *Investigative Ophthalmology and Visual Science* and *Experimental Eye Research*.

2. To establish using high-throughput DNA microarray a global gene expression profile in chick RPE after long-term (38 days) imposed hyperopic defocus, which induces ocular elongation and myopia. Myopia carries a high risk of retinal complications that compromise vision, some of which could plausibly reflect altered RPE gene expression and thus RPE function. Genes showing altered expression in RPE may also play important roles in maintaining myopia.

3. To investigate the effects of apomorphine (APO) on TGF-βs secretion in cultured hfRPE cells. Dopamine (DA) receptor agonists are known to inhibit myopic growth, although their site of action and other details of the signal pathway involved are not well understood. As the RPE is known to have DA receptors, it is also a plausible site of action for this effect.

In the last chapter, we summarize the findings from this dissertation study, and discuss the future directions and development based on the current results.

Chapter 2

Bidirectional, Optical Sign-Dependent Regulation of BMP Gene Expression in Chick RPE

Abstract

This study explored the role of Bone Morphogenetic Proteins (BMPs), BMP2, BMP4, and BMP7 in defocus-induced ocular growth changes using gene expression changes in retinal pigment epithelium (RPE) as a surrogate. Young White-Leghorn chickens were used in this study. Normal gene expression of BMP2, BMP4, BMP7 and their receptors was also examined in retina, RPE, and choroid, and the expression profiles of all three BMP proteins were assessed in the same tissues using Western blots and immunohistochemistry. Semi-quantitative PCR (qPCR) was used to assess the effects of short-term exposure (2 or 48 hours) to monocular +10 and +10 diopter (D) lenses, on RPE gene expression of BMPs and their receptors. Ocular growth was measured using high frequency A-scan ultrasonography. In the eyes of untreated (normal) chickens, expression of all three BMP mRNAs was high in RPE compared to retina and choroid and all three tissues expressed the related BMP proteins. At the level of gene expression, all three receptors also were detected in these tissues, with BMPR2 showing the highest, and BMPR1B, the lowest expression. BMP2, 4, and 7 were up-regulated in the RPE from eyes wearing +10 D lenses, which exhibited shorter than normal vitreous chamber depth (VCD) and thickened choroid, while BMP gene expression was down-regulated in the RPE from eyes wearing -10 D lenses, which developed enlarged VCD and thinned choroid. In contrast, the BMP receptors did not show differential expression changes in RPE in response to these defocus treatments. That mRNA expression of BMPs in chick RPE shows bidirectional, defocus sign-dependent changes is suggestive of a role for BMPs in eye growth regulation, although the diffuse ocular expression of BMPs and their receptors suggests complex growth-modulatory signal pathways.

Chapter 2 was reproduced with modification from the following published papers:

Zhang Y, Liu Y, Wildsoet CF. 2012. Bidirectional, optical sign-dependent regulation of BMP2 gene expression in chick retinal pigment epithelium. *Invest Ophthalmol Vis Sci*. 2012. 53:6072-6080.

Yan Zhang, Yue Liu, Carol Ho, Christine F. Wildsoet. Effects of imposed defocus of opposite sign on temporal gene expression patterns of BMP4 and BMP7 in chick RPE. *Experimental Eye Research*. 2013; 109:98-106.

2.1 Introduction

Uncorrected refractive errors are one of the world's leading causes of blindness and significant contributors to the global burden of eye disease.[6, 8, 9, 228] Ocular refractive errors reflect the imbalance between the refracting power of the eye, to which the cornea and crystalline lens contribute, and its optical axial length, which defines the position of the retina relative to the latter optical elements. Mismatches between these parameters can result in either myopia, where the eye is too long in relative terms, or hyperopia, where the eye is too short. Babies are typically born with refractive errors, which are corrected during early development through a process of coordinated ocular growth known as emmetropization.[3, 4, 229-231] However, myopia may also occur in childhood as a failure of emmetropization, when the eye continues to elongate after emmetropia is achieved.[9, 232]

Studies using animal models have provided convincing evidence for the role of visual input in the emmetropization process and its abnormalities.[16, 233, 234] For example, both spatial form-deprivation and negative defocusing lenses accelerate the rate of eye elongation while positive defocusing lenses slow eye elongation. The net results in refractive terms are induced myopia and hyperopia respectively. A variety of studies, including neural lesioning ones, support a model of local regulation of eye growth, with the retina being the presumed origin of growth modulatory signals, linked via one or more local signal cascades directed at the two outer layers of the eye wall – the choroid and sclera, which ultimately determine eye size.[34-37] Although the nature of these regulating pathways remains poorly understood, one investigational approach has been to look for genes showing differential regulation in one or more of these key tissues during altered eye growth.[26, 39-41] Because emmetropization is bidirectional, at least in chicks, bidirectional, optical defocus sign-dependent regulation of genes has been interpreted as evidence of their roles in emmetropization.[16] Excepting the data published from this dissertation, only expression of the ZENK protein in a subset of retinal amacrine cells exhibits this profile (i.e., optical defocus sign-dependence).[16, 51, 53]

The retinal pigment epithelium (RPE) is a unique tissue, lying between the retina and choroid, and comprising a single layer of polarized cells interconnected by tight junctions. It serves not only to absorb stray light within the eye but to tightly regulate the exchange of molecules, including ions and water, between the retina and choroid. Thus the RPE hosts a variety of receptors and transporters.[135, 137] Our interest in the RPE is as a likely conduit for growth regulatory signals originating in the retina. By examining gene expression patterns in the RPE from eyes undergoing altered growth, we hope to obtain insight into how such retinal signals are relayed to the choroid/sclera complex, with the possibility of identifying key growth regulatory molecules underlying myopic eye growth.[40, 135]

BMPs represent a large family of multi-functional growth factors that belong to the transforming growth factor-β superfamily, with important roles in embryogenesis and osteogenesis.[235-239] So far, at least 15 members of the BMP family have been reported (Table 2-1).[239, 240] Based on amino acid sequence homology, BMP2 and BMP4 belong to one subgroup, being very similar to each other, while BMP7 belongs to another.[239] Of this

family, BMP2 has already been linked to ocular development and growth regulation.[133, 241, 242] Importantly, BMP2 gene expression in chick retina/RPE is down-regulated in form-deprivation myopia.[133] BMP2 has also been reported to inhibit serum-induced human RPE cell proliferation, consistent with the profile of a negative growth regulator,[243] although BMP2 is reported to have the opposite action *in vitro* on human scleral fibroblasts, of stimulating the proliferation and differentiation.[208] Previous studies have also linked both BMP4 and BMP7 to embryonic eye morphogenesis as well as diseases of the adult retina.[243-247] For example, a genetics study using a loss-of function mutation of BMP7 in mouse reported severe defects in the developing eye,[248] and a recent human genetic study proposed BMP4 as a possible candidate gene for myopia. Both studies provided additional motivation for the current study.[249]

To investigate the roles of BMP2, BMP4, and BMP7 in defocus-mediated eye growth regulation, we used short exposures to both positive and negative lenses, to limit the magnitude of induced ocular dimensional changes, which may themselves affect gene expression in one or more tissues. We observed defocus sign-dependent, bidirectional regulation of BMP2, BMP4, and BMP7 gene expression in RPE but not of its RPE receptors, although the expression of all three BMP receptors was confirmed in RPE, as well as retina and choroid, along with all three BMPs.

Table 2-1. Members of the BMP family

BMPs	Synonyms
BMP1	PCP (procollagen C-endopeptidase)
BMP2	BMP2A
BMP3	Osteogenin
BMP4	BMP2B
BMP5	
BMP6	Vgr-1
BMP7	OP-1 (osteogenic protein 1)
BMP8	OP-2
BMP9	Gdf-2 (growth/differentiation factor 2)
BMP10	
BMP11	Gdf-11
BMP12	Gdf-7
BMP13	Gdf-6
BMP14	Gdf-5
BMP15	Gdf-9B

2.2 Materials and Methods

2.2.1 Animals and Lens Treatments

White-Leghorn chickens were obtained as hatchlings from a commercial hatchery (Privett, Portales, NM) and raised under a 12 h-light/12-h dark cycle. To induce myopic and hyperopic growth patterns, 19 day-old (adolescent) chickens wore monocular -10 and +10 D lenses respectively, for either 2 or 48 h. To characterize the effects of the lens treatments on eye growth, the axial ocular dimensions of both eyes of individual birds were measured under isoflurane anesthesia (1.5% in oxygen), at both the beginning and end of the lens treatment periods, using high-frequency A-scan ultrasonography (n = 53). Only data for ocular parameters showing significant change are reported, i.e., vitreous chamber depth (VCD), choroidal thickness (CT) and axial length (AL; the distance between of the anterior corneal and posterior scleral surfaces). The same treatments were applied to a separate set of chickens for use in gene expression studies, to avoid the potentially confounding influence of anesthesia on gene expression. In this case, each of the 4 treatment groups comprised a total of 4-6 birds, made up from 3 independent repetitions of the experiment (n =16 for 2 h of -10 D lens treatment group; n = 14 for all three other treatment groups); age-matched untreated birds, i.e., no lens treatment, were also included (n = 24).

Experiments were conducted according to the ARVO Statement for the Use of Animals in Ophthalmic and Vision Research and approved by the Animal Care and Use Committee (ACUC) at University of California, Berkeley.

2.2.2 Tissue Sample Collection for RNA and Protein Studies

Retina, RPE, and choroid samples collected from 19-day and 21-day old untreated chicks were used to study normal BMP (BMP2, -4, -7) and BMP receptor (BMPR1A, -1B, -2) gene expression. BMP protein expression in the same three tissues was characterized using Western blots. Additional posterior eyecups were collected from untreated chicks and processed for immunohistochemistry, to localize the proteins in the tissues making up the posterior eye wall – retina, RPE, choroid and sclera. Only RPE was collected from the lens experiments, in the interest of obtaining samples in minimal time. The expression of BMP2, -4, -7 and their receptors was examined in samples from lens-treated and untreated fellow eyes of experimental subjects, after lens-wearing periods of both 2 and 48 h. The method of sample collection was as described in details in Chapter 1. Briefly, chicks were sacrificed, eyes enucleated and then retina, RPE, and choroid isolated and collected over ice.

For RNA samples, all three ocular tissues were lysed with RLT buffer from RNeasy Mini kits (Qiagen, Valencia, CA). Ocular protein samples were lysed with RIPA buffer (Sigma-Aldrich, St. Louis, MO) containing a protease inhibitor cocktail (Sigma-Aldrich). All samples were stored at -80 °C immediately for later use.

2.2.3 RNA Purification and Quantification

Total RNA from retina and RPE samples was purified using RNeasy Mini kits, while total RNA from choroid was purified using RNeasy Fibrous Tissue Mini Kits (Qiagen, Valencia, CA), with on-column DNase digestion, according to the manufacturer's protocol. RNA concentration and A_{260}/A_{280} optical density ratio were measured for quantification and quality control with a spectrophotometer (NanoDrop 2000, NanoDrop Technologies, Inc., Wilmington, DE). RNA quality was also examined by gel electrophoresis, using a 1.2 % agarose gel, with ethidium bromide (EB) staining.

2.2.4 Reverse Transcription

Total RNA was first reverse transcribed to cDNA (SuperScript III First-Strand Synthesis System for RT-PCR, Invitrogen, Carlsbad, CA). Genomic DNA contamination was examined using RNA samples without RT enzymes. The amount cDNA used in each PCR reaction varied across tissues and between genes, according to expression levels.

2.2.5 Primer Design and Validation

Primers for these studies were designed using Primer Express 3.0 (Table 2-2; Applied Biosystems, Foster City, CA). Ten-fold serial dilutions of cDNA were used for generating standard curves for each pair of primers. The efficiency (E) of each primer was calculated using the following equation, $E=10^{(-1/slope)}$. Melt curves were performed for all genes examined; all PCR tests yielded single peak products. Amplification of each gene was performed in triplicate.

Table 2-2. Primer information for BMPs and BMP receptors

Gene	NCBI Access Number	Sequences (5'-3')	Efficiency	Amplicon
BMP2	NM_204358	Forward: 5'-AGCTTCCACCACGAAGAAGTTT-3' Reverse: 5'-CTCATTAGGGATGGAAGTTAAATTAAAGA-3'	93.6%	96 bp
BMP4	NM_205237.2	Forward: 5'-CCAGCAAATCAGCCGTCAT-3' Reverse: 5'-CGGACTGGAGCCGGTAGA- 3'	97.5 %	57 bp
BMP7	XM_417496.3	Forward: 5'-GGTGGCAGGACTGGATCATC-3' Reverse: 5'-GCGCATTCTCCTTCACAGTAATAC-3'	100 %	64 bp
BMPR1A	NM_205357.1	Forward: 5'-TGTCACAGGAGGTATTGTTGAAGAG-3' Reverse: 5'-AAGATGGATCATTTGGCACCAT-3'	93.8%	68 bp
BMPR1B	NM_205132.1	Forward: 5'-GGGAGATAGCCAGGAGATGTGT-3' Reverse: 5'-GGTCGTGATATGGGAGCTGGTA-3'	105%	66 bp
BMPR2	NM_001001465.1	Forward: 5'-GCTACCTCGAGGAGACCATTACA-3' Reverse: 5'-CATTGCGGCTGTTCAAGTCA-3'	100%	62 bp
GAPDH	NM_204305.1	Forward: 5'-AGATGCAGGTGCTGAGTATGTTG-3' Reverse: 5'-GATGAGCCCCAGCCTTCTC-3'	95.6%	71 bp

2.2.6 Real-time PCR

QuantiTect SYBR Green PCR Kits (Qiagen, Valencia, CA) and a StepOnePlus Real-Time PCR System (Applied Biosystems, Foster City, CA) were used for gene expression quantification. Mean normalized expression (MNE) values were used to express mRNA levels in RPE from lens-treated eyes, their fellow (control) eyes, and normal eyes from untreated birds. Calculation for MNE values, mRNA levels and fold changes has been described in Chapter 1 (Table 1-2). Chick glyceraldehyde 3-phosphate dehydrogenase (GAPDH) was used as the housekeeping gene.

2.2.7 Western Blot

Normal BMP2, BMP4, and BMP7 protein expression profiles were established for chick retina, RPE and choroid using Western blots and samples from untreated birds. The ocular tissues were collected and lysed at 4 °C with RIPA buffer (Sigma-Aldrich, St. Louis, MO), containing a protease inhibitor cocktail (Sigma-Aldrich, St. Louis, MO). Total protein concentration was measured using a BCA assay (Pierce Biotechnology, Rockford, IL). Protein samples were prepared in NuPAGE LDS sample buffer (Invitrogen), with or without DTT as a reducing agent, and heated at 95 °C for 5 minutes. Protein samples (20 μg) were then electrophoresed under non-reducing and reducing conditions on 4%-12% gradient gels (NuPAGE 4-12% Bis-Tris Gel, Invitrogen), before being transferred to nitrocellulose membranes (iBlot Gel Transfer Stacks, Invitrogen). Membranes were blocked (StartingBlock T20 [TBS]; Pierce Biotechnology), then incubated with anti-human BMP antibody (Abcam, San Francisco, CA, # ab6285 for BMP2, # ab93939 for BMP4, # ab93636 for BMP7), and finally labeled with HRP-conjugated secondary antibody (Pierce, Rockford, IL, # 31430 or Millipore, MA, # AP132P). Immunoreactive bands were detected with chemiluminescence (Supersignal Pico ECL; Pierce Biotechnology) and imaged with a bioimaging system (FluorChem Q, Alpha Innotech; San Leandro, CA).

The choice of antibody was based on results of database searches; mature human BMP2 and chicken BMP2 have 96.5% identity and human and mouse BMP2 have 100% identity. For BMP4, there is 95.7% similarity between chick and mouse, and chick and human sequences. For BMP7, the equivalent figures are 99.3% and 98.6% respectively. Protein sequence alignment for human, mouse, and chick BMP2, BMP4, and BMP7 are shown in Figure 2-1.

The specificity of the BMP2 primary antibody was verified using commercial BMP2 protein (Abcam, # ab87065). Mouse brain lysates were used as positive controls. As a negative control the commercial BMP2 protein was also used as a pre-absorbed blocking peptide for the BMP2 antibody. Commercial mature BMP4 protein (# ab87063, Abcam) and mouse brain lysates were used as positive controls for testing the BMP4 antibody, while human kidney lysates (# ab30203, Abcam) and mouse brain lysates were used as positive controls for BMP7 antibody. Assays involved three independent biological samples and triplicate repeats.

Figure 2-1. Protein sequence alignment for human, mouse, chick BMP2 (A), BMP4 (B), & BMP7 (C).

2.2.8 Immunohistochemistry

Posterior eyecups were prepared from enucleated eyes, immersed in OCT (Ted Pella Inc., Redding, CA) and stored at -80 °C immediately for later use. Seven-micron cryostat sections were dried at room temperature, fixed with acetone, washed with PBS, and then blocked with 10% normal goat serum in PBS containing 2% bovine serum albumin (BSA). Immunostaining used the BMP2, BMP4, and BMP7 primary antibodies, as described in previous section covering Western blots, and fluorescence-conjugated secondary antibodies. Isotype control (Invitrogen) was also included. Sections were labeled and then mounted on glass slides with medium containing the nuclear stain, DAPI (Vector Labs, Burlingame, CA), and photodocumented with a Zeiss Axioplan 2 microscope (Carl Zeiss, Inc., Germany).

2.2.9 Statistical Analysis

Data were expressed as mean ± SEM. Paired Student's *t*-tests were used to compare lens-treated eyes with their fellow (contralateral) control eyes; one-way ANOVAs combined with post-hoc analysis (Fisher's Least Significant Difference) were used for comparisons involving more than 2 groups. In analyzing gene expression data, comparisons were made both between the two eyes of treated birds, as a measure of the primary treatment effects, and also between the fellow eyes of treated birds and eyes of untreated birds, to look for effects on the fellow untreated eyes that would imply interocular yoking influences.

2.3 Results

2.3.1 RNA Yield & Quality

Mean RNA concentrations and A_{260}/A_{280} optical density ratios for retina, RPE and choroid are shown in Table 2-3. Retinal samples had highest RNA yield (16.9 ± 0.8 µg/eye), followed by choroidal samples (8.7 ± 1.1 µg/eye), with RPE samples giving the lowest yield (1.9 ± 0.1 µg/eye). A_{260}/A_{280} ratios for all three tissues were about 2.0. Gel electrophoresis confirmed the integrity of RNA in the samples (Fig. 2-2).

Table 2-3. RNA concentration, A_{260}/A_{280} ratio, and total yield per eye for retina, RPE, and choroid samples

	RNA conc. (ng/ul)	A_{260}/A_{280}	Total yield (ng)/eye
Retina	338.8 ± 17.0	2.0 ± 0.003	16942 ± 848
RPE	38.7 ± 1.79	2.0 ± 0.009	1935 ± 90
Choroid	173.1 ± 22.7	2.0 ± 0.008	8655 ± 1135

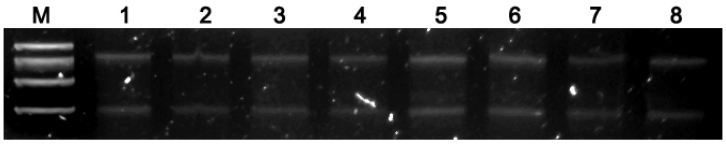

Figure 2-2. Results of electrophoresis using a 1.2% agarose gel and EB staining for 8 RPE RNA samples checked for RNA integrity. Lane M, marker; samples in lanes 1-8.

2.3.2 mRNA Expression of BMPs and BMP Receptors in Normal Chicks

BMP2, BMP4, BMP7 and all three BMP receptor subtypes examined - BMPR1A, BMPR1B and BMPR2, were expressed in all three tissue types examined - retina, RPE, and choroid (Fig. 2-3). The expression levels of each gene relative to housekeeping gene GAPDH are summarized in Table 2-4. In relative terms, BMP2, -4, and -7 appeared more highly expressed in RPE compared to retina and choroid. Of the BMP receptors, BMPR2 and BMPR1A showed much higher expression than BMPR1B across all 3 tissues. Note that differences in baseline expression of GAPDH between these ocular tissues were also

evident when Ct values were normalized against total RNA amount. The ratio of GAPDH expression – retina:RPE:choroid was 15:3:1.

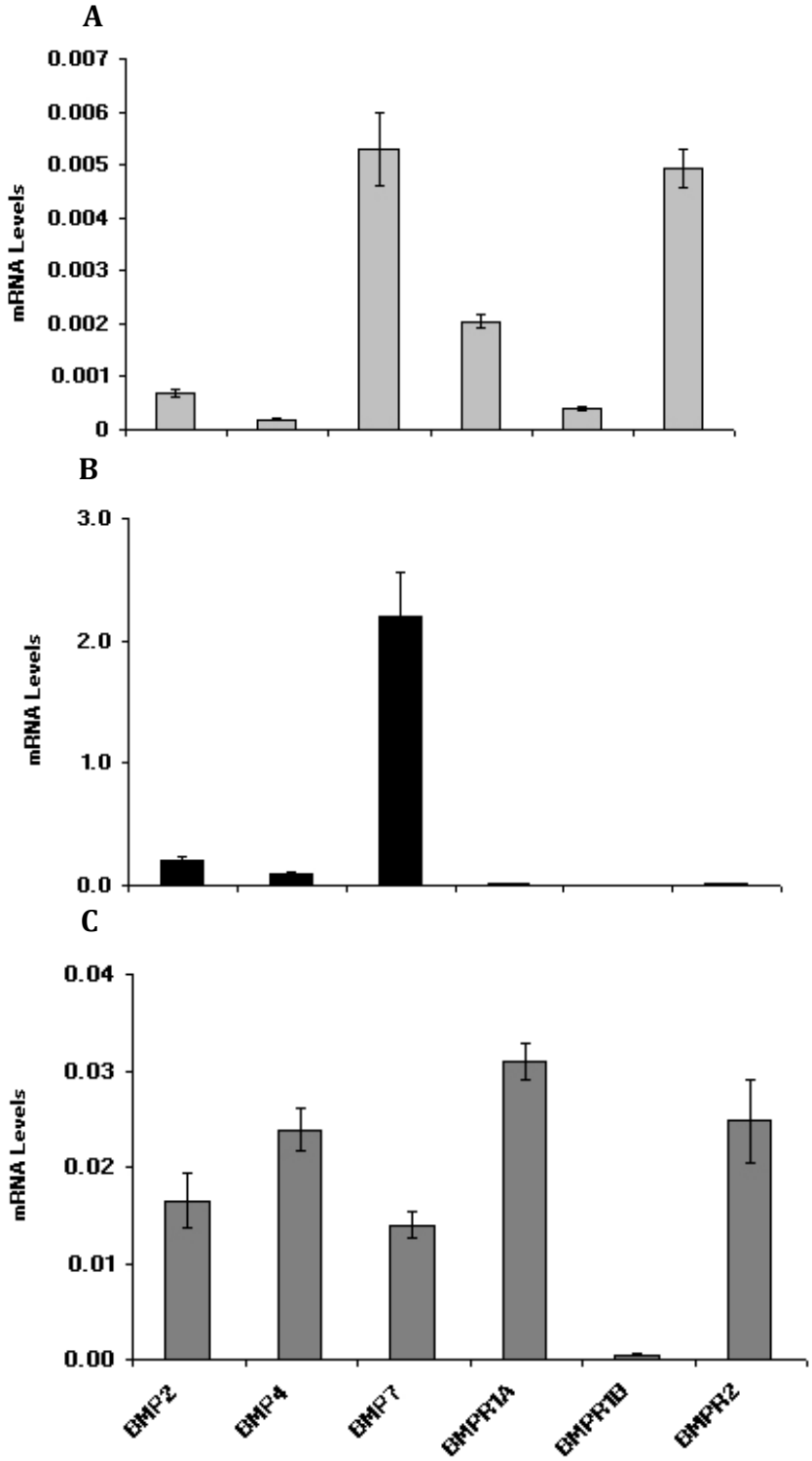

Figure 2-3. mRNA expression of BMP2, BMP4, BMP7, and BMP type I and II receptors (BMPR1A, BMPR1B, BMPR2) in normal (untreated) chick retina (A), RPE (B), and choroid (C). GAPDH used as the housekeeping gene. Data are expressed as mean MNE ± SEM.

Table 2-4. mRNA levels for BMPs and BMP receptors.

	BMP2	BMP4	BMP7	BMPR1A	BMPR1B	BMPR2
Retina	0.0007 ± 0.00008 (n = 20)	0.0002 ± 0.00002 (n = 20)	0.005 ± 0.0007 (n = 12)	0.002 ± 0.0001 (n = 14)	0.0004 ± 0.00003 (n = 12)	0.005 ± 0.0004 (n = 12)
RPE	0.21 ± 0.02 (n = 48)	0.10 ± 0.01 (n = 38)	2.20 ± 0.37 (n = 32)	0.013 ± 0.002 (n = 18)	0.0002 ± 0.00003 (n = 20)	0.019 ± 0.003 (n = 26)
Choroid	0.017 ± 0.003 (n = 16)	0.024 ± 0.002 (n = 16)	0.014 ± 0.001 (n = 8)	0.0309 ± 0.002 (n = 16)	0.0005 ± 0.00009 (n = 16)	0.025 ± 0.004 (n = 8)

2.3.3 Protein Expression of BMP2 in Normal Chicks

Western blots indicated the presence of BMP2 protein in chick retina, RPE and choroid (Fig. 2-4). To understand the complex banding patterns observed under both non-reducing and reducing conditions, it is important to note that both mature and proprotein of BMP2 have been reported for the chick (http://www.uniprot.org/uniprot/Q90751), as well as other animals.[236, 250] The mature protein has 114 amino acids (aa; 13 kDa), while the proprotein is much larger (353 aa, 40.3 kDa), with some glycosylation sites at which further protein modification may occur.[251, 252] The presence of the amino acid, cysteine, also allows dimers to form from monomers via disulfide bonds (Fig. 2-5).[250, 253, 254] In describing our results, we have made tentative assignments to observed bands, based on this background knowledge. Under non-reducing conditions (Fig. 2-4A), the retinal sample (lane 2) showed 4 strong bands corresponding to the dimer of the proprotein (~ 80 kDa), a modified (glycosylated) monomer of the proprotein (~ 50 kDa), a monomer of the proprotein (~40 kDa), and a dimer of the mature protein (~ 28 kDa). The dimer of the mature BMP2 (~ 28 kDa) was not detected in either RPE (lane 3) or choroid (lane 4). Interestingly, in lane 4 (choroid), there was an additional weak band at ~39 kDa, which may represent either a trimer of the mature protein or other forms of BMP2.[255] In lane 5, to which BMP2 protein (0.02 μg) was added as a control, a band at ~13 kDa was detected. Compared to the non-reducing conditions, the reducing conditions (Fig. 2-4B), generated stronger bands and in some cases, additional bands (e.g. lane 4, choroid), presumably reflecting improved binding of the antibody, although the results for the two conditions were generally similar. In both cases, no mature protein of BMP2 was detected in RPE. No obvious bands were visible in the negative control test, for which the BMP2 primary antibody was first neutralized, implying very low nonspecific binding. The masses for human, mouse, and chick proprotein and mature protein of BMP2 are presented in Table 2-5.

2.3.4 Protein Expression of BMP4 in Normal Chicks

BMP4 protein was detected in Western blots prepared under reducing conditions from chick retina, RPE and choroid samples (Fig. 2-6). Lanes 1 and 2 were loaded with positive controls, while lanes 3 - 6 were loaded with chick tissue samples. To understand the complicated patterns of BMP4 protein expression, it is important to note that monomers

and dimers of the BMP4 proproteins and mature proteins, as well as other forms have been reported in published literature, and databases (in the public domain at http://www.uniprot.org/uniprot/Q90752).[255-258] Masses for different forms of BMP4 protein are also presented in Table 2-5.

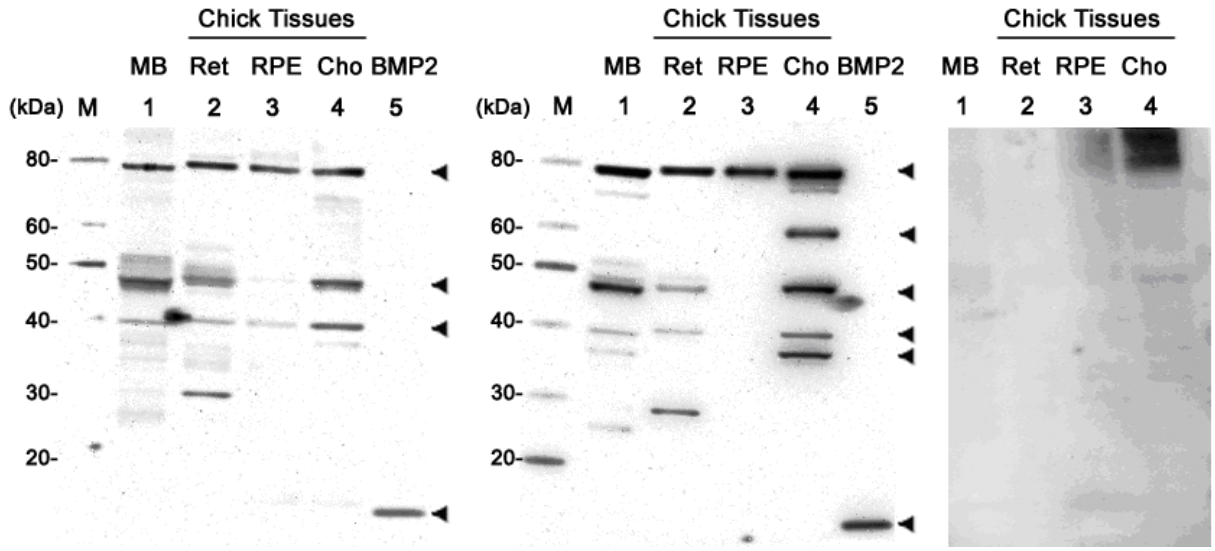

Figure 2-4. Western blots showing protein expression of BMP2 for both non-reducing (A) and reducing (B) conditions. In both cases, lane M was loaded with marker, lane 1 with mouse brain lysates (positive control), and lanes 2, 3, and 4, with chick retina, RPE and choroid respectively, lane 5 with commercial BMP2 protein. Differences in BMP2 expression, both between tissues and between conditions, were evident, with the choroid showing the highest expression and multiple forms. Molecular weights of main mature and proprotein of BMP2 are 13.0 and 40.3 kDa respectively. Negative control using BMP2 peptide preabsorbed primary antibody was included (C). Primary antibody concentration 1:500. MB, mouse brain; CB, chick brain; Ret, retina; Cho, choroid.

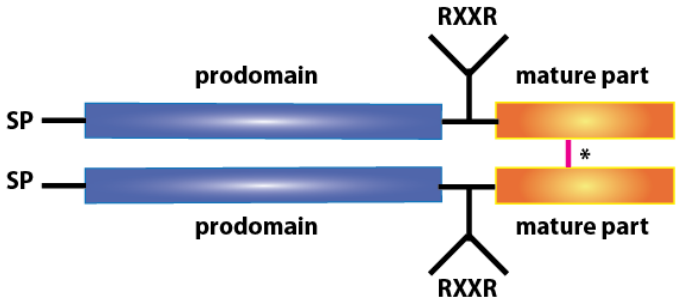

Figure 2-5. Diagram of BMP proprotein and mature protein. BMPs are synthesized as dimeric proproteins including an N-terminal signal peptide (SP), a large prodomain and a C-terminal mature component with a characteristic cystine-knot motif. Proteolytic processing by furin proteases occurs at the RXXR motif. There is also an intermolecular disulfide bond linking the mature components of the dimer (see asterisk).

Table 2-5. Masses corresponding to different forms of BMP2, BMP4 and BMP7 for different species.

	Human		Mouse		Chick	
	Proprotein	Mature	Proprotein	Mature	Proprotein	Mature
BMP2	44.7 (396 aa)	12.9 (114 aa)	44.5 (394 aa)	12.9 (114 aa)	40.3 (353 aa)	13.0 (114 aa)
BMP4	46.6 (408 aa)	13.1 (116 aa)	46.5 (408 aa)	13.2 (116 aa)	46.5 (405 aa)	12.8 (114 aa)
BMP7	49.3 (431 aa)	15.7 (139 aa)	49.2 (430 aa)	15.6 (139 aa)	49.5 (435 aa)	15.7 (139 aa)

For BMP4, the retina (lane 4, Fig. 2-6) produced the most complex banding pattern. Two bands correspond to the dimer and monomer of the proprotein (~ 90 and ~ 46 kDa, respectively), and another band at ~ 35 kDa represents the dimer of mature protein. There also are two additional bands at ~ 60 and ~ 70 kDa, possibly representing the glycosylated proprotein. The choroid (lane 6) yielded only 2 bands, corresponding to the dimer of the proprotein (~ 90 kDa) and the monomer of mature BMP4 (~ 13 kDa, as in lane 1, which was loaded with commercial BMP4 protein, and shows single band at ~ 13 kDa). The RPE (lane 5) yielded the simplest pattern, with only one band, at ~ 40 kDa, which may represent a nuclear variant of BMP4 or mature BMP4, based on its molecular weight.[255, 257, 259] The pattern of BMP4 expression showed variability both between individual chicks and between the 3 ocular tissues analyzed, with one bird showing negligible choroidal expression of BMP4. Samples prepared from mouse and chick brain show similar, albeit complex patterns. No obvious bands were detected in the negative control (data not shown).

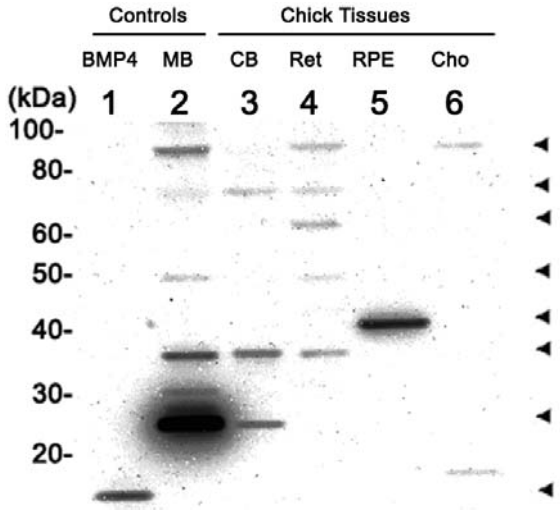

Figure 2-6. Western blots showing protein expression profiles for BMP4 in retina, RPE, and choroid from adolescent chicks, prepared under reducing conditions. Lane M was loaded with protein marker. Lane 1 was loaded with denatured, reduced BMP4 protein (0.02 μg), lanes 2 and 3 with mouse brain and chick brain respectively, and lanes 4 to 6 with chick retina, RPE, and choroid, respectively. MB, mouse brain; CB, chick brain; Ret, retina; Cho, choroid.

2.3.5 Protein Expression of BMP7 in Normal Ocular Tissues

In chick retina, RPE and choroid samples, BMP7 protein was detected in Western blots prepared under reducing conditions (Fig. 2-7). Lane 1 and 2 were loaded with positive controls, while lanes 3 - 6 were loaded with chick tissue samples. Database (in the public domain at http://www.uniprot.org/uniprot/F1NUT2) and literature searches[260] showed the proprotein and mature protein information for chick BMP7. Masses corresponding to the different forms of BMP7 in different species are listed in Table 2-5.

The BMP7 protein was detected in chick retina, RPE and choroid under reducing conditions (Fig. 2-7). The retina (lane 4), RPE (lane 5), and choroid (lane 6) all showed bands at ~ 30 kDa, corresponding to the dimer of the mature protein. The RPE (lane 5) yielded an additional weak band at ~ 49 kDa, which represents the proprotein. The choroid (lane 6) showed another weak band at 15 kDa, corresponding to the monomer of mature BMP7. Human kidney lysates (lane 1), which served as a positive control, yielded a single band at ~ 50 kDa. Mouse and chick brain samples showed similar patterns (lane 2 and 3); in each case, there are two visible bands at ~ 30 and 15 kDa, corresponding to the dimer and monomer of mature BMP7, respectively. No obvious bands were detected in the negative control (data not shown).

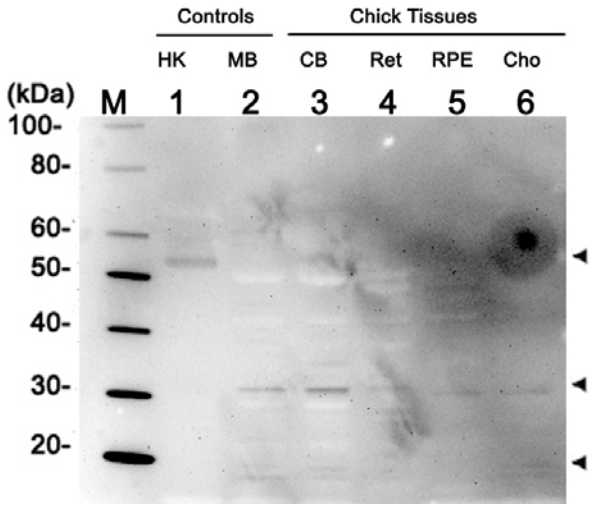

Figure 2-7. Western blots showing protein expression profiles for BMP7 in chick retina, RPE, and choroid. Lane M was loaded with protein marker. Lane 1 was loaded with human kidney lysates, and lanes 2 and 3 were loaded with mouse and chick brain, respectively. Lanes 4 to 6 were loaded with chick retina, RPE, and choroid, respectively. MB, mouse brain; CB, chick brain; Ret, retina; Cho, choroid. HK, human kidney lysates.

2.3.6 Protein Localization of BMP2, BMP4, and BMP7 in Normal Chicks

BMP2, BMP4, and BMP7 labeling were observed in all layers making up the wall of the posterior eyecup, with similar localization patterns (Fig. 2-8, 2-9, 2-10). In the retina, there is intense BMP labeling in regions corresponding to the inner plexiform layer (IPL), outer plexiform layer (OPL), and photoreceptor outer segments. In the ganglion cell layer (GCL), the inner nuclear layer (INL), and the outer nuclear layer (ONL), BMP staining seems to be distributed throughout the cytoplasm of cells, while in the RPE, labeling appears limited to the basal (choroid) side of RPE, although this may represent an artifact of the heavy pigmentation elsewhere in this layer. The choroid shows diffuse labeling while the sclera shows more variable staining; there is intense labeling at the choroid-sclera boundary and throughout the outer fibrous component, but more localized labeling in the inner cartilaginous layer, confined to the chondrocytes. The negative control, which was prepared by incubating sections in both mouse isotype IgG and secondary antibody, shows only very low background labeling for all three BMPs (Fig. 2-8 E, 2-9 E, 2-10 D). These immunostaining data are consistent with the above Western blot results, which detected the BMP2, BMP4, and BMP7 proteins in retina, RPE and choroid.

2.3.7 Ocular Dimensional Changes after Lens Treatment

With the +10 D lenses, VCD was significantly decreased in treated eyes relative to their fellows after only 2 h of wear ($p < 0.001$, n = 6. Fig. 2-11A). The longer exposure period of 48 h yielded a similar response pattern although the change in VCD was significantly larger than that recorded with the shorter, 2 h period of lens wear and CT was now significantly increased ($p < 0.001$ in both cases, n = 6). Although this lens treatment is expected to slow axial elongation, no statistically significant interocular differences in AL were seen over the short treatment durations used in this study.

The -10 D lens treatment also induced changes in ocular dimensions (Fig. 2-11B), although they reached statistical significance only after the longer, 48 h period of lens wear. At this time, lens-treated eyes had longer VCDs and ALs and thinner choroids compared to their fellows, with interocular differences reaching statistical significance in all 3 cases ($p < 0.001$, n = 18). The interocular VCD and AL difference data for 2 (n = 11) and 48 h were also significantly different from each other ($p < 0.001$).

The two eyes of normal, untreated birds typically had similar dimensions and thus as expected, no significant interocular differences in VCD, CT, and AL were observed (data not shown, n =12). Chicks used for the collection of ocular biometry data were not used in gene expression experiments, to avoid potentially confounding effects from the measurement procedure, which included brief exposure to isoflurane and unobstructed vision.

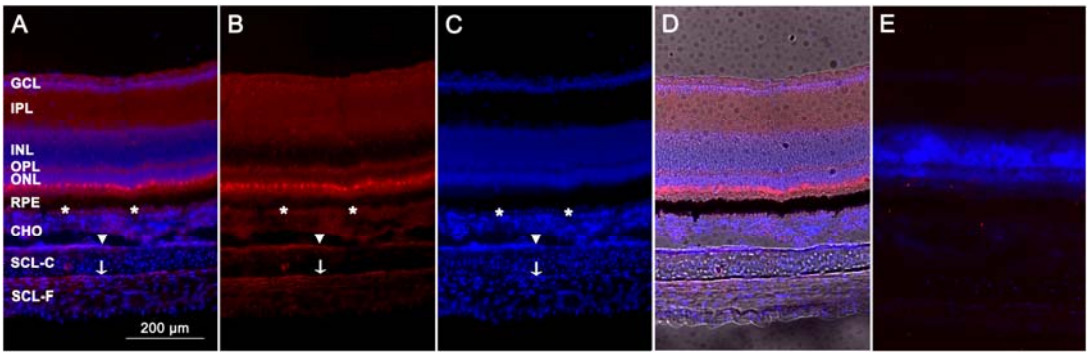

Figure 2-8. Representative sections from the posterior wall of the eyecup labeled for BMP2 (in red), with nuclei stained with DAPI (in blue) (A), labeled for BMP2 alone (B), or stained with DAPI alone (C); double-labeled section overlaid on image of unstained section (D); negative isotype control imaged in blue and red channels (E). GCL, ganglion cell layer; IPL, inner plexiform layer; INL, inner nuclear layer; OPL, outer plexiform layer; ONL, outer nuclear layer; RPE, retinal pigment epithelium; CHO, choroid; SCL-C, sclera cartilaginous layer; SCL-F, sclera fibrous layer. * Basal side of RPE, ▼ Inner boundary between choroid and sclera, ↓ Border between cartilaginous and fibrous layers of sclera. Scale bar, 200 µm.

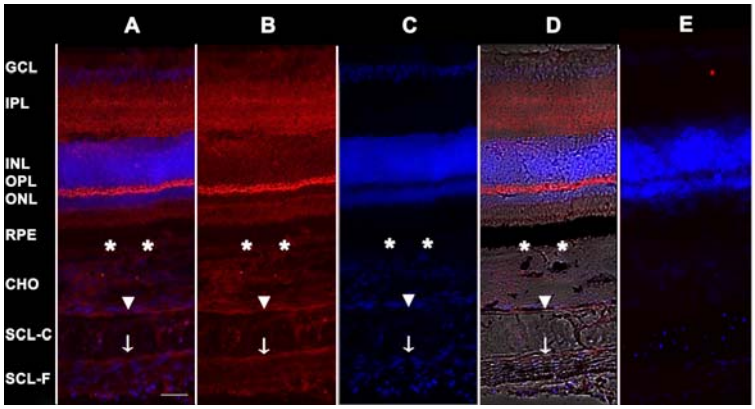

Figure 2-9. Representative sections from the posterior wall of the eyecup labeled for BMP4 (in red), with nuclei stained with DAPI (in blue) (A), labeled for BMP4 alone (B), or stained with DAPI alone (C); double-labeled section overlaid on image of unstained section (D). Negative control imaged in blue and red channels (E). GCL, ganglion cell layer; IPL, inner plexiform layer; INL, inner nuclear layer; OPL, outer plexiform layer; ONL, outer nuclear layer; RPE, retinal pigment epithelium; CHO, choroid; SCL-C, sclera cartilaginous layer; SCL-F, sclera fibrous layer. * Basal side of RPE, ▼ Inner boundary between choroid and sclera, ↓ Border between cartilaginous and fibrous layers of sclera. Scale bar, 50 µM.

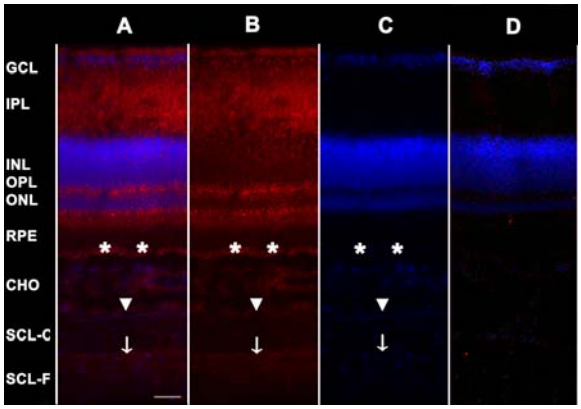

Figure 2-10. Representative sections from the posterior wall of the eyecup labeled for BMP7 (in red), with nuclei stained with DAPI (in blue) (A), labeled for BMP7 alone (B), or stained with DAPI alone (C). Negative control for BMP7 (D) was imaged in blue and red channels. Scale bar, 50 µM.

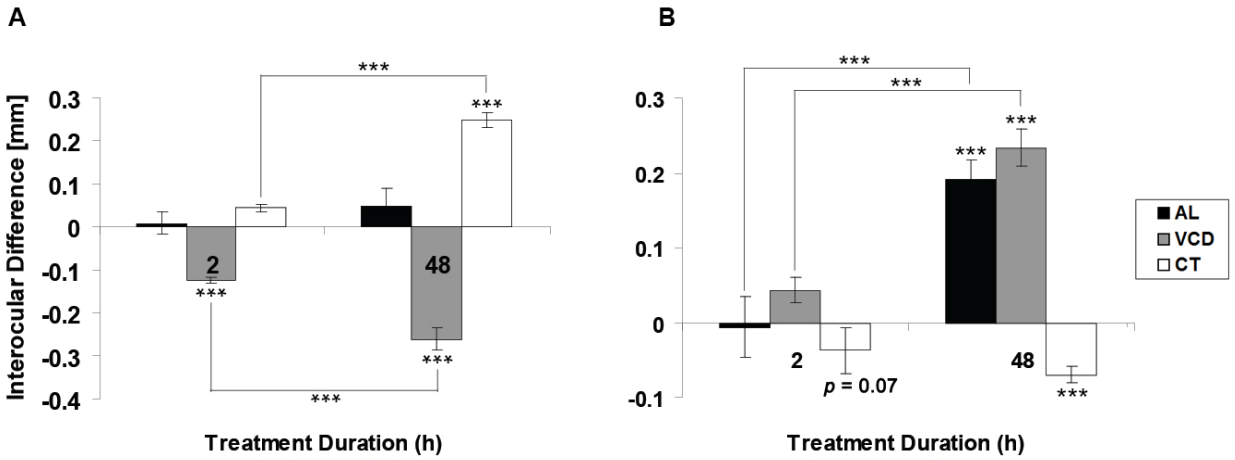

Figure 2-11. Effects of +10 D (A) and -10 D (B) lens treatments on axial length (AL), vitreous chamber depth (VCD), and choroidal thickness (CT) following 2 h (n= 6, 11 resp.) and 48 h (n=6, 18 resp.) of lens wear, shown as interocular differences (treated-control eyes) (mean ± SEM). Shown also are treatment-induced statistically significant changes from baseline (* on top of bars) and significant differences between 2 and 48 h treatment effects (* & connecting lines). *** $p < 0.001$.

2.3.8 Defocus-Induced Gene Expression Changes of BMP2, BMP4, and BMP7 in RPE

The +10 D lens treatment induced an up-regulation of BMP2 in the RPE, with the largest increase being recorded after only 2 h (Fig. 2-12A). Expression of BMP2 was increased by 7.2- and 4.1-fold in treated eyes compared to their fellow (control) eyes, with 2 and 48 h of treatment respectively ($p < 0.001$, n = 14 for both cases). The opposite trend was observed with the -10 D lens treatment, which induced a down-regulation of BMP2, and here also, the change recorded with the 2 h treatment was larger (Fig. 2-12B). Expression of BMP2 was decreased by 13.3- and 3.7-fold in treated eyes compared to their fellow eyes, with 2 and 48 h of treatment respectively ($p < 0.001$, n = 16; $p < 0.01$, n = 14). No significant interocular difference in BMP2 gene expression was observed in RPE from eyes of age-matched untreated birds (data not shown).

Both the +10 and -10 D lens treatments altered BMP4 gene expression, with the direction of change being again defocus sign-dependent and consistent in direction for both treatment durations (Figs. 2-13), and with the patterns described for BMP2. Specifically, with the +10 D lenses, BMP4 gene expression was up-regulated by similar amounts after both 2 and 48 h of treatment, by 3.6- and 4.4-fold, respectively ($p < 0.01$, n = 18 in both cases; Fig. 2-13A). With the -10 D lenses, BMP4 gene expression was down-regulated, albeit slightly more with the shorter 2 h than the longer 48 h treatment period, by 3.8- and 1.4-fold, respectively ($p < 0.001$; $p < 0.01$, n = 19 for both cases; Fig. 2-13B). No significant interocular difference in BMP4 gene expression was observed in RPE from eyes of age-matched untreated birds (data not shown).

While BMP7 also showed bidirectional changes in gene expression in response to optical defocus, the patterns differed in their temporal profiles from those described for BMP2 and BMP4. Specifically, the +10 D lens induced 2.9-fold up-regulation of BMP7 only after 48 h of treatment ($p < 0.05$, n = 18. Fig. 2-14A); a shorter 2 h exposure to this lens did not affect

gene expression ($p > 0.05$, n = 18). In contrast, gene expression of BMP7 was down-regulated with both 2 and 48 h of -10 D lens treatment, by 1.37- and 1.38-fold respectively ($p < 0.01$, n = 20; $p < 0.01$, n = 17; Fig. 2-14B). As expected, RPE from eyes of untreated age-matched birds showed no significant interocular differences in expression (right & left eyes compared; data not shown).

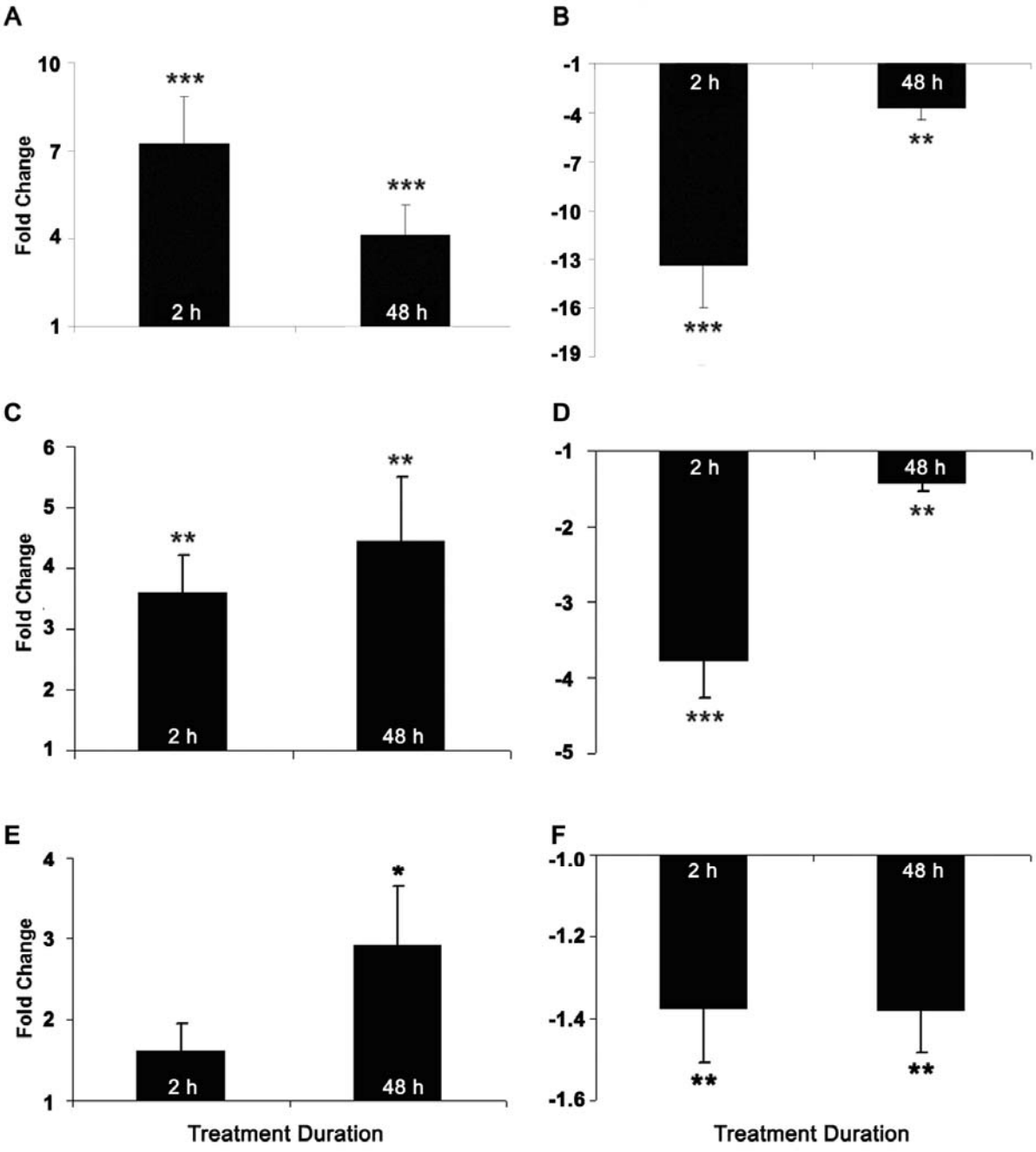

Figure 2-12. Differential expression of BMP2, BMP4, and BMP7 mRNA in RPE after 2 and 48 h of imposed defocus (+10 D, A, C, E; -10 D, B, D, F). Comparison between treated and fellow control eyes; data are expressed as mean ± SEM. GAPDH was used as the housekeeping gene. ** $p < 0.01$, *** $p < 0.001$.

2.3.9 Yoking Effects of Lens Treatments on BMP Gene Expression in RPE

For all three BMPs, gene expression in RPE from the contralateral fellow eyes of lens-treated birds from eyes of untreated birds were compared to look for indirect evidence of interocular yoking effects, which cannot be detected by the within-bird interocular comparisons reported above. With the longer 48 h, -10 D lens treatment, both BMP4 and BMP7 expression levels in RPE from the fellows of the lens-treated eyes showed significant down-regulation relative to values for RPE of eyes of untreated chicks ($p < 0.01$ for BMP4 and BMP7, Fig. 2-13D, F). For BMP2, gene expression levels in both treated eyes and their fellows appeared reduced relative to levels in the eyes of untreated birds, hinting at yoking; however, the difference between fellow and untreated eyes did not reach statistical significance ($p = 0.077$, Fig. 2-13B). No equivalent trends were apparent with the +10 D lens treatment (Fig. 2-13A, C, E).

2.3.10 Gene Expression Changes of BMP Receptors in RPE after Lens Treatments

None of the three genes - BMPR1A, BMPR1B, BMPR2 - showed differences in expression between treated eyes and their fellows, for either of the lens treatments, irrespective of their duration (Fig. 2-14A). However, when gene expression (MNEs) in the eyes of lens-treated birds was compared with equivalent data for untreated birds, BMPR2 was found to be significantly down-regulated in both treated and fellow eyes with -10 D lens treatment, for both the 2 and 48 h treatment durations, implying yoked down-regulation of this receptor ($p < 0.01$, Fig. 2-14B).

2.3.11 Validation of Using GAPDH as a Housekeeping Gene

The stability of GAPDH expression across different treatment conditions was assessed by comparing the expression of GAPDH / total RNA (μg) in RPE from untreated, treated, and fellow eyes. Its expression was not significantly affected by the lens treatment conditions (Fig. 2-15).

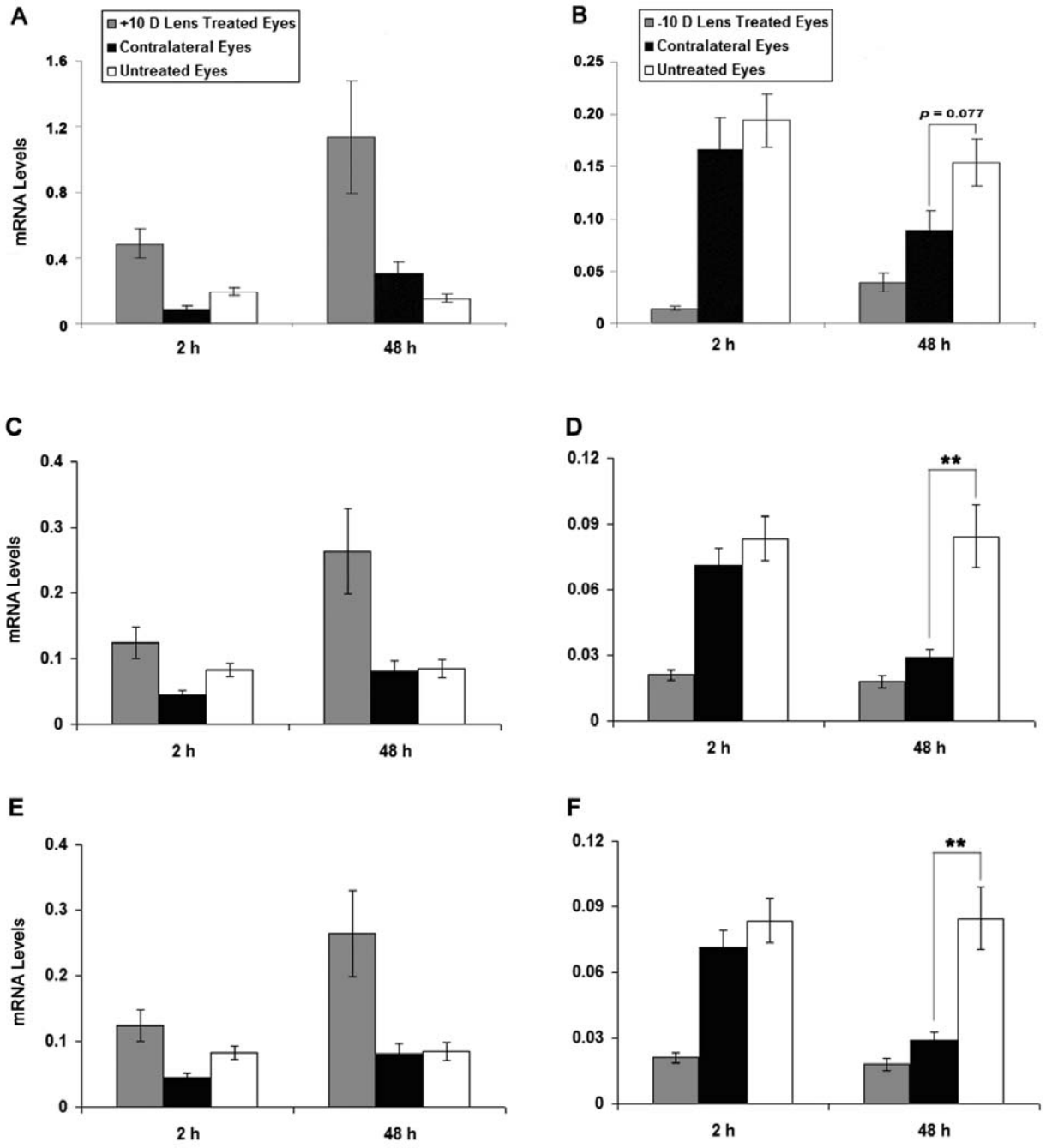

Figure 2-13. BMP2, BMP4, and BMP7 mRNA levels in RPE after +10 D (A, C, E) and -10 D (B, D, F) lens treatments applied for 2 or 48 h. The fellows to eyes wearing -10 D lenses showed similar, albeit smaller down-regulation of BMP gene expression after 48 h of treatment compared to untreated eyes (only differences for BMP4 and BMP7 reached statistical significance, ** $p < 0.01$; BMP2, $p = 0.077$). No such yoking is evident in the +10 D lens data. Data are expressed as mean ± SEM. GAPDH was housekeeping gene.

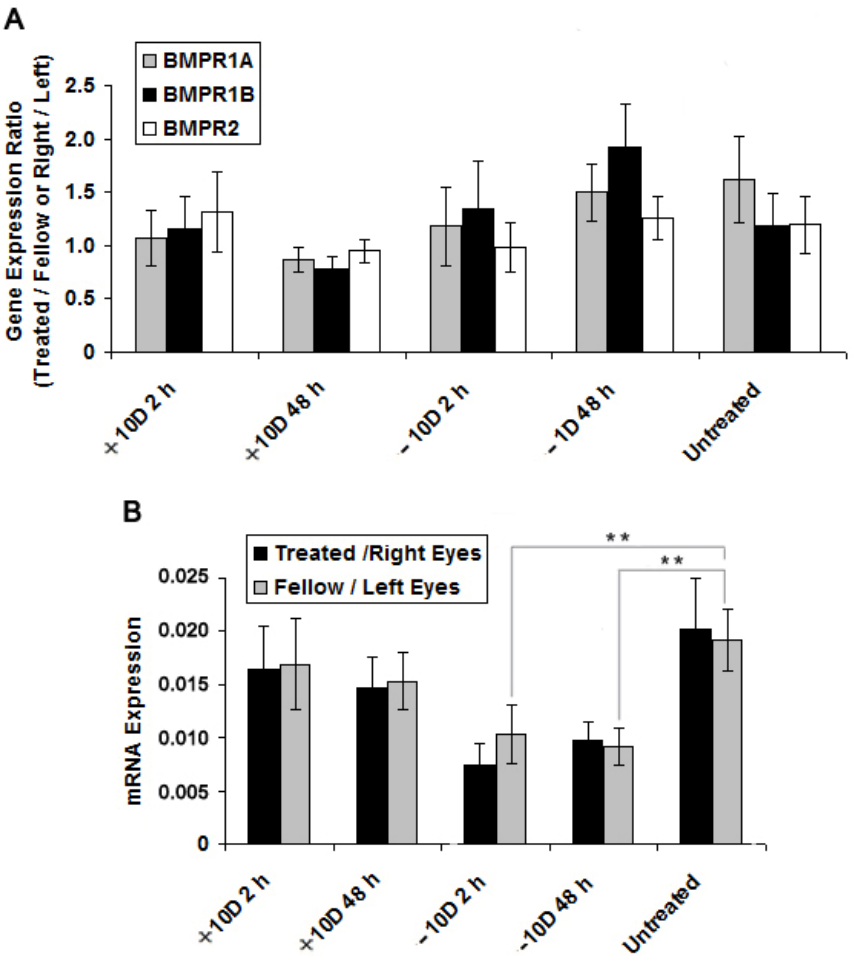

Figure 2-14. BMP receptor mRNA expression in RPE after +10 and -10 D lens treatments and in eyes of untreated birds. No differences in gene expression between lens-treated and fellow eyes, or between right and left eyes of untreated birds were observed (A, $p > 0.05$). mRNA expression of BMPR2 was significantly down-regulated in both treated and fellow eyes compared to untreated eyes after -10 D lens treatment for 2 and 48 h ($p < 0.01$, **).

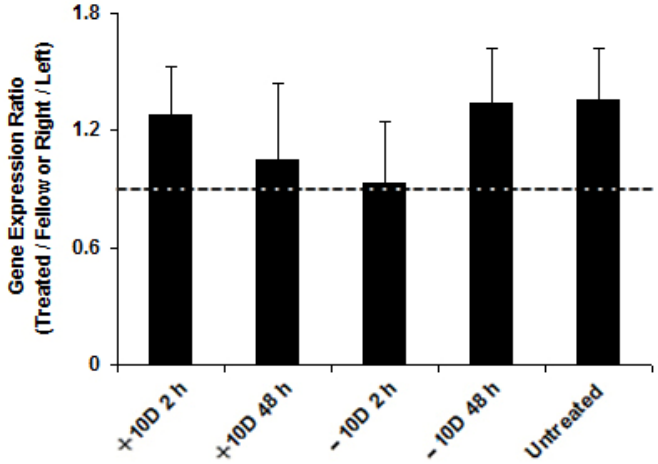

Figure 2-15. Expression of GAPDH in RPE, normalized to total RNA (µg); data plotted as the ratio of expression levels in treated and fellow eyes for treated birds, and for untreated birds, the ratio of levels in right and left eyes. Dotted line indicates a ratio of 1.0, representing no difference.

2.4 Discussion

In the present study, we demonstrated in normal chickens the gene and protein expression of BMP2, BMP4, and BMP7 as well as the gene expression of three different subtypes of BMP receptors in three posterior ocular tissues – retina, RPE and choroid, and for the first time, the optical defocus-sign-dependent, bidirectional regulation of BMP2, BMP4, and BMP7 gene expression in chick RPE. The latter results are consistent with, although not definitive evidence for a role of these three BMPs in defocus-induced modulation of eye growth.

The initial discovery that BMPs could induce ectopic bone and cartilage formation underlies the name of this family of growth factors.[261, 262] However, they are better described as multifunctional regulators, with influences on cell proliferation, differentiation, apoptosis and extracellular matrix accumulation, as well as on the development of many organs.[235, 236, 238, 239, 263-265] BMP2, BMP4, and BMP7 are three of the most widely studied growth factors in the BMP family. While several studies have focused on the roles of BMPs in embryonic eye development, investigations into their roles in postnatal ocular development and function in adult eyes are very limited.[133, 143, 242, 243, 247, 263, 266] In early embryonic chick eyes (E3 eyes at Hamburger and Hamilton stages 15–18), BMP2 mRNA was not detected in the eye. However, BMP2 expression was detectable throughout most of the retina with stronger expression in dorsal regions in E8 retina. The dorso-ventral asymmetry expression of BMP2 maintained to the late developmental stage (E18).[241] BMP4 mRNA expression was found to be initially restricted to the dorsal retina, with the expression pattern becoming less regionally localized and also weaker in later embryonic development. More mature retinas also express BMP4 although dorso-ventral asymmetries in expression are no longer apparent.[241] Apart from studies in chicks, ocular studies of BMP4 expression are very limited in number. In the human embryonic eye, BMP4 expression has been observed in the optic vesicle, developing optic cup and developing lens.[249, 263] Scleral expression of BMP4 has also been described for both guinea pig and adult human eyes.[208, 267] In the adult mouse, all cells in the retina were shown by *in situ* hybridization to express BMP4 and the RPE, to highly expressed it.[243] The distribution of BMP7 in early embryonic chick eyes was strong in the ventral RPE, and later on throughout the retina, with strong expression in the dorsal region. In the early embryonic stage, BMP7 had a more laminar distribution, initially confined to the presumptive INL (pINL), pGCL, pONL, and restricted to the INL and GCL at a more mature stage.[241] BMP7 has also been reported to enhance chick photoreceptor outer segment development *in vitro*.[268] In another study, BMP7 protein expression was observed in all humans retinal layers, and a similarly diffuse pattern of BMP7 expression was observed in rat retina.[269] Overall, the observations for the retina of other species are similar to the results reported here for the chick retina.

The current study represents the most comprehensive study to-date of BMP2, BMP4, BMP7 and BMP receptor gene and protein expression in the posterior ocular tissues of adolescent chickens, complementing and expanding on an earlier investigation of retina/RPE BMP2 expression in 7 day-old chicken.[133] While the expression of three BMPs was found to be

only low in the retina, they were all highly expressed in the RPE, consistent with RPE being a major ocular source of this growth factor. Furthermore, the gene expression profiles for the BMP receptors suggest that they act at multiple sites within the posterior layers of the eye, with potentially multiple functions. Specifically, we were able to confirm the presence in all three ocular tissues of the receptors involved in downstream signaling of BMPs, i.e., the heterodimerized type I (either BMPR1A or BMPR1B) and type II (BMPR2).[235] Although there were receptor-related differences in gene expression patterns, nonetheless the implied broad ocular distribution of these receptors is compatible with both paracrine and autocrine signaling.

Because BMPs exist in multiple forms, including dimers and monomers of proprotein and mature protein, and further, that gene expression levels do not reliably predict translation into protein, we also examined for these three BMPs, both their protein expression and their localization in posterior ocular tissues. The Western blots detected various forms of BMPs in all three tissues - retina, RPE and choroid, and also showed tissue-related differences in protein expression profiles. Of note was the detection of both the biologically active forms and proprotein of BMPs in RPE. Thus it seems likely that the RPE serves as a storage site for BMPs. Indeed, the high level of BMP gene expression in the RPE compared to the two neighboring tissues (retina & choroid), is consistent with it being a major source of BMPs for these tissues, which nonetheless also appear have the capacity to synthesize and secrete BMPs locally, based on our gene expression data. The immunohistochemistry data in our study lend further support for this interpretation; BMP labeling was found throughout the retina, choroid and adjacent sclera. These profiles are also consistent with secretion of BMPs by RPE as part of a paracrine signaling pathway, modulating as yet unknown ocular functions.

In the context of ocular growth regulation and myopia, the most significant findings from our study were the optical defocus, sign-dependent bidirectional changes in gene expression in chick RPE. Specifically, BMP2, BMP4, and BMP7 gene expression all showed significant up-regulation in response to imposed myopic defocus (+10 D lens treatment), while expression of these genes was down-regulated with imposed hyperopic defocus (-10 D lens treatment). These patterns of up- and down-regulation of BMP expression correspond to slowed and accelerated ocular elongation, respectively. In the case of all three BMPs (except for BMP7 with +10D treatment), changes in gene expression were seen soon after treatments were initiated (i.e., at 2 h). The rapid onset of the gene expression changes are compatible with roles for BMP2, BMP4 and BMP7 in initiating defocus-driven eye growth changes, and also tend to rule out the possibility that the changes were a byproduct of altered ocular growth, which would have been minimal at this time. With both lens treatments, the early changes in expression of these three BMPs persisted out to 48 h of treatment. That the same patterns of differential gene expression were still evident after 48 h of negative lens wear, when eyes were growing faster than normal, as evident from ultrasonography data, suggest a further role for BMP2, BMP4, and BMP7 in maintaining this altered growth pattern. These prolonged changes in gene expression tend to argue against them being simply responses to the altered visual (retinal defocus) conditions. Note that the apparent reduction in the magnitude of the change after 48 h compared to 2 h of treatment is at least partly a product of yoked changes in the fellow eye at the latter time

point (see Figure 2-13). However, the mechanisms underlying the regulation of BMP expression in RPE remain largely unknown and its role in postnatal eye growth regulation is yet to be directly demonstrated. While high basal level of BMP expression in the RPE, as observed, is not a necessary pre-requisite for bidirectional changes in expression, it could plausibly extend the range of response, although this point has not been emphasized in relevant previous gene expression studies.

Of the few other molecules known to be bidirectionally regulated in the eye by optical defocus, ZENK, an immediate early gene, has been shown to undergo optically modulated expression changes in retina.[51, 58, 117, 118, 120] For example, the number of ZENK-expressing glucagon amacrine cells was found to be increased with positive lenses, after as little as 30 minutes of wear, and decreased after 2 hours of negative lens wear in chicks. It remains to be determined whether or not these cells are part of a signal pathway mediating the observed changes in BMP expression in the RPE. It is possible that BMP expression is regulated by an independent, yet-to-be identified retinal cell population.

It is also noteworthy that retinoic acid (RA), which has been put forward as a potential eye growth regulator, has also been linked to the regulation of BMP expression in other studies.[270-273] The data tying RA with eye growth regulation in chicks also exhibit bidirectionality; retinal RA levels are increased in eyes wearing negative lenses and diffusers and levels are decreased in eyes wearing positive lenses, with the opposite trends being true for choroidal RA levels.[117-120] While RA could be acting up-stream from BMPs on the retinal and/or choroidal side of RPE - these possibilities are not distinguishable based on currently available data - a signal pathway linked to eye growth regulation would argue for an upstream retina-RA, RPE-BMP association. Nonetheless, retina, choroid and sclera are all plausible sites of action of BMPs, based on our immunohistochemistry and Western blot results.

Our results raise the possibility that BMPs are themselves negative growth modulators, acting on the choroid and/or sclera. Roles for BMP2 and BMP4 as growth inhibitors, as suggested by these gene expression profiles, are in line with the results of another study describing BMP2 and BMP4 as negative growth regulators.[243] In two separate studies involving cultured human scleral fibroblasts, BMP2 was shown to promote cell proliferation and differentiation and also alter the expression of key extracellular matrix (ECM) genes and proteins.[207, 208] The addition of exogenous BMP4 is reported to alter eye shape and reduce eye size in the mouse embryo.[266] There has been no equivalent study in chicks although intraocular injection of BMP4, given before treatment with a neuron toxin, is reported to suppress the proliferation of Müller glia and thus reduce retina damage in young chicks.[244] Assuming that differentially expressed BMP genes in RPE are translated into protein, and subsequently secreted into the choroid, these BMPs may affect changes in ocular dimensions through changes in ECM remodeling in either or both the choroid and sclera.[239, 274] Local tissue-specific manipulations of BMP levels may be required to dissect this apparently very complex signaling cascade (Figure 2-20).[255]

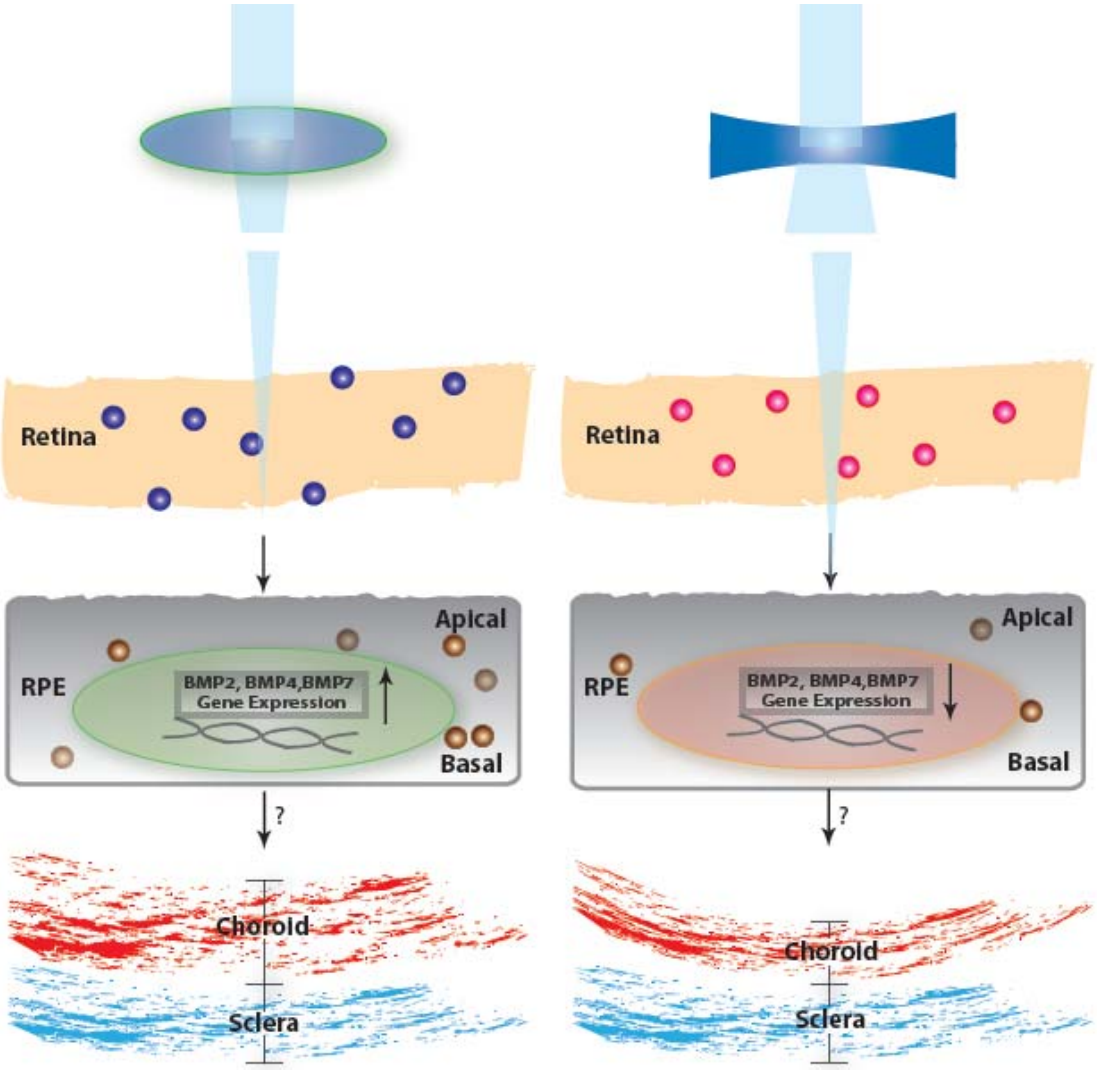

Figure 2-16. Cartoon summary diagram showing BMP gene expression changes in RPE with lens treatments.

While BMP2, BMP4 and BMP7 are closely related structurally, and all three BMPs activate the same subtypes of BMP receptors, studies of embryonic eye development in the chick describe spatially and temporally distinct expression patterns for these BMPs. [235, 239, 241, 270, 275, 276] Nonetheless, the latter observations are consistent with general behavior of these growth factors; their effects on developmental regulation, cell proliferation and differentiation can be similar or different, depending on the developmental stage and cell type.[208, 243, 277] The close similarity of the RPE gene expression profiles of BMP2, BMP4 and BMP7 for the optical defocus conditions imposed in our studies suggests that these three BMPs are co-regulated and/or may play similar roles in refractive error and eye growth regulation.

Interestingly, BMP2 gene expression was reported to be down-regulated in chick retina/RPE with form-deprivation myopia,[133] in the same direction as that induced by our

negative lens treatment, which also induces myopia. While there is accumulating evidence that the mechanisms underlying these two types of myopia are different,[104, 278] our results add to other data suggest that some components of the regulatory pathways are shared.[33, 51] As the effects on retinal image quality of these treatments are generally quite different and thus likely to elicit different retinal responses, we speculate that the RPE was the site of BMP2 gene expression changes in the previous form-deprivation study, with the RPE serving as a conduit or point of convergence of different retinal signal pathways.

In the current study, we found no evidence of defocus-dependent differential regulation of BMP receptor expression, although we did observe yoked down-regulation of BMPR2 in response to the negative lens treatment. The experimental myopia literature contains many examples of interocular yoking involving gene expression, as well as refractive error and ocular growth rate changes in response to lenses and drug treatments.[35, 51, 58, 197, 279-281] Further examples are provided by our findings for BMP4 and BMP7, that gene expression was significantly down-regulated in both -10 D lens-treated eyes and their fellows after 48 h of lens wear. A hint of similar yoking for BMP2 with -10 D lenses was also observed, although the effect was not statistically significant (p = 0.077). This interocular yoking phenomenon was not evident with either the shorter 2 h exposure for the -10 D lens treatment or with either the 2 or 48 h + 10 D lens treatments. While the mechanisms underlying such interocular yoking remain to be elucidated, there appear to be treatment- and gene-dependent differences that need to be accounted for. For example, for BMP2, BMP4 and BMP7, the yoking effects on RPE gene expression was limited to our negative lens treatment, while yoking of ZENK protein expression in retina has been reported with both positive and negative lens treatments, as well as with recovery from form-deprivation myopia.[51, 53] In a previous study, we found that sectioning of the optic nerve in chicks eliminated the inhibitory effect of monocular atropine on lens-induced myopia in fellow eyes.[282] While neural feedback loops may also be involved in these yoked gene expression changes, a humoral mechanism is also plausible.[51]

Although it is now generally accepted that both genetic and environmental factors are likely to contribute to the development of human myopia, there appears little overlap in the genes implicated in human myopia and those linked to eye growth regulation in animal models of myopia.[11] Our findings implicating BMP2 and BMP4 in eye growth regulation in the chick represents a departure from this trend and a potentially important break-through, with both BMP2 and BMP4 being recently put forward as candidate genes for human myopia.[249, 283] The recent meta-analyses of human genetic studies using genome-wide single-nucleotide polymorphism (SNP) identified BMP2 as a new locus for refractive error and myopia.[283] The latter study also reported a mutation in BMP4 in a range of subjects presenting with anophthalmia, microphthalmia, or myopia although a causal link is yet to be established. In terms of animal studies, also of potential relevance is the finding in zebrafish of severe myopia linked to a mutation of low density lipoprotein receptor-related protein 2 (*lrp2*), which serves as an endocytic receptor for BMP4, in addition to other bioactive molecules.[284] These observations lend weight to our data suggesting that BMP4 plays an important role in eye growth regulation.

In summary, we demonstrated the expression of genes for BMP2, BMP4, and BMP7 and their receptors, as well as of the three BMP proteins throughout the tissues making up the posterior ocular wall, implying that they serve important regulatory functions in these tissues. Key ocular growth modulatory roles for these growth factors and a key role of the RPE as a signal transducer or relay in the related retino-scleral cascade are suggested by the further observations of sign-dependent, optical defocus-induced changes in gene expression in the RPE for all three BMPs – BMP2, BMP4 and BMP7. The latter results also raise the possibility of targeting these BMP signaling pathways as a novel therapeutic intervention for myopia.

Chapter 3

Long-Term Imposed Hyperopic Defocus Induced Gene Expression Changes in Chick RPE: a Microarray Study

Abstract

This study examined the effect on gene expression in the retinal pigment epithelium (RPE) of long-term, lens-induced myopia. To induce myopia, 5 White-Leghorn chicks wore monocular -15 D lenses from 10-days of age for 38 days. Retinoscopy and high-frequency A-scan ultrasonography were used to monitor refractive errors (RE) and axial ocular dimensions of both treated and untreated fellow eyes, which served as controls. RPE was isolated from enucleated eyes and total RNA purified. After the verification of the quality of RNA, it was subjected to cDNA synthesis, *in vitro* transcription, labeling, and hybridization with Affymetrix GeneChip Chicken Genome Arrays. Microarray data were analyzed using BioConductor package and bioinformatic databases. Seventeen candidate genes were validated with real-time PCR. Expression patterns for RPE from myopic and fellow eyes were compared. Significant myopia, axial length (AL) increases, and choroidal thinning were recorded in treated eyes compared to their fellows after 38 days of treatment. Eight hundred and fifty-two transcripts were up- or down-regulated in myopic compared to fellow eyes, by at least 1.5-fold ($p<0.05$). Real-time PCR confirmed the differential expression of many genes, including the up-regulation of FIGF ($p = 0.053$), NOG, PDGFA, and down-regulation of BMP2, 4, 7, DRD4, RARB, and RRH. Of the genes exhibiting differential expression, many could plausibly be involved in ocular growth regulation in RPE, based on their known actions in other tissues, although functional changes in RPE secondary to myopic growth may underlie the changes in some affected genes.

Some of the data reported in this chapter were previously published in the following conference abstract:

Zhang Y, Liu Y, Xu J, Nimri N, Wildsoet CF. Microarray analysis of RPE gene expression in chicks during long-term imposed hyperopic defocus. *Invest. Ophthalmol. Vis. Sci*. 2010; 51: E-Abstract 3680.

3.1 Introduction

Myopia describes the condition in which images of distant objects are focused in front of the retina, due to a mismatch between the optical power and axial length of the eye. Most myopia is caused by excessive ocular elongation,[285] leading in high myopia to sight-threatening complications such as retinal degeneration, retinal detachment, choroidal neovascularization, myopic maculopathy, cataract, and glaucoma.[6, 286, 287] In a recently published study, the overall prevalence of myopia in the US was given as 41.6%, and the prevalence of high myopia (≤ -7.9 D) as 1.6% for persons aged 12 to 54 years.[9] These figures represent significant increases over previous figures,[9, 288] mirroring trends in equivalent statistics from East Asia.[232, 289-291] Because of these altered prevalence figures and the complications of high myopia, it has become a significant public health problem world-wide. For effective clinical intervention, it is thus imperative to elucidate the mechanisms underlying the development of myopia and associated complications.

Studies using animal models, such as chickens, guinea pigs, tree shrews, and monkeys, have provided significant insights into postnatal eye growth regulation, and specifically, the role of the retina as a source of myopia-generating stimuli.[16, 26, 292] Myopia can be generated in two different ways, using diffusers to impose form-deprivation or negative lenses to impose hyperopic defocus. In both cases, the result is an increase in the rate of axial elongation. Of the above experimental models, chickens are both the most widely used and most reliable, responding rapidly to imposed hyperopic defocus, with choroidal thinning being detectible within 1 hour of the initiation of lens treatment, ahead of detectible changes in overall eye length.[179, 180] With imposed optical defocus, the growth changes are compensatory, with emmetropia being achieved with the lenses in place, provided the size of the defocus stimulus is not too large or the animals too old. In young chickens, around 9 days old, near complete compensation (80%) is seen after just one week of treatment with –10 D lenses.[226] Compensation occurs more slowly in older birds.[35, 227] In all cases, treated eyes will continue to grow at a faster rate with the lenses in place, to maintain compensation after it has been achieved.

Since localized manipulation of retinal images induces localized changes in the adjacent sclera, and optic nerve section, which prevents communication between the retina and brain, does not prevent the induction of experimental myopia, it is generally accepted that local ocular circuits underlie myopic growth, and that the retina is the origin of growth modulating signals.[36, 37]

Because the retina is separated from the two target tissues, the choroid and sclera, by the retinal pigment epithelium (RPE), it is likely to play an important role as a signal relay. RPE cells express many different types of receptors, for both neurotransmitters and growth factors, and also secretes a variety of growth factors and cytokines, many of which could plausibly be components of a growth modulatory signal transduction pathway, and/or be affected by excessive ocular enlargement.[40, 65, 66, 135] As the RPE is increasingly stretched and thinned during this enlargement process, it is also plausible that it is adversely affected

in this process, and so contributes to some of the ocular complications of myopia, such as choroidal neovascularization and myopic maculopathy.[293-295]

DNA microarray technology makes it possible to screen a large number of genes in a single experiment, to look for effects of applied treatments.[296] To-date, the use of this technology in myopia research has been largely limited to retina or retina/RPE, with relevant studies in mice, chickens, and monkeys, involving retinal image contrast manipulation (e.g. form-deprivation), as well as optical defocus.[127, 133, 161, 297-299] In these case, RPE was not separated from the adjacent retina or choroid.

In the study described here, chickens wore monocular -15 D lenses over an extended period, i.e. 38 days, to induce long-term high myopia, after which RPE cells were isolated for gene expression studies. With this experimental protocol, changes in gene expression in the RPE may occur as a part of the signal cascade underlying myopic "growth", or as a consequence of changes in RPE secondary to the excessive expansion of the vitreous chamber.

3.2 Materials and Methods

3.2.1 Animals & Lens Treatment

White-Leghorn chickens were obtained as hatchlings from a commercial hatchery (Privett, Portales, NM), and were reared in a 12 h: 12 h light-dark cycle. Five (5) birds in total were used for this study. Four birds (1, 2, 3, 4) were used for the microarray screening. RNA from an additional bird (5) was included in follow-up qPCR validation experiments. To induce myopia, chicks wore -15 D lenses over their right eyes from 10-day of age for 38 days. Their contralateral (fellow) untreated eyes were used as controls. Lenses were cleaned twice a day. Both eyes of each bird had refractive errors (RE) and axial ocular dimensions, including vitreous chamber depth (VCD) and choroidal thickness (CT), measured under isoflurane anesthesia (1.5% in oxygen) with retinoscopy and high-frequency A-scan ultrasonography respectively, after 18 and 38 days of lens wear.

3.2.2 RPE Isolation & RNA Extraction

The RPE was collected from both eyes at least 2 h after the last biometry measurements. Birds were euthanized with an overdose of pentobarbital injection, after eyes immediately enucleated, anterior segments removed, RPE isolated and lysed with RLT buffer from RNeasy Mini kits (Qiagen, Valencia, CA), and then immediately stored at -80 °C for later use. RNA was extracted from RPE cells and purified using RNeasy Mini kits and RNeasy MinElute Cleanup kits (Qiagen, Valencia, CA), according to the manufacturer's protocol. RNA concentration and optical density ratio of A_{260}/A_{280} were measured using a DU 650 Spectrophotometer (Beckman Coulter, Fullerton, CA). The quality of extracted RNA was further analyzed in the Functional Genomic Lab at the University of California, Berkeley, using an Agilent 2100 bioanalyzer in combination with an RNA 6000 Pico Chip kit (Agilent Technologies, Inc., Santa Clara, CA).[300-302]

3.2.3 Microarray Analyses

cDNA synthesis, in vitro transcription, and microarray hybridization: Affymetrix GeneChip Chicken Genome Arrays (Affymetrix, Santa Clara, CA) were used in this study. First, cDNA was synthesized from 1.4 μg samples of RNA from each eye of the 4 chicks, using SuperScript One-Cycle cDNA Kit (Invitrogen, Carlsbad, CA), according to the manufacture's protocol. The synthesized double-stranded cDNA was then cleaned up and used as a template to synthesize biotinylated complementary RNA (cRNA) in an *in vitro* transcription (IVT) reaction. The synthesized cRNA was then cleaned up, quantified, and fragmented into 35-200 base fragments. Finally, 30 μg samples of fragmented cRNA were hybridized onto the chips, followed by washing, staining and scanning.

Microarray data analysis: Raw microarray data (.CEL files) were analyzed using both Bioconductor project R and Affy packages.[303-305] Robust multiarray averaging (RMA) was used as a normalization method.[306, 307] The Affy package includes a suite for probe-level quality control checks of signal intensity and variance. Boxplots of perfect match (PM) probe data provide the information of the overall distribution of probe intensities on each array. Three quality control (QC) analyses were performed to check array qualities. Relative Log Expression (RLE) represents the log ratio of the expression of a probe set on an individual array to the median expression of this probe set across all arrays. The RLE provides information about the overall distribution of probe intensity. Normalized Unscaled Standard Error (NUSE) represents the ratio of expression of the standard error of an individual probe set and median standard error for this probe set across all arrays. The NUSE provides information about the overall distribution of probe variance. RLE and NUSE data for each eye are shown graphically as box plots, as is RNA degradation data, which shows mean expression of all probe sets as a function of relative position (5' end to 3' end).[302, 308] Identification of differentially expressed genes was based on an MA plot, which shows M (log2 fold-change) plotted as a function of mean expression level A (log2 intensity).[309] For each gene, the log2 fold change in expression was derived from the ratio of treated to control eye data. The criteria applied in selecting candidate genes for export were fold ≥ 1.5 and $p \leq 0.05$. Up-regulation by ≥ 1.5 fold is equivalent to M ≥ 0.585 and down-regulation by ≤ -1.5 fold is equivalent to M ≤ -0.585.

Identified differentially expressed (candidate) genes were analyzed using NetAffx,[310] with functional annotations obtained from the Database for Annotation, Visualization and Integrated Discovery (DAVID), and NCBI databases (GenBank, PubMed).[311] Canonical pathway information was obtained using Ingenuity Pathways Analysis software (Ingenuity® Systems, www.ingenuity.com).[133, 299] Heatmaps were prepared for 55 candidate genes using MultiExperiment Viewer (http://www.tm4.org/mev.html).[312, 313]

3.2.4 Real-Time PCR

From the candidate genes identified in the microarray analyses, 17 genes were selected for further real-time PCR validation study. Using extracted RNA from RPE, reverse transcription was performed to synthesize cDNA (SuperScript III First-Strand Synthesis System for RT-PCR, Invitrogen, Carlsbad, CA). Custom-designed primers and QuantiTect

SYBR Green PCR Kits (Qiagen, Valencia, CA) were used in combination with a StepOnePlus Real-Time PCR System (Applied Biosystems, Foster City, CA). Primers were designed using Primer Express 3.0 (Applied Biosystems, Foster City, CA). Chick glyceraldehyde-3-phosphate dehydrogenase (GAPDH) was used as the housekeeping gene. Gene symbols, NCBI (National Center for Biotechnology Information, Bethesda, MD) access numbers, sequences, and sizes of amplicons of candidate genes are listed in Table 3-1. The PCR cycling conditions included an initial denaturation for 10 min at 95 °C, followed by 40 cycles of denaturation for 15 s at 95 °C, annealing for 1 min at 60 °C. Ten-fold serial dilutions of cDNA were used for generating standard curves for each pair of primers. Amplification of each gene was performed in triplicate. Mean normalized expression (MNE) values were used to compare gene expression levels in RPE from lens-treated eyes and their fellow control eyes.

3.2.5 Statistical Analysis

Paired Student's *t*-test were used to compare lens-treated eyes with their fellows, both in terms of biometric data (axial length, vitreous chamber depth, choroidal thickness, refractive error), as well as gene array and real-time PCR data.

Table 3-1. Primer information for candidate genes

Gene	NCBI Access Number	Sequences (5'-3')	Amplicon
AQP4	NM_001004765.1	Forward: 5'-TGGGAGTCACTGCGGTACAC-3' Reverse: 5'-TGAATCACAGCTGGCAAAAATAG-3'	107 bp
BMP2	NM_204358	Forward: 5'-AGCTTCCACCACGAAGAAGTTT-3' Reverse: 5'-CTCATTAGGGATGGAAGTTAAATTAAAGA-3'	96 bp
BMP3	NM_001034819.1	Forward: 5'-GGAATGAGCCACGGTATTGTG-3' Reverse: 5'-GCCAATGTCAGCAAAATCCA-3'	59 bp
BMP4	NM_205237.1	Forward: 5'-GCACAGACTCATCAGGGCAAA-3' Reverse: 5'-GCCGTGCCCCTGAGGTA-3'	60 bp
BMP6	XM_418956	Forward: 5'-TCATGGTGGCATTCTTCAAAGT-3' Reverse: 5'-TGCCGCTGACCTCGTAGTC-3'	59 bp
BMP7	XM_417496.2	Forward: 5'-CGGGAATTTGGAAATCAGTCA-3' Reverse: 5'-GCCATCTGGTCTGGATTTGG-3'	66 bp
DRD4	NM_001142849.1	Forward: 5'-GCTCAAGACCACCACCAACTATT-3' Reverse: 5'-GGAGGGCGAGCAGAAGGT-3'	65 bp
FGF1	NM_205180.1	Forward: 5'-TCCTGTATGGCTCGCAGCTA-3' Reverse: 5'-TGGAGATGTATGTGTTGTAATGGTTCT-3'	84 bp
FGFR2	NM_205319.1	Forward: 5'-ACACGTAGAGAGGAATGGCAGTAA-3' Reverse: 5'-AACACCGGCAGCCTTTAAAA-3'	76 bp
FIGF	NM_204568.1	Forward: 5'-CTCATGGGTCACAAAGCAAAGA-3' Reverse: 5'-GCAGTGGATTTCTGGAGAACTGA-3'	65 bp
GAPDH	NM_204305.1	Forward: 5'-AGATGCAGGTGCTGAGTATGTTG-3'	71 bp

		Reverse: 5'-GATGAGCCCCAGCCTTCTC-3'	
KDR	NM_001004368.1	Forward: 5'-TCTGGCGCTCACCAATACC-3' Reverse: 5'-ACACCACCTCCCCCACCTAT-3'	67 bp
NOG	NM_204123.1	Forward: 5'-CAGAAGGCATGGTCTGCAAA-3' Reverse: 5'-CGCCACCTCAGGATCGTTA-3'	58 bp
PDGFA	NM_204306.1	Forward: 5'-GTGCACTAGACCGCGATGAG-3' Reverse: 5'-GGACAGGTAGCCAAAACCTATCA-3'	63 bp
PDGFRA	NM_204749.1	Forward: 5'-GCCTGAGAATGAAAGGGAGAGA-3' Reverse: 5'-CAACGCTGAGATGCTCATAAAGTAC-3'	85 bp
RARB	NM_205326.1	Forward: 5'-CCACCCCCGCGTGTTTA-3' Reverse: 5'-AAAGCCCTTACATCCCTCACAA-3'	96 bp
RRH	NM_001079759	Forward: 5'-GGGCGTCCATGCCTACTGTA-3' Reverse: 5'-AGTTGCTCCAGTCGGATCTGA-3'	59 bp
TGFB2	NM_001031045.1	Forward: 5'-CGCCTGCAGAACTCAAAGG-3' Reverse: 5'-TTCAGAACCTGGTACAGCTCTATCC-3'	62 bp

3.3 Results

3.3.1 Ocular Effects of Lens Treatment

Monocular -15 D lenses, worn for an extended period of time, induced choroidal thinning and excessive ocular elongation that was largely limited to the vitreous chamber (Figure 3-1), and as a consequence of the increase in ocular length, treated eyes were highly myopic. At the end of the lens treatment period of 38 days, treated eyes had a mean refractive error of -14.1 ± 0.60 D, compared to +2.5 ± 0.29 D (mean ± SEM) for their fellows, this difference being highly significant ($p < 0.01$, paired Student's *t*-test). In statistical terms, treated eyes had significantly longer anterior chamber depths ([distance from anterior cornea to anterior lens] 2.49 ± 0.10 mm vs. 2.03 ± 0.03 mm, $p < 0.01$), vitreous chamber depths (8.63 ± 0.19 mm vs. 6.91 ± 0.14 mm, $p < 0.001$ [interocular difference is 1.72mm]), thinner choroids (0.18 ± 0.02 mm vs. 0.24 ± 0.01 mm, $p < 0.05$), and, longer overall lengths (axial length: 14.50 ± 0.24 mm vs. 12.56 ± 0.17mm, $p < 0.001$, paired Student's *t*-test [interocular difference is 1.94mm]).

3.3.2 RNA Quality Analysis & cRNA Quantification

The yield of total RNA from RPE was approximately 1.5-2.8 µg/eye, and the optical density ratio of A_{260}/A_{280} was 1.76 ± 0.02. RNA integrity number (RIN), which measures the integrity of total RNA using the electrophoretic trace of the RNA sample on an RNA 6000 Pico Chip, was 8.27±0.10. The concentration of cRNA was 2.47 ± 0.11 µg/µl. These data are consistent with high yield and high integrity.

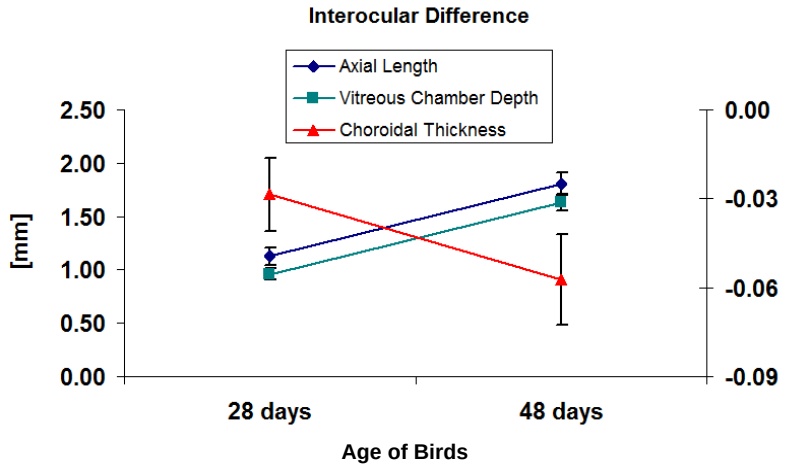

Figure 3-1. Interocular differences (treated - control eyes), in axial length, vitreous chamber depth (left axis), and choroidal thickness (right axis), after 18 and 38 days of continuous -15 D lens treatment (mean ± SEM, n = 7).

3.3.3 Microarray Analyses

Quality control analyses of microarray data: In the boxplot showing Relative Log Expression (RLE) for each array (representing 4 treated eyes and their fellows; Figure 3-2A), all boxes are centered close to 0, and distributions of probe intensity of all arrays are similar to each other. In the boxplot of Normalized Unscaled Standard Error (NUSE) (Figure 3-2B), the median standard error lies close to 1 for all arrays. In RNA degradation plot (Figure 3-2C), which represents the average degradation for the complete probe set, the signal intensity ratio for the housekeeping gene 3' to 5' probe sets was ≤ 3.0. The consistency across all 8 arrays in their RLE and NUSE profiles, as evidenced from the boxplots, and the similarity of their RNA degradation profiles validates the comparisons subsequently made within genes across the arrays.[305, 308, 314]

Differentially expressed genes: The MA plot (Figure 3-3) shows a broad spread in the data, with many points showing a greater than 1.5 fold change in expression in absolute terms, implying that many genes had been significantly up- or down-regulated by the lens treatment. More genes were up-regulated than down-regulated. Specifically, a total of 851 transcripts out of 32,773 chick transcripts or 670 genes were up- or down-regulated by more than 1.5 fold by the lens treatment ($p \leq 0.05$), and of the differentially expressed genes, 520 were up-regulated and 150 were down-regulated.

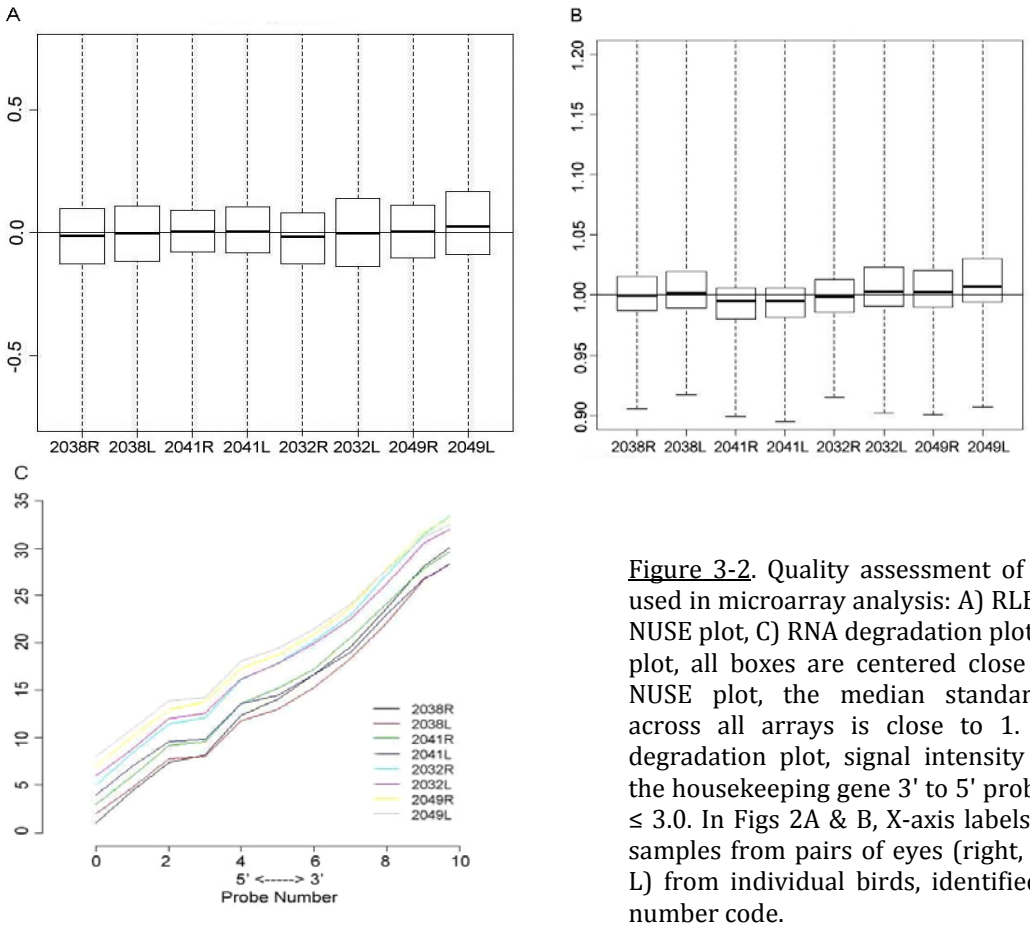

Figure 3-2. Quality assessment of samples used in microarray analysis: A) RLE plot, B) NUSE plot, C) RNA degradation plot. In RLE plot, all boxes are centered close to 0. In NUSE plot, the median standard error across all arrays is close to 1. In RNA degradation plot, signal intensity ratio of the housekeeping gene 3' to 5' probe sets is ≤ 3.0. In Figs 2A & B, X-axis labels refer to samples from pairs of eyes (right, R & left, L) from individual birds, identified by the number code.

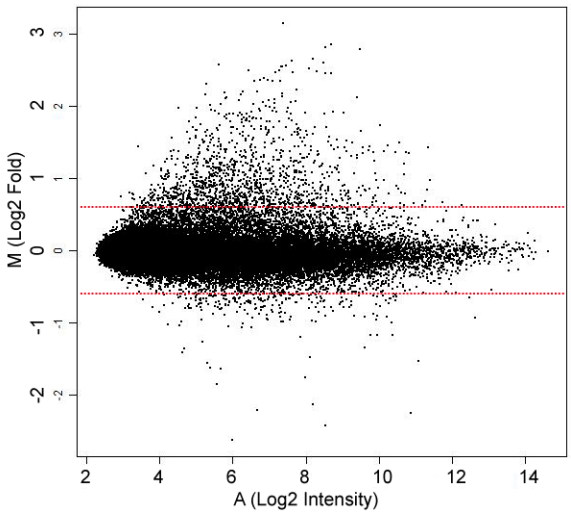

Figure 3-3. Plot of M (log2 fold-change) as a function of mean expression level A (log2 intensity). Data from 8 arrays representing 4 treated and 4 control eyes are shown. Fold change represents the ratio of expression in treated and control eyes. The superimposed redlines indicate a 1.5 fold change in expression; genes lying outside the central zone defined by the red lines were considered to be significantly up- or down-regulated.[309]

In further analyses of the 851 differentially expressed transcripts, using NetAffx, DAVID, and NCBI databases to classify them, particular attention was paid to genes that had already been linked to either myopia or eye growth regulation in other studies, or could plausibly play a role in ocular growth regulation or myopia pathogenesis, based on their known functions. Selected genes are listed in Table 3-2, clustered into groups according to the gene ontology terms for molecular function. Among the up-regulated genes were a number of growth factors (BMP3, BMP6, FIGF, INHBA, PDGFA, TGFB2), a variety of receptors (EDNRA, FGFR2, KDR, PDGFRA), protein/lipid binding molecules (FN1, NOG), and water/ion channels (AQP4, CACNA1G). Among the down-regulated genes were other growth factors (BMP2, BMP4, BMP7), receptors (ADRA2C, DRD4, RARB, RRH), and ion channels (CLCN5, CLCN7).

A heatmap of 55 candidate genes (Table 3-2) that could plausibly regulate RPE and choroidal/scleral function and ocular growth is shown in Figure 3-4.

3.3.4 Real-Time PCR

Treatment-induced changes in expression as well as results of statistical analyses of the PCR data collected for nine genes are summarized in Table 3-3. These nine genes represent a subset of the seventeen candidate genes whose microarray results were validated with real-time PCR (Figure 3-5). A comparison of gene expression changes from both the microarray and real-time PCR experiments are shown in Figure 3-6. All nine genes showed similar expression patterns with the two techniques. Specifically, with real-time PCR, FIGF, NOG, and PDGFA once again showed up-regulation in treated relative to control eyes, and BMP2, BMP4, BMP7, DRD4, RARB, and RRH all showed down-regulation.

3.4 Discussion

In this study, we found in eyes made highly myopic 851 transcripts in RPE to be differentially expressed using microarrays and confirmed the observed trends for a subset of nine genes using real-time PCR. Below we discuss the possible growth regulatory roles of the latter genes, based on already established links to eye growth regulation or plausible links, based on their function. Because of the relatively long treatment period used in this study, and relatively high myopic errors induced, we also consider the possibility that the changes in gene expression could be a product of excessive eye elongation, secondary to stretching and thinning of RPE, and thus perhaps linked to the retinal pathology described in myopic eyes.

One family of genes selected for further investigation were the bone morphogenetic proteins (BMPs), which belong to the transforming growth factor β (TGF-β) superfamily that has been linked to eye growth regulation in other studies. The BMPs represent multi-functional growth factors, first linked to cell proliferation and extracellular matrix synthesis in bone and cartilage formation,[236, 261, 262, 315, 316] and now known to play crucial roles in embryonic morphogenesis, as well as postnatal development and cellular functions in adult animals.[235, 236, 246, 248, 317, 318]

Table 3-2. List of genes, showing significant treatment-related differential expression changes in RPE in microarray analyses, and with plausible links to eye growth regulation and/or myopia.

Probe Set ID	Gene Symbol	Gene Title	Fold	P Value
GO:0015267~channel activity				
Gga.11374.1.S1_at	AQP4	aquaporin 4	1.56	0.022
GgaAffx.4763.4.S1_s_at	CACNA1G	calcium channel, voltage-dependent, T type, alpha 1G subunit	1.76	0.043
Gga.1805.1.S1_at	CLCN5	chloride channel 5 (nephrolithiasis 2, X-linked, Dent disease)	-1.56	0.004
GgaAffx.292.1.S1_s_at	CLCN7	chloride channel 7	-1.80	0.019
GO:0008083~growth factor activity				
Gga.3950.1.S2_at	BMP2	bone morphogenetic protein 2	-6.47	0.005
GgaAffx.6892.1.S1_at	BMP3	bone morphogenetic protein 3 (osteogenic)	2.41	0.049
Gga.686.1.S1_at	BMP4	bone morphogenetic protein 4	-3.15	0.002
GgaAffx.23995.1.S1_at	BMP6	bone morphogenetic protein 6	3.05	0.05
Gga.6770.2.S1_s_at	BMP7	bone morphogenetic protein 7	-1.97	0.006
Gga.3219.1.S1_at	FIGF	c-fos induced growth factor (vascular endothelial growth factor D)	2.83	0.012
Gga.648.1.S2_at	FGF1	fibroblast growth factor 1 (acidic)	1.91	0.032
Gga.3982.1.S1_at	INHBA	inhibin, beta A	1.96	0.045
Gga.3899.3.S1_a_at	PDGFA	platelet-derived growth factor alpha polypeptide	1.87	0.041
GgaAffx.22982.1.S1_at	TGFB2	transforming growth factor, beta 2	1.86	0.023
GO:0005515~protein binding				
Gga.4285.1.S1_at	CEBPB	CCAAT/enhancer binding protein (C/EBP), beta	-1.82	0.007
Gga.4941.2.S1_a_at, Gga.4941.1.S1_at	CDH11	cadherin 11, type 2, OB-cadherin (osteoblast)	2.35	0.0006
Gga.1917.1.S1_at, GgaAffx.21844.1.S1_s_at	CDH2	cadherin 2, type 1, N-cadherin (neuronal)	2.01	0.045
GgaAffx.6053.1.S1_at	COL1A2	collagen, type I, alpha 2	2.87	0.031
Gga.2592.1.S1_at	COL5A1	collagen, type V, alpha 1	2.10	0.015
GgaAffx.21771.1.S1_at	COL6A1	collagen, type VI, alpha 1	2.49	0.011
Gga.4257.1.S1_at	COL6A2	collagen, type VI, alpha 2	2.13	0.008
Gga.4965.2.S1_at	COL12A1	collagen, type XII, alpha 1	2.06	0.03
Gga.17860.1.S1_at	DOK7	docking protein 7	1.92	0.015
Gga.9293.1.S1_at	FN1	fibronectin 1	3.12	0.048
Gga.5710.1.S1_a_at	HTRA3	HtrA serine peptidase 3	3.29	0.013
Gga.8434.1.S1_at	IGFBP4	insulin-like growth factor binding protein 4	1.66	0.043
Gga.19049.1.S1_at	IL18	interleukin 18 (interferon-gamma-inducing factor)	1.68	0.037
Gga.3199.1.S1_at	MMP2	matrix metallopeptidase 2 (gelatinase A, 72kDa gelatinase, 72kDa type IV collagenase)	2.73	0.009
Gga.449.1.S1_at	NOG	noggin	4.28	0.036
GgaAffx.25896.1.S1_at,	SLC1A3	solute carrier family 1 (glial high affinity	4.37	0.039

GgaAffx.25896.1.S1_s_at		glutamate transporter), member 3		
GO:0004872~receptor activity				
Gga.8371.1.S1_s_at	ADIPOR2	adiponectin receptor 2	-1.56	0.004
GgaAffx.9949.1.S1_at	ADRA2C	adrenergic, alpha-2C-, receptor	-2.09	0.05
Gga.2733.1.S1_at	CNR1	cannabinoid receptor 1 (brain)	2.05	0.008
GgaAffx.3186.1.S1_at	DRD4	dopamine receptor D4	-1.50	0.003
Gga.137.1.S1_at	EDNRA	endothelin receptor type A	2.21	0.046
Gga.694.1.S1_at	EPHB1	EPH receptor B1	1.57	0.011
Gga.633.1.S1_at	EPHB6	EPH receptor B6	1.82	0.049
Gga.11368.1.S1_at	F2RL2	coagulation factor II (thrombin) receptor-like 2	-2.10	0.003
Gga.14338.1.S1_at	FGFR2	fibroblast growth factor receptor 2	1.58	0.043
Gga.3907.1.S1_at	LOC395603	fibroblast growth factor receptor FREK	-1.69	0.001
Gga.8771.1.S1_at	FGFRL1	fibroblast growth factor receptor-like 1; similar to fibroblast growth factor receptor-like protein	1.72	0.012
Gga.2908.1.S1_at	LOC395407	fibroblast growth factor receptor-like embryonic kinase	-1.70	0.03
Gga.1941.1.S1_at	FZD4	frizzled homolog 4 (Drosophila)	1.87	0.009
Gga.2690.1.S1_at	FZD6	frizzled homolog 6 (Drosophila)	1.53	0.005
Gga.311.1.S1_at	FZ-8	frizzled-8	2.91	0.04
Gga.2529.1.S1_a_at	IL1RL1	interleukin 1 receptor-like 1	3.52	0.017
Gga.7339.1.S1_at	KDR	kinase insert domain receptor (a type III receptor tyrosine kinase)	2.18	0.007
Gga.4738.1.S1_at	NEO1	neogenin	1.67	0.001
Gga.14911.1.S1_at	OXTR	oxytocin receptor	-2.03	0.03
Gga.274.1.S1_at	PDGFRA	platelet-derived growth factor receptor, alpha polypeptide	2.18	0.043
GgaAffx.3811.1.S1_at	PLXNA1	plexin A1	-1.69	0.008
Gga.8211.1.S1_at	PLXNB2	plexin B2	2.12	0.018
Gga.2668.4.S1_a_at	RARB	retinoic acid receptor, beta	-1.84	0.029
GgaAffx.7723.3.S1_at	RRH	retinal pigment epithelium-derived rhodopsin homolog	-1.60	0.037
Gga.679.1.S1_at	VLDLR	very low density lipoprotein receptor	2.28	0.031

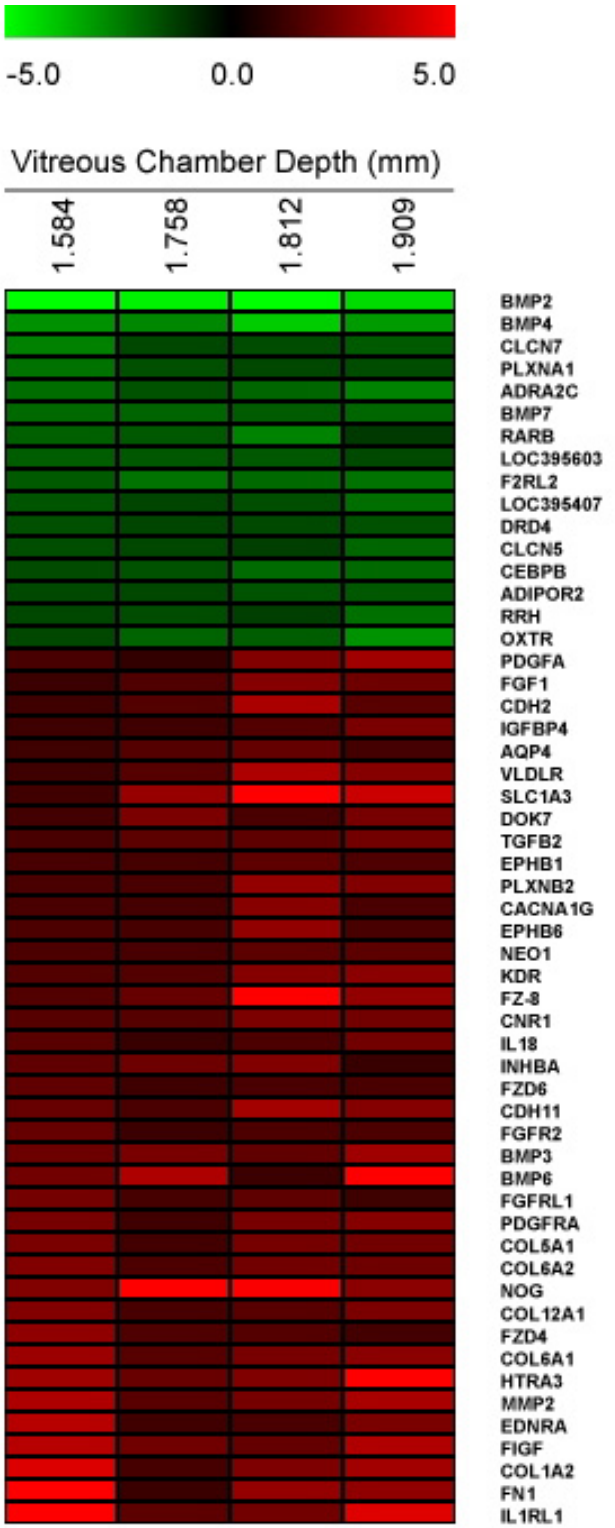

Figure 3-4. Heatmap from microarray analysis showing results for 55 candidate genes with plausible roles in regulating ocular growth and/or RPE functions. Each column shows the fold change of RPE gene expression for each of 4 birds, i.e., ratio of expression in treated and control eyes (n=4). Down-regulated genes are represented in green, and up-regulated genes are in red. Interocular difference of vitreous chamber depth (mm) is shown for each bird on top of the relevant column.

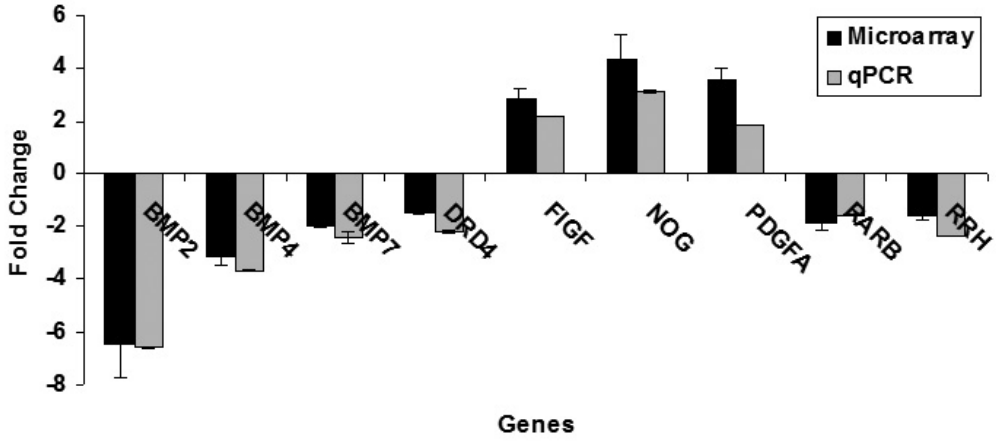

Figure 3-5. Comparison of microarray and real-time PCR gene expression results (treated vs. fellow control eye); microarray findings of up-regulation for FIGF, NOG, and PDGFA, and down-regulation for BMP2, BMP4, BMP7, DRD4, RARB, and RRH were confirmed with real-time PCR (mean ± SEM, n = 4).

Table 3-3. Results of real-time PCR validation experiments for nine genes showing differentially expression in microarrays; negative values signify down-regulation & positive values, up-regulation.

Gene Symbol	Gene Name	Fold change	*p* value
BMP2	bone morphogenetic protein 2	-6.47	0.011
BMP4	bone morphogenetic protein 4	-3.66	0.015
BMP7	bone morphogenetic protein 7	-2.40	0.007
DRD4	dopamine receptor 4	-2.19	0.005
FIGF*	c-fos induced growth factor (vascular endothelial growth factor D)	2.21	0.053
NOG	noggin	3.11	0.022
PDGFA	platelet-derived growth factor alpha polypeptide	1.86	0.049
RARB	retinoic acid receptor, beta	-1.55	0.001
RRH	retinal pigment epithelium-derived rhodopsin homolog	-2.34	0.015

* *p* value for FIGF is 0.053

In the current study, we observed defocus-induced down-regulation in RPE of three BMPs, including BMP2, which was also reported to be down-regulated in retina/RPE with 6 h and 3 days of form-deprivation in a previous study involving young chicks.[133] We also found BMP2, BMP4, and BMP7 gene expression to be down-regulated with short-term exposure to negative lenses, as well up-regulation in response to short-term exposure to positive lenses.[140] The consistency of the pattern of altered gene expression with very short and longer term myopia-inducing treatments suggests an on-going role for BMP2 in myopic eye growth. Furthermore, while this family of growth factors has been implicated in embryonic retinal patterning and differentiation in the chick,[241] nonetheless, a RPE site for the induced changes in BMP2 expression would explain why two different myopia-inducing stimuli with likely different retinal signal pathways, had the same effect on RPE gene expression,

assuming that distinct retinal signal pathways converge at the RPE. A study that hint at such a role for BMP2 as a growth inhibitor in eye growth regulation found the BMP2 protein to be localized in human sclera, and observations of increased human scleral fibroblasts proliferation, increased secretion of TIMP2 and decreased secretion of MMP2 in response to treatment with recombinant human BMP2 are consistent with reduced scleral remodeling and reduced axial elongation, opposite that expected for reduced BMP2 gene expression and protein secretion.[207] Nevertheless, to definitively establish BMP2 to be part of a myopia-inducing signal cascade, it will be necessary to establish that these same myopia-inducing stimuli decrease the secretion of the BMP2 protein from basal (choroid) of the RPE.

Of the other two BMPs showing altered gene expression, BMP4 has been placed in the same subgroup as BMP2, based on the similarity of their amino acid sequences. It has also been linked to eye growth and scleral fibroblast function. Specifically, mutations in the BMP4 gene may lead to developmental ocular abnormalities including microphthalmia,[249] and in cultured human scleral fibroblasts, mechanical stress causes the down-regulation of BMP4 expression.[267] This growth factor also appears to influence wound healing and tissue repair. Of particular note, transgenic mice that over express BMP4 in the RPE show less severe choroidal neovascularization (CNV); this action appears to be through the modulation of TNF-α induced MMP9 expression.[319] Extrapolation from this observation to assume a role for BMP4 in the maintenance of choroidal structure and function, it is plausible that sustained down-regulation in RPE in myopic eyes may contribute to the associated pathological complications involving the choroid.

BMP7 (osteogenic protein-1, or OP-1) belongs to another subgroup of BMPs along with BMP5 and BMP6.[320] Compared to other members of this group, including BMP2, 4, and 6, BMP7 exhibits stronger pro-anabolic activities as well as anti-catabolic activities in cartilage repair.[316] While the effect on BMP7 protein secretion from the RPE was not studied, the predicted effect of reduced secretion would tend to rule out the sclera as a target as reduced proteoglycan synthesis is opposite to the results expected for the chick eye, whose sclera adds to its cartilage component during eye enlargement. The choroid is a plausible alternative target, as the observed thinning during myopic growth is accompanied by reduced glycosaminoglycan (GAG) synthesis.[124]

In contrast to the consistent patterns of down regulation for the BMP genes, the gene for Noggin (NOG), a BMP binding protein, was up-regulated.[236, 321-323] In binding to BMPs, NOG also inactivates them. It appears to play a critical role in bone and cartilage development. For example, over-expression of Noggin in mice impairs bone formation,[324, 325] while the NOG null mutation results in excess cartilage, a consequence of elevated BMP activity.[326] Since the chick sclera includes a cartilage layer, it is plausible target for NOG. In terms of eye growth regulation, NOG may modulate the activity of secreted BMPs since it is known to bind to all three of the BMPs whose genes showed differential expression with our myopia-inducing lens treatment. The up-regulation of the NOG gene would serve to amplify the effects of the reduced expression of the BMP genes observed, assuming comparable trends in protein secretion in all cases. More direct evidence of NOG's involvement in myopic eye growth would be confirmation that neutralizing antibodies inhibit or attenuate

myopic eye growth. Such a result would be of potential therapeutic interest, assuming it can be generalized to the mammalian eye.

In this study, gene expression for *c-fos* induced growth factor (FIGF), also known as vascular endothelial growth factor D (VEGF-D) was up-regulated 2.21-fold in treated eyes. FIGF is a member of the PDGF/VEGF superfamily, whose members play critical roles in embryonic vessel development, angiogenesis and lymphogenesis under physiological conditions, and they have also been implicated, either directly or indirectly, in a range of ocular pathologies including age-related macular degeneration (AMD), diabetic retinopathy and pathologic myopia.[287, 327-334] Target receptors for FIGF include VEGFR-2 and -3, whose activation leads to angiogenesis and lymphangiogenesis in tumors.[330, 335] Both VEGFR-2 and -3 have been localized to the choriocapillaris in monkey and human eyes[295, 336] and VEGFR-2 mRNAs has also been detected in monkey choroid-retinal pigment epithelial complex.[337] It is note worthy that in the chick, the defocus-induced changes in choroid thickness are largely limited to suprachoroidal layer, where lymphatic-like vessels or lacunae expand or flatten to achieve thickening or thinning respectively.[175, 177, 338-340] Changes in the permeability of the choroidal vasculature have also been reported with form-deprivation in the chick.[174] The FIGF may play a role in the choroidal component of the emmetropization processes, although choroidal thickness changes tend to occur early, within the first few days of defocus treatment (unpublished data). The sustained choroidal thinning observed in this study, after 38 days of treatment, is likely to partly reflect the stretching of the choroid, as the scleral cup expanded. While neither neovascularization nor lymphogenesis have been reported with shorter term myopia-inducing treatment regimens in chicks, intraocular neovascularization has been observed with long term treatments, extending out to 12 months or more, raising the question of whether the observed change in FIFG gene expression could be a stimulus for such pathology.[328] Nonetheless, three further observations are compatible with a role for FIGF in ocular growth regulation. FIGF expression is regulated, at least in fibroblasts, by *c-fos*, a member of the immediate-early gene family,[341] and the expression of FIGF in RPE is also reported to be regulated by *c-fos*.[342] Finally, expression of *c-fos* in retinal amacrine cells is known to be responsive to light and to visual stimuli known to alter eye growth.[51, 343]

PDGF-A was included among the genes selected for further analysis based on the large amount of data localizing members of the platelet-derived growth factor (PDGF) and receptor proteins to RPE, and their apparent roles in both development and ocular pathology, including proliferative diabetic retinopathy as well as corneal and choroidal neovascularization.[344-346] Both freshly isolated human RPE and cultured human RPE cells are reported to express all isoforms of PDGF mRNA, and secret PDGF into culture medium.[347-350] Native human RPE and cultured RPE cells also express PDGF receptor mRNA as well as PDGFR-α and-β protein.[348, 349] This pattern of co-expression of PDGF and its receptors suggests autocrine regulation of PDGF secretion by RPE.[348, 349] In the adjacent choroid, both PDGFR-α and-β have been detected in the normal human eyes; cultured choroidal fibroblasts also express PDGFR-α mRNA,[346, 351] and human recombinant PDGF stimulates their proliferation and migration.[351] Further studies are warranted to explore the possible roles of this growth factor in the signal pathway underlying myopic eye growth and/or related pathology.

The finding that gene expression for dopamine D4 receptors was down-regulated is perhaps not surprising, given the many studies linking retinal dopamine with eye growth regulation. The D4 receptor is one of five subtypes of DA receptors, which have been categorized based on their properties into two subfamilies D1-like (D1, D5) and D2-like (D2, D3, D4).[70] Reduce levels of dopamine (DA) and its metabolite in the retina of form-deprived eyes is a consistent finding across relevant studies in chicks, as is the complementary finding that apomorphine, a nonselective DA agonist, inhibits both form deprivation- and defocus-induced myopic eye growth.[74, 79, 104] Results from another more recent pharmacological study, also in chicks, pointed to involvement of D2-like dopamine receptors, which we find to have the highest expression in human fetal RPE cells.[80, 151] In related studies, applied apomorphine was shown to stimulate the secretion of TGFβ-1 and -2 from cultured human fetal RPE cells, offering a plausible signaling pathway for ocular growth modulation, given that the latter growth factors have been implicated in scleral extracellular matrix remodeling.[151] Nonetheless, our finding of down-regulation rather than up-regulation of D4 receptor gene expression would seem in the opposite direction to that expected if retinal DA release had remained depressed, although such changes have only been observed in one of a number of studies involving defocus-induced myopia.[77, 85] Species differences also do not explain changes were limited to D4 rather than D2 receptors in our study, although they are members of the same subfamily and it is possible that there is some overlap in their roles.

Retinoic acid (RA) is known to be a potent regulator of cell growth and differentiation, acting via nuclear receptors (RARs and RXRs), to activate or repress the expression of other genes.[115, 116] Interestingly, many of the growth factors showing differential expression in the current study, including BMP-2, -4, -7, FIGF, PDGFA, have been shown to be regulated by RA in a variety of cells and tissues, either *in vivo* or *in vitro*, and directly or indirectly.[270, 271, 352-358] There are already extensive data linking RA with ocular growth regulation in a number of different species, although there are also subtle species-related differences. Specifically in the chick, negative lens treatments up-regulate retinal mRNA expression of aldehyde dehydrogenase-2 (AHD2), one of the enzymes involved in RA synthesis, and retinal RA levels are increased by both form-deprivation or negative lens treatment.[117, 119, 120, 123] In contrast, choroidal RA synthesis is decreased significantly by the latter treatments. The opposite trends have been observed in eyes recovery from form-deprivation and ones wearing positive lenses in chick.[118] Mammals and primates show similar retinal trends to those described for chicks but opposite trends for choroidal RA synthesis.[16, 118, 120, 124] Since the RPE is interposed between the retina and choroid, it is likely that it is affected by both retinal and choroidal RA levels. Thus our finding of down-regulation of RAR-β mRNA in RPE is more consistent with a response to treatment-induced elevation of retina RA levels, assuming RA synthesis remains high with extended negative lens treatments. However, it is also acknowledged that the regulation of expression of retinoic acid receptors in RPE and thus effects of myopia-inducing stimuli may be more complicated than the mechanisms underlying expression changes in myopic chick retina and sclera, as reported by other studies.[122, 123, 135, 158, 159, 359-361]

The last of the nine genes targeted for additional investigation with real time PCR was RRH or peropsin. In mice, this visual pigment-like protein is expressed exclusively in RPE, and

prominently in the microvilli surrounding photoreceptor outer segments in mice.[362] In chick, RRH is expressed in both the retina and pineal gland,[363] although its expression in RPE has not been confirmed, perhaps due to the heavy pigmentation of this layer. It has been assigned various roles, including providing an index of the concentration of retinoids and/or other photoreceptor-derived compounds in RPE, and acting as a photoisomerase, facilitating the conversion of *all-trans*-retinal to *11-cis*-retinal in response to light.[362, 364] The down-regulation of RRH gene expression observed in our study may signify altered levels of retinoids in the RPE or altered photoreceptor functions. Both are plausible consequences of long-term negative lens treatment, given the altered anatomy of the myopic eye, and previous reports of altered photoreceptor morphology and disk shedding in form-deprived chick eyes.[365, 366]

On the technical side, it is important to acknowledge two potential limitations of our data. The first limitation relates the RPE isolation procedures used to collect our samples. The tips of photoreceptor are an unavoidable contaminant, as they are embedded in the RPE microvilli. While dark adaptation prior to sacrifice is sometimes used in retinal research, to more cleanly separate the RPE from the retina, this technique was not used in the current study, because of the likely impact of dark adaptation on gene expression. For example, the expression of retinal ZENK, a gene linked to eye growth regulation, is known to be affected by the number of hours of light exposure after lights-on.[51] Thus we cannot rule out that changes in retinal gene expression contributed to our results. The second limitation relates to our use of the fellow eyes as controls or references. Interocular yoking has been observed in gene expression changes involving the retina and sclera of the chick,[53, 280] as well as in the RPE for some BMP genes (see Chapter 2). While the origins of these yoking effects are not fully understood, nonetheless, we cannot rule out similar intraocular yoking for some of the genes examined in this study. However, as most reported yoking effects are manifest as a similar but weaker trend in the control eye, thereby reducing rather than exaggerating treatment effects, our use of fellow eyes as controls strengthens rather than weakens the cases tying changes in gene expression to the applied treatments.

In summary, long-term, myopia-inducing lens (hyperopic defocus) treatments applied to chicks result in the differential expression of a variety of genes in the RPE, among which are growth factors, a growth factor antagonist protein, a neurotransmitter receptor, and a retinoic acid receptor. Plausible explanations linking them with either ocular growth regulation, including myopic growth, and pathological complications of myopia were presented. Follow-up studies are needed to directly investigate these possibilities, and to understand the inter-relationship between them.

Chapter 4

Apomorphine Regulates TGF-β1 and TGF-β2 Secretion in Human Fetal Retinal Pigment Epithelial Cells

Abstract

This study investigated dopaminergic regulation of TGF-β secretion from human retinal pigment epithelium (RPE) as a possible mechanism by which inhibitory eye growth signals may be relayed from retina to choroid/sclera. Using primary cultures of human fetal (hf) RPE as a model, RPE gene expression for dopamine (DA) and TGF-β receptors and TGF-β isoforms was examined using real-time PCR, receptor protein expression with Westerns blots, and receptor localization with immunocytochemistry. Cultures were also subjected top treatment with the DA agonist, apomorphine (APO; 0–20 μM), applied to the apical (retinal) side of cells, and the secretion of TGF-β isoforms into the medium measured after 24 h with ELISAs. Dopamine D1, D2, D5 as well as TGFBR1, 2, 3 receptors, and TGF-β1, -β2 isoforms were all detected in hfRPE, with D2 and TGFBR2 receptors showing the highest expression of receptors. D2 and TGFBR1 receptors were also detected by Western blots and immunocytochemistry. In untreated cells, the mRNA expression of TGF-β1 was 4.6-fold higher than TGF-β2 and both TGF-β1 and TGF-β2 were constitutively secreted, mainly from the apical side. In contrast, apically applied APO (0.2–2.0 μM) increased the secretion of both isoforms, mainly from the basolateral (choroidal) side. The polarized nature of this pharmacological effect provides a plausible explanation for how activation of DA receptors on the apical membrane of human RPE, i.e. facing the retina, could initiate signals that act on the choroid/sclera to inhibit eye growth.

Some of the data reported in this chapter were previously published in the following conference abstract:

Zhang Y, Maminishkis A, Zhi C, Li R, Agarwal R, Miller SS, Wildsoet CF. Apomorphine Regulates TGF-β1 and TGF-β2 Expression in Human Fetal Retinal Pigment Epithelial Cells. *Invest. Ophthalmol. Vis. Sci*. 2009; 50: E-Abstract 3845.

4.1 Introduction

Myopia, or near-sightedness, is one of the most common ocular disorders in humans, affecting 41.6% of U.S. population aged 12 to 54 years.[9] The prevalence and the severity of myopia have risen worldwide during the past several decades, stimulating increased research into the underlying mechanisms, an essential step in developing effective therapies.

Animal studies provide convincing evidence for the importance of retinal signaling in eye growth regulation. Currently there are two different experimental paradigms for inducing myopia, utilizing form-depriving diffusers and negative defocusing lenses, respectively. Both paradigms have been shown to elicit robust responses in chickens, guinea pigs, tree shrews and monkeys.[16] In all cases, the induced myopia is characterized by expansion of the posterior vitreous chamber of the eye, reflecting the remodeling of the outer choroidal and scleral support layers. The preservation of these response patterns in eyes isolated from the brain by optic nerve section points to local growth regulation.[34, 35] The RPE serves to protect the health and integrity of the neural retina and is known to be an important source of growth factors that may have autocrine or paracrine functions.[40, 135, 367-369] By virtue of its anatomical location, it is also ideally suited to relay retinal paracrine signals regulating the growth of the choroid and sclera.

Previous studies of experimental myopia in chicks have provided strong evidence for a role for retinal dopamine (DA) in eye growth regulation.[74, 75, 79-81] Direct evidence for a role of DA in eye growth regulation is provided by observations that ocular administration of apomorphine, a nonselective DA receptor agonist, slows both form deprivation- and lens-induced myopia. DA has been localized to subsets of retinal amacrine and interplexiform cells and DA receptors have also been identified on both neural cells within the retina and RPE.[64-68] There are five subtypes of DA receptors (D1-D5), and based on their biochemical and pharmacological properties they have been categorized into D1-like (D1, D5), and D2-like (D2-D4) subfamilies.[69, 70] In chicks, D2/3 receptors have been identified on the basal side of the RPE, with their presence on the apical surface of RPE cells being left unresolved due to the heavy pigmentation in this region.[65] D2 receptors have also been demonstrated on the RPE of other mammals, including cat and cow, while their presence on human RPE is controversial.[149, 150]

The transforming growth factor-β (TGF-β) superfamily encompasses structurally-related proteins that function as regulatory cytokines. They are involved in a wide variety of functions, including the modulation of chemotaxis, wound healing, angiogenesis, stimulation or inhibition of cell proliferation, and extracellular matrix (ECM) remodeling.[239] TGF-β is known to modulate fibroblast proliferation, as well as ECM protein expression and degradation, all of which have been tied to scleral growth modulation.[185, 239, 280, 370-372] Non-polarized efflux of TGF-β from RPE has been measured in several preparations,[165, 166, 373-375] and while the effects of dopamine analogs on TGF-β secretion from RPE have not been previously studied, both dopamine and DA agonists have been shown to induce dose-

dependent increases in TGF-β1 secretion and TGF-β1 mRNA expression coupled to inhibited proliferation in pituitary lactotropic cells.[376, 377]

In the present study, we determined the expression and localization of dopamine and TGF-β receptors on primary hfRPE monolayers in culture and measured the constitutive and apomorphine induced polarized secretions of TGF-β1 and -β2. We found that activation of dopaminergic receptors on the retina-facing, apical membranes of human RPE results in increased TGF-β secretion, predominately from the basolateral (choroidal) side of the epithelium. These results suggest that retina-derived dopaminergic signals may be relayed to the choroid and sclera via modulated growth factor secretion from the RPE for the modulation of eye growth.

4.2 Materials and Methods

4.2.1 Human Fetal RPE Cell Culture

Retinal pigment epithelial cells were obtained from 16-18 weeks old human fetal eyes (Advanced Bioscience Resources, Alameda, CA) and cultured as described previously.[367] Briefly, hfRPE cells from donor eyes were seeded into tissue culture flasks with a 15% FBS-containing culture medium (P0). The culture medium was replaced the next day with 5% FBS-containing medium, which was changed every 2 to 3 days thereafter. After the cells became confluent and pigmented, they were trypsinized and passaged onto cell culture transwell inserts coated with human extracellular matrix (ECM, 10 µg/well, BD Biosciences, Bedford, MA) at a density of 2.0×10^5 per well (P1). For use in the studies reported here, we used confluent P1 cells with total tissue resistance of > 200Ω • cm^2. The cell culture set-up used in this study is shown schematically in Figure 4-1.

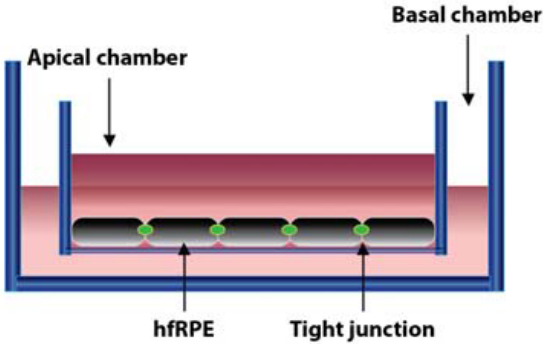

Figure 4-1. hfRPE were cultured on ECM-coated inserts of transwells that allowed isolation of medium bathing apical and basal sides of cells, and thus their separate sampling and analysis.

4.2.2 Characterization of RPE Receptors

Real-time PCR: Real-time PCR targeting human dopamine receptors (D1, D2 and D5), TGF-β receptors (TGFBR1, 2, 3), and TGF-β isoforms (TGF-β1, TGF-β2), was performed on

cultured hfRPE after incubating in serum-free medium (SFM) for 24 h. Total RNA from six culture inserts was extracted using RNeasy Mini Kit (Qiagen, Valencia, CA), with on-column DNase treatment, before being reverse transcribed to cDNA (SuperScript III First-Strand Synthesis System for RT-PCR, Invitrogen, Carlsbad, CA). Real-time PCR assays were performed according to the manufacturer's instructions (TaqMan & ABI Sequence Detection System 7900; Applied Biosystems, Foster City, CA). TaqMan assay IDs are listed in Table 4-1. Standard curves were generated by 10-fold serial dilutions of cDNA. The mRNA concentration of each sample was normalized against human GAPDH levels. Testing for each gene was performed using six samples, with two technical repeats. Because some of the qPCR primers used were not designed to flank exon-exon junctions, controls for genomic contamination were included.

Table 4-1. TaqMan qPCR assay information

Assay	ID
DRD1	Hs00377719_g1
DRD2	Hs01024460_m1
DRD5	Hs00361234_s1
TGFBR1	Hs00610318_m1
TGFBR2	Hs00234253_m1
TGFBR3	Hs01114253_m1
TGFB1	Hs00998130_m1
TGFB2	Hs00234244_m1
GAPDH	Hs999999905_m1

Western Blots: Western blots were used to confirm the presence of the D2 receptor and TGFBR1 proteins in hfRPE cells. While still attached to the inserts, confluent monolayers of hfRPE were lysed at 4°C with RIPA buffer (Sigma-Aldrich, St. Louis, MO) containing a protease inhibitor cocktail (Roche Diagnostics, Indianapolis, IN), and the total protein was measured (BCA; Pierce Biotechnology, Rockford, IL). Western blot samples (30 μg) were denatured and then electrophoresed on a 4%-12% gradient gel (NuPAGE 4-12% Bis-Tris Gel, Invitrogen), before being transferred to nitrocellulose membranes (iBlot Gel Transfer Stacks, Invitrogen). Membranes were blocked (StartingBlock T20 [TBS]; Pierce Biotechnology) and then incubated with either goat anti-human polyclonal antibody against the D2 receptor (Santa Cruz Biotechnology, Santa Cruz, CA, # sc-7522), or goat anti-human polyclonal antibody against TGFBR1 (R&D Systems, Minneapolis, MN, # AF3025), and subsequently labeled with HRP-conjugated rabbit anti-goat IgG (HRP; Pierce Biotechnology). Immunoreactive bands were detected with chemiluminescence (Supersignal Pico ECL; Pierce Biotechnology) and images developed using a bioimaging system (Autochemie; UVP, Upland, CA).[348, 369] Assays involved three separate biological samples and triplicate repeats. Human brain and heart lysates and mouse brain lysates were used as positive controls for both receptors.

Immunocytochemistry: hfRPE cells were fixed with 4% formaldehyde, permeabilized with 0.2% Triton X-100, blocked with a signal enhancer (Image-iT FX; Invitrogen). RPE monolayers were incubated with antibodies against human D2 receptors (Santa Cruz Biotechnology, # sc-7522) and TGFBR1 (R&D Systems, # AF3025), and ZO-1 (Zymed, South

San Francisco, CA, # 339100), prelabeled with different fluorophores using Zenon Labeling Technology (Invitrogen), following manufacturer's instructions. Normal goat serum pre-labeled with fluorophore was used as a negative control. Cells were then stained with Hoechst 33342, mounted on glass slides with antifade reagent (Prolong Gold; Invitrogen), and imaged with a Zeiss Axioplan 2 microscope with apotome and Axiovision 3.4 software (Carl Zeiss AG, Germany).

4.2.3 Effect of Apomorphine (APO) on TGF-β1 and TGF-β2 Secretion from RPE

Dose-response study: Confluent monolayers of hfRPE cells on inserts were incubated in serum-free medium (SFM) for 24 h prior to drug treatment. One of 4 different concentrations, 0, 0.2, 2, 20 μM of APO (Sigma, St. Louis, MO), was then added to the SFM medium bathing the apical side of the hfRPE cells. After 24 h, culture medium was collected from both apical and basal chambers and assayed for TGF-β1 and -β2 (pg/ml) using ELISA kits. The total amounts (pg) of TGF-β1 and -β2 secreted into apical and basal culture medium were calculated form measured concentrations, accounting for the difference in the volumes of culture medium in the apical and basal chambers, i.e. 0.5 and 1.5 ml respectively. The effect of each dose of APO was studied in triplicate.

ELISA: Samples of media were clarified by centrifugation and subjected to immunoassays for TGF-β1 and -β2, carried out according to the manufacturer's instructions (R&D Systems, Minneapolis, MN). In brief, acid-activated samples were added to a 96-well microplate coated with monoclonal antibodies specific to either TGF-β1 or -β2, incubated for 2 h at room temperature, and then reacted with horseradish peroxidase (HRP)-conjugated polyclonal antibodies specific for TGF-β1 and -β2. Finally, a color reagent mixture was added to the wells and optical densities at 450 nm measured with a microplate reader, using a wavelength correction setting of 540 nm.

4.2.4 Statistical Analysis

Data reported in both the text and figures are expressed as mean ± SEM. Statistical comparisons made use of Student's *t*-tests (unpaired, two-tailed), when two groups were involved, and one-way ANOVA, when more than 2 groups were involved.

The described research followed the tenets of the Declaration of Helsinki and the National Institutes of Health Institutional Review Board.

4.3 Results

4.3.1 Characterization of Dopamine and TGF-β Receptors on Cultured hfRPE

Gene/protein expression for dopamine and TGF-β receptors Real-time PCR results for six of the genes coding for dopamine and TGF-β receptors are shown in Figure 4-2. While D1, D2 and D5 receptors were all expressed at relatively low levels, D2 receptor expression was approximately 22-fold higher than D1 receptor expression, and 2.5-fold higher than of D5 receptor expression (Fig. 4-2A, $p < 0.001$ for both cases). In contrast, all three TGF-β receptors were strongly expressed, although TGFBR2 expression was approximately 4.4-fold higher than TGFBR1 expression (Fig. 4-2B, $p < 0.01$) and 2.3-fold higher than TGFBR3 expression ($p < 0.05$). Western blots confirmed the presence of both D2 receptor and TGFBR1 proteins (Fig. 4-3). Figure 4-3A shows results with a Santa Cruz antibody (sc-7522) used to label the D2 receptor and includes positive controls of brain (human and mouse) and heart (human). In one blot this antibody showed three bands, all of which were reproduced with different antibodies from other sources (Chemicon: AB5084, Abcam: ab21218, ab32349 and ab30743). The band at 51 kDa, which is best described in the literature, was detected in all of our hfRPE samples (lanes 1-3) and confirmed with the positive controls in human heart (lane 5) and mouse brain (lane 6).[378] The two additional bands, at 68 and 90 kDa, have also been described in the literature.[378] The specificity of the 68 kDa for DRD2 has been confirmed using pre-immune serum and peptide-blocked immune serum.[378] This larger band represents the receptor in a different state of glycosylation and was the major band in mouse brain lysates revealed with another antibody (Chemicon: AB 5084, unpublished data). We also detected a 90 kDa band, which likely represents a DRD2 dimer protein (http://www.scbt.com/datasheet-7522-d2dr-n-19-antibody.html). Both the Abcam ab32349 and Santa Cruz antibodies to the D2 receptor produced an additional band at 37 kDa. For TGFBR1, there was just one band at 50 kDa (Fig. 4-3B), which was evident in all three hfRPE samples (lanes 1-3) as well as in the positive control (mouse brain, lane 4).

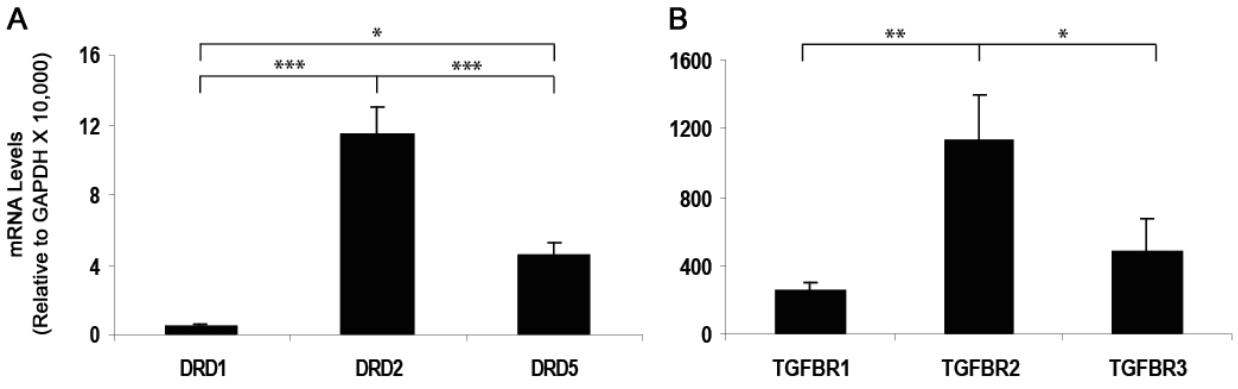

Figure 4-2. mRNA levels for (A) dopamine receptors and (B) TGF-β receptors in cultured hfRPE normalized to GAPDH. Data are expressed as mean ± SEM (n = 6). * $p < 0.05$, ** $p < 0.01$, *** $p < 0.001$.

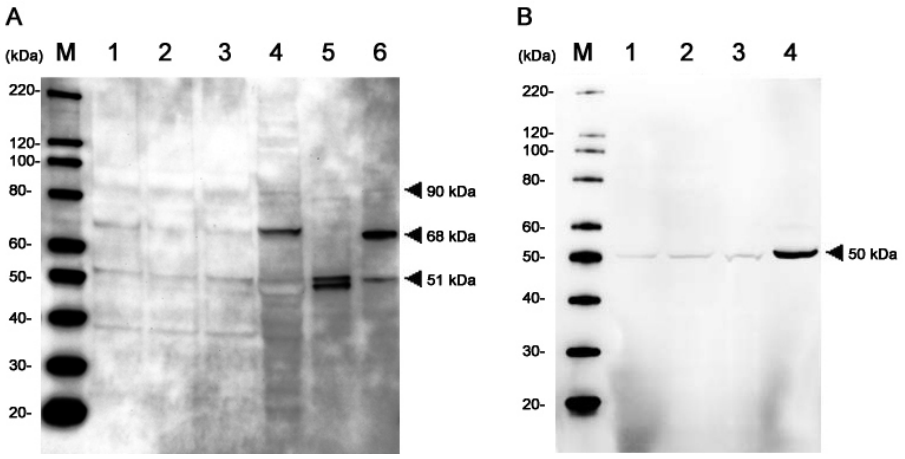

Figure 4-3. Expression in cultured hfRPE of the D2 receptor protein (A), detected at 90, 68, and 51kDa, and TGFBR1 protein (B), detected at 50 kDa. In both cases, lanes 1, 2, and 3 were loaded with hfRPE cell lysates from 3 different donors. Lanes 4, 5, and 6 in (A) include positive controls for the D2 receptor from human brain and heart lysates, and mouse brain lysates, respectively. In (B) mouse brain lysates were used as a positive control for TGFBR1 (lane 4).

Localization of dopamine and TGF-β receptors Immunocytochemistry labeling was used to localize D2 and TGFBR1 receptors on hfRPE grown on transwells. Additional ZO-1 labeling of tight junctions allowed the apical and basolateral membrane regions to be distinguished. Sample results are shown in Figure 4-4; the upper part of each panel shows a cross sectional view of the epithelium. Both D2 and TGFBR1 receptors were largely confined to the apical membranes.

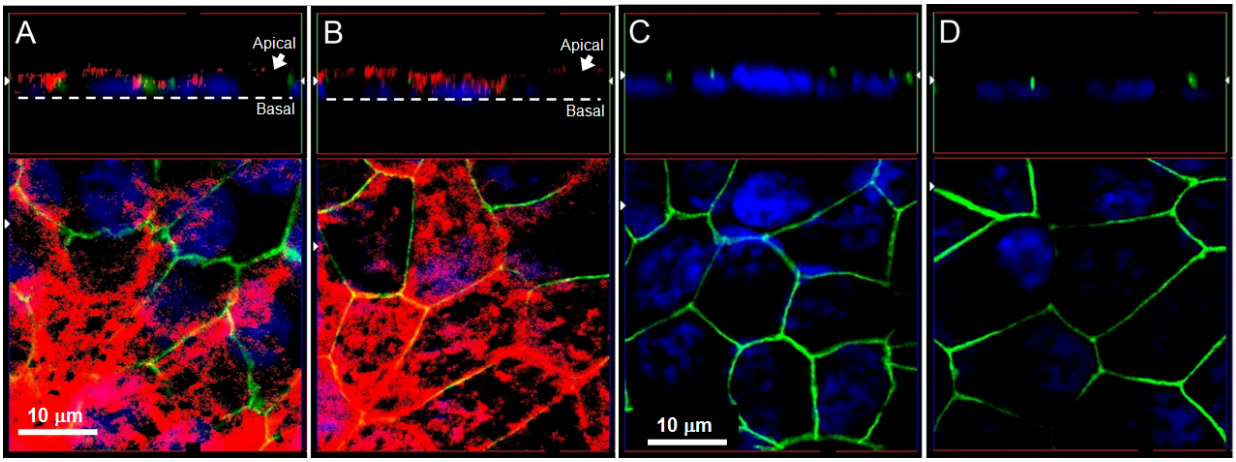

Figure 4-4. Immunocytochemistry of cultured hfRPE for D2 receptors (A) and TGFBR1 (B), shown in red, ZO-1 shown in green, and nuclei shown in blue. The upper part of each panel shows a cross section of the monolayer; the dotted white line indicates the basal surface of the cells and the white arrows indicate their apical surface. The lower part of each panel shows an optical section obtained from a z-stack. Negative controls are also shown, for both DRD2 (C) and TGFBR1 (D).

4.3.2 Expression and constitutive secretion of TGF-β1 and TGF-β2

Real-time PCR results for untreated cultured hfRPE showed TGF-β1 mRNA expression to be 4.6-fold higher than TGF-β2 expression (data normalized to GAPDH; Fig. 4-5, $p < 0.001$). Consistent with constitutive secretion of these cytokines, both TGF-β1 and -β2 were also detected in the culture medium (Fig. 4-6), and in each case, the secretion was polarized, predominantly from the apical side of cells, whether measured in terms of concentration (pg/ml, Fig. 4-6A) or total amount (pg, Fig. 4-6B). However, while gene expression data was biased in favor of TGF-β1, TGF-β2 was the dominant isoform in the secreted product, its concentration in the apical chamber being approximately 5.5-fold higher than that of TGF-β1 (Fig. 4-6A). Similar trends are evident in volume-adjusted total protein data (Fig. 4-6B).

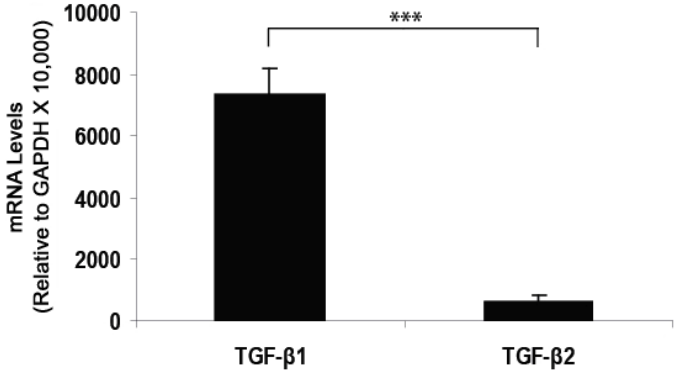

Figure 4-5. TGF-β1 and -β2 mRNA expression in untreated cultured hfRPE normalized to GAPDH. Data expressed as mean ± SEM (n = 6).

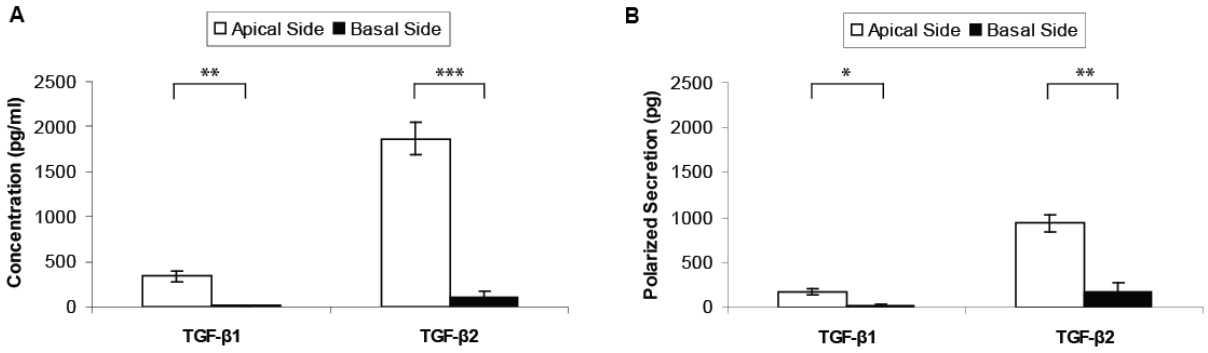

Figure 4-6. Constitutive polarized secretion of TGF-β1 and TGF-β2 from untreated cultured hfRPE, determined by ELISAs and expressed in (A) as concentrations (pg/ml) and in (B) as total amount (pg). For each chamber, the amount (pg) of secreted product was calculated as concentration (pg/ml) x bath volume (ml), using 0.5 and 1.5 ml for apical and basal chambers respectively. TGF-β2 was the dominant isoform secreted, and mainly into the apical bath (n = 3). * $p < 0.05$, ** $p < 0.01$, *** $p < 0.001$.

4.3.3 Apomorphine-Induced Alterations in TGF-β1 and TGF-β2 Secretion

Apomorphine (APO) increased the secretion of both TGF-β1 and -β2 in a polarized, dose-dependant fashion (Table 4-2, Fig. 4-7). Specifically, APO stimulation of apical dopamine receptors significantly increased the basal (but not the apical) secretion of both TGF-β1 and TGF-β2. The total protein data (Figs. 4-7 B & D) show that APO, at both 0.2 and 2 μM concentrations, reversed the direction of polarized secretion from the apical side, in the absence of APO, to the basal side of the monolayer. This change from predominantly apical constitutive secretion to predominantly basal secretion with the addition of APO is not evident in the protein concentration data (Figs. 4-7A & C), which does not account for the differences in the volumes of apical and basal chambers.

In the absence of APO, the total secretion of TGF-β1 (apical+basal chambers) was 196 pg/well. The main effect of apically applied APO was to increase secretion of TGF-β1 from the basal side of cells. Secretion was very low in control (0 APO) and 20 μM APO (25 & 33 pg/well respectively), but was significantly increased with 0.2 and 2 μM APO, by 68- and 44-fold over the control value (1700 & 1101 pg/well, respectively; $p < 0.01$ & 0.05, respectively). In contrast, the change in secretion of TGF-β1 from the apical side of cells did not reach statistical significance for any dose of APO.

In the absence of APO, the total secretion of TGF-β2 was 1099 pg/well. As with APO-induced changes in TGF-β1 secretion, the main effect of apically applied APO was increased TGF-β2 secretion from the basal side of the epithelium. Basal secretion was significantly increased with both 0.2 and 2 μM APO treatments (1878 & 2040 pg/well, respectively; $p < 0.001$ for both cases). These increases correspond to 11.4- and 12.4-fold increases compared to the control value. As with TGF-β1, secretion of TGF-β2 was minimally affected by 20 μM APO.

Table 4-2. Dose-dependent effects of apically-applied APO on TGF-β secretion by cultured hfRPE (24 h treatment).

	TGF-β1 (pg)			TGF-β2 (pg)		
APO (μM)	Apical	Basal	Total*	Apical	Basal	Total*
0	171 ± 30	25 ± 13	196 ± 17	934 ± 93	165 ± 104	1099 ± 72
0.2	312 ± 89	1700 ± 500	2012 ± 423	776 ± 95	1878 ± 50	2654 ± 54
2.0	365 ± 177	1101 ± 356	1466 ± 187	921 ± 46	2040 ± 340	2962 ± 353
20	193 ± 65	33 ± 16	225 ± 51	786 ± 78	108 ± 78	893 ± 155

*Total secretion represents combined secretions of TGF-β into apical and basal chambers (0.5 & 1.5 ml respectively). Data expressed as mean ± SEM (n = 3)

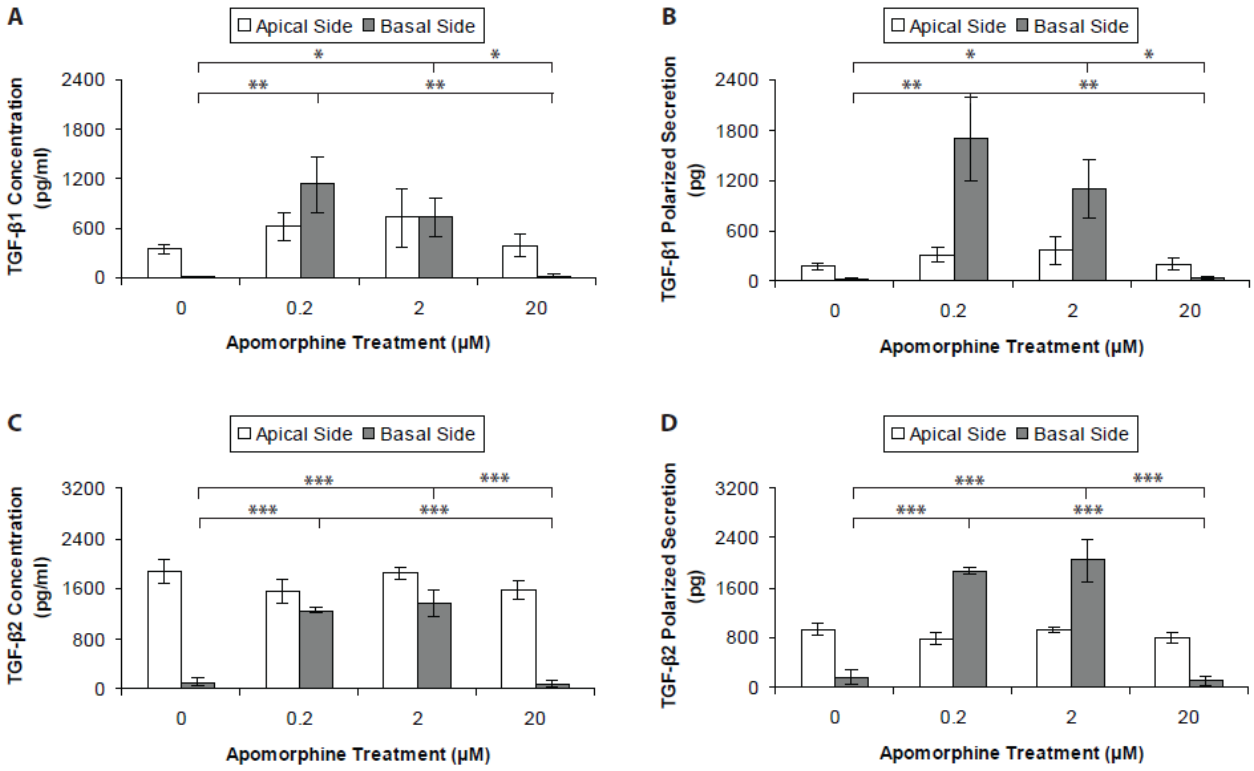

Figure 4-7. Dose-dependent effects of apically-applied APO on secretion by cultured hfRPE of TGF-β1 (A & B), and TGF-β2 (C & D). TGF secretion is expressed as either concentration (pg/ml) or amount (pg). The APO-induced changes in TGF-β1 and -β2 secretion were greater from the basal compared to apical sides of cells. * $p < 0.05$, ** $p < 0.01$; *** $p < 0.001$.

4.4 Discussion

It is known that dopamine receptor agonists such as apomorphine (APO) can inhibit form-deprivation and lens-induced myopia in chicks and monkeys.[74, 79-81, 84] APO is a nonselective dopamine receptor agonist that activates D2-like receptors at nanomolar concentrations and D1-like receptors at micromolar concentrations.[69, 82, 379, 380] The observation that sulpiride, a D2 receptor antagonist, enhances form-deprivation myopia in chick represents further evidence implicating D2 receptors in eye growth regulation.[85] The present study identified D2 receptors on apical membrane of hfRPE, offering a plausible a site of action for APO and relay mechanism for visually-regulated dopaminergic signals from the retina.

The hfRPE constitutively secretes a wide range of cytokines, chemokines and growth factors, with presumed roles in maintaining the homeostatic environment of the distal retina and the choroid.[368, 381, 382] In the present study, we demonstrated the presence of TGF-β receptors on the apical membrane of hfRPE and showed for the first time, polarized (apical) constitutive secretion of TGF-β from hfRPE. Localization of TGFBR1 to the RPE apical membrane is consistent with autocrine regulation of TGF-β secretion into the retina, which is thought to help protect the retina from extreme variations in TGF-β levels and plays an important role in maintaining normal retinal physiology.[375, 383, 384]

The apical bias in the constitutive secretion of both TGF-β isoforms was reversed with apically applied APO (0.2 and 2 μM), which increased the secretion of TGF-β into the basal (choroidal) chamber. The dose-response curve for APO-induced TGF-β secretion had an inverted U-shape, with intermediate concentrations, 0.2 and 2 μM APO, resulting in highest secretion. Interestingly, 20 μM APO had minimal effect on the secretion of both TGF-β1 and -β2, consistent with a previous *in vivo* observation.[81] The reduced efficacy of this high concentration of APO is most likely due to receptor desensitization or secondary effects mediated by binding to other receptors, such as D5 receptors (also detected in hfRPE), and β-adrenoceptors.[385]

Given that APO is known to inhibit the development of myopia in both chick and monkey models,[74, 75, 81, 84] our observation of APO-induced secretion of TGF-β into the basal chamber opens the possibility that this cytokine may act as an inhibitor of ocular elongation. Figure 4-8 is a schematic diagram illustrating APO "rescue of myopia". A parallel is drawn between the lowest concentration of apical APO tested in our human RPE model (Fig. 4-8A), and the decreased retinal dopamine level recorded in experimental myopia (Fig. 4-8E). A further parallel is drawn between the intermediate concentrations of APO (Fig. 4-8B), and the retinal conditions encountered in untreated normal eyes (Fig. 4-8D), and APO-treated form-deprived myopic eyes (Fig. 4-8F).

The model for dopamine mediated TGF-β secretion from RPE shown in Figure 4-8 indicates the sclera to be the target of TGF-β, although the choroid represents another possible target.[41] Nonetheless, in tree shrews, which have a primate-like fibrous sclera, mRNA expressions of TGF-β1, -β2, and -β3 were all found to be down-regulated following form-deprivation, consistent with a role of TGF-β as an ocular growth inhibitor.[371] Other *in vitro* studies involving tree shrew sclera are also consistent with a scleral site of action for TGF-β and an inhibitory role on eye elongation.[371, 386] Our study did not distinguish between the active and latent forms of TGF-β1 and -β2. However, other studies indicate that both isoforms were secreted in their latent forms from the hfRPE.[374, 387] Activation of TGF-β isoforms by plasmin, matrix metalloprotease-2 and -9, thrombospondin, integrins and other factors provide mechanisms for their controlled release in target tissues (choroid and sclera).[239, 388-391]

In addition to dopamine, other paracrine signals may also contribute to the regulation of TGF-β2 secretion from RPE. For example, a recent study described cholinergic regulation of TGF-β2 secretion from human RPE.[392-394] The role of cholinergic receptors on RPE in eye growth regulation is strengthened by the identification in recent genome-wide association studies of susceptibility loci for myopia on chromosome 15,[20, 395] which implicate several cholinergic receptors, one of which (CHRNA3) is a highly expressed signature gene for human RPE.[394]

In summary, key findings from this study - the apical localization of D2 receptors on hfRPE cells and the polar nature of the APO-induced secretion of TGF-β, from the basal side - support a role for RPE as a relay for retinal dopamine signals underlying visually-regulated eye growth.

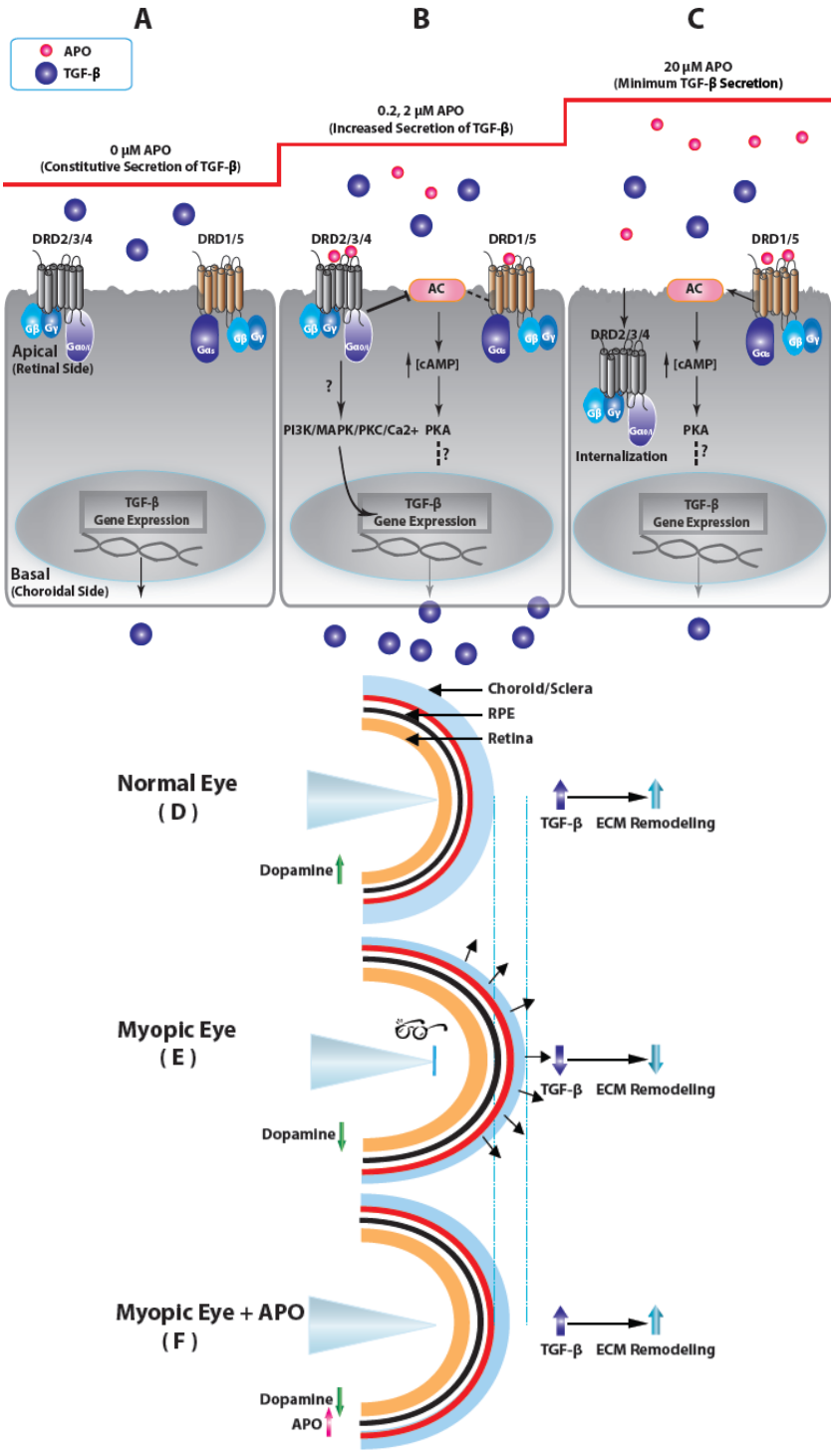

Figure 4-8. Diagram illustrating a model for retinal dopamine-regulated eye growth. The decreased level of retinal dopamine reported in experimental myopia models (E) is mimicked by the low APO condition (< 0.2 µM; A), leading to low secretion of TGF-β from the basal side of RPE. In (B), intermediate doses of APO (0.2 µM ≤ [APO] ≤ 2 µM) increase basal secretion of TGF-β, to levels in normal untreated eyes (D); APO treatment of form-deprived eyes (F), normalizes TGF-β secretion to slow myopia progression. The dose-response curve for APO is U-shaped; thus high doses of APO (> 20 µM, C), like very low doses, are without effect on TGF-β secretion.

Chapter 5

Dissertation Summary and Future Directions

5.1 Dissertation summary

Myopia is one of the most common ocular disorders in human. The ocular change underlying myopia is accelerated eye growth, which results in a mismatch between the axial length of eye and its refractive power, and in turn, blurred retinal images without optical correction. In high myopia, generally categorized as - 6.0 D or higher, the associated stretching of internal ocular structures with the increase in axial length may lead to blinding complications such as retinal degeneration, retinal detachment, myopic maculopathy, choroidal neovascularization and glaucoma. Understanding of the mechanism underlying myopic eye "growth" is an essential prerequisite to developing effective anti-myopia treatments. The research described in this dissertation focused on the role of retinal pigment epithelium (RPE) in eye growth regulation, with special attention to its potential role as a relay in retino-sclera signal cascades modulating eye growth. An overarching motivation was the possibility that this line of research might uncover novel approaches to controlling myopia.

This dissertation research addressed two questions in relation to the role of RPE in eye growth regulation: (1) what is its role in accelerated, i.e. myopic, eye elongation, and (2) what is its role in slowed eye elongation, as required to control myopia. The first question was investigated in Chapters 2 and 3. Experiments using negative lenses to induce myopia *in vivo* in young chicks revealed differential gene expression in RPE with both short-term (2 and 48 h) and long-term (38 days) lens treatments. The second question was investigated in Chapters 2 and 4, using both our *in vivo* chick model and an *in vitro* hfRPE cell culture model. We identified genes that are bidirectionally regulated, showing altered expression in opposite directions according to whether negative lens or positive lens treatment are imposed, the latter resulting in slowed eye growth. We also documented with a dopamine agonist known to inhibit myopia in animal studies, increased secretion from cultured hfRPE of a growth factor already linked to myopia growth. The major key findings from this dissertation work may be summarized as follows:

1. In investigations into the effects of imposed optical defocus on gene expression changes in chick RPE, we found that gene expression of the bone morphogenetic proteins (BMPs), BMP2, BMP4, and BMP7 to be bidirectionally regulated by short-

term (2 and 48 h) imposed defocus of opposite sign. Because changes in gene expression were elicited before significant changes in ocular dimensions had occurred, these genes are assumed to play important roles in initiation and maintaining early responses to imposed optical defocus rather than being a consequence of altered eye growth. These genes represent potential targets in the development of molecular-based anti-myopia treatments.

2. In investigating, the effects of long-term (38 days), myopia generating, imposed hyperopic defocus on gene expression in chick RPE using high-throughput DNA microarray technology, we identified a group of genes that could plausibly be involved in maintaining the myopic phenotype and/or pathological complications of myopia. This group included BMPs, NOG, dopamine receptor D4 (DRD4), retinoic acid receptor, beta (RARB), and retinal pigment epithelium-derived rhodopsin homolog (RRH).

3. In investigating the effects on TGF-β secretion from cultured hfRPE cells of apomorphine (APO), a dopamine receptor agonist with known anti-myopia action, we documented a pattern of regulation, i.e., apical application of APO leading to increased TGF-βs secretion from the basal side of cells, consistent with the myopia inhibitory effect of APO and offering a plausible mechanism for the same.

This dissertation work can be considered novel and innovative in the following respects: (1) the Wildsoet lab is the only myopia research lab focused on the role of RPE in eye growth regulation and the finding that RPE-derived BMPs are up-regulated under conditions that slow eye growth is new to the myopia field and opens up the possibility that they may be used as novel anti-myopia therapies; (2) the attempt to tie retinal DA to RPE-TGF-β regulation is also a new idea and approach used novel; previous studies have looked at neurotransmitters and growth factors in isolation, and have never focused on the RPE as a potential site for such regulation.

In summary, we investigated the role of RPE in myopia development and control, focusing on the molecular and cellular mechanisms underlying the altered eye growth, using changes in gene expression in RPE as a key signature. The findings reported herein represent the first studies to implicate the RPE in postnatal eye growth regulation, as a relay or conduit for retina-derived growth modulatory signals directed at the choroid and sclera. The genes and molecules identified in these studies may lead to novel therapeutic approaches to controlling of myopia. This study also opens up the possibility of targeting the RPE with some form of anti-myopia gene therapy.

5.2 Future directions

Based on the findings reported in this dissertation, there are a number of logical directions for future research. For example, roles for BMPs in eye growth regulation are strongly suggested by results from gene expression studies but these results are not definitive. Thus there is a need for more direct evidence. The are also many unresolved questions related to

the pathways mediating the regulation of RPE-BMPs and the potential roles in eye growth regulation and/or myopia-related pathology of other genes showing altered expression in the RPE of myopic eyes. Some avenues for follow-up studies are outlined below.

1. Further characterization of the ocular roles of BMPs:
    (1) Quantification of BMPs at protein level in different myopia and hyperopia animal models.

    (2) Application of BMPs and BMP signaling pathway inhibitors to directly study the role of BMPs in eye growth regulation. BMPs (BMP2, BMP4, and/or BMP7 protein) and signaling pathway inhibitors such as LDN-193189 and BMP antibodies can be administrated through intravitreal and subconjunctival injections and their effects on eye growth examined.

    (3) Direct manipulation of BMP gene expression in RPE to investigate the role of RPE-BMPs in eye growth regulation, ocular morphology and functions. Possible approaches include the over-expression and knock-down of BMP genes in RPE, which has been demonstrated to be an ideal target tissue for gene transfer.

    (4) Deployment of a gene therapy approach for myopia control targeting RPE. Since positive lens treatments up-regulate BMP2, BMP4, and BMP7 gene expression in RPE, and the opposite tends are seen with negative lenses, the over-expression of these BMPs is predicted to slow eye elongation, while knock-down of these genes should accelerate eye growth. Although gene therapy has never been evaluated in any myopia animal models, promising results have been obtained with gene therapy for some human retinal diseases and this approach has also been tested experimentally in the chick, as a treatment for one blinding retinal condition.

    (5) Investigation of the effects of RPE-derived BMPs on (i) retinal remodeling and neurogenesis and (ii) choroidal/scleral remodeling, using both *in vivo* animal and *in vitro* cell and tissue culture models.

2. Characterization of the retinal mechanisms regulating RPE-BMP expression, using a similar approach to that used for RPE-TGFβ in this dissertation research, starting with a study of the effects of dopamine receptor agonists on BMP secretion from RPE using *in vivo* animal and *in vitro* hfRPE cell culture models. The latter model avoids potentially confounding influences of nearby ocular structures. The *in vivo* approach would be to examine the effect of apomorphine (APO), as an example of a nonselective DA agonist, on BMP expression in RPE of chicks undergoing myopia-inducing treatments. The *in vitro* approach would be to characterize APO's effect on BMP secretion from cultured hfRPE.

3. Identification of novel genes involved in eye growth regulation. Increasing our understanding of the genes involved in myopia development potentially opens up

the possibility of new therapeutic targets; the microarray study reported in this dissertation identified a number of genes showing altered expression in myopic eyes and thus warranting follow-up studies.

From the perspectives of basic science and clinical practice, the successful accomplishment of one or more of the above proposed lines of research should provide new insights into the molecular and cellular mechanisms underlying eye growth regulation and myopia development. Targeting specific genes in RPE as a therapeutic intervention for myopia represents a novel approach but one with potential long term benefits to myopes, if successfully accomplished. Given the now high prevalence of myopia world-wide, many would also stand to benefit.

Bibliography

1. McBrien NA, Millodot M. A biometric investigation of late onset myopic eyes. *Acta Ophthalmol (Copenh)* 1987;65:461-468.
2. Whitmore WG. Congenital and developmental myopia. *Eye (Lond)* 1992;6 (Pt 4):361-365.
3. Mehra KS, Khare BB, Vaithilingam E. Refraction in Full-Term Babies. *Br J Ophthalmol* 1965;49:276-277.
4. Chen J, Xie A, Hou L, Su Y, Lu F, Thorn F. Cycloplegic and noncycloplegic refractions of Chinese neonatal infants. *Invest Ophthalmol Vis Sci* 2011;52:2456-2461.
5. Jones D, Luensmann D. The prevalence and impact of high myopia. *Eye Contact Lens* 1999;38:188-196.
6. Saw SM, Gazzard G, Shih-Yen EC, Chua WH. Myopia and associated pathological complications. *Ophthalmic Physiol Opt* 2005;25:381-391.
7. Flitcroft DI. The complex interactions of retinal, optical and environmental factors in myopia aetiology. *Prog Retin Eye Res* 2012;31:622-660.
8. Ono K, Hiratsuka Y, Murakami A. Global inequality in eye health: country-level analysis from the Global Burden of Disease Study. *Am J Public Health* 2010;100:1784-1788.
9. Vitale S, Sperduto RD, Ferris FL, 3rd. Increased prevalence of myopia in the United States between 1971-1972 and 1999-2004. *Arch Ophthalmol* 2009;127:1632-1639.
10. Pan CW, Ramamurthy D, Saw SM. Worldwide prevalence and risk factors for myopia. *Ophthalmic Physiol Opt* 2012;32:3-16.
11. Morgan IG, Ohno-Matsui K, Saw SM. Myopia. *Lancet* 2012;379:1739-1748.
12. Saw S, Yang A, Chan Y, Tey F, Nah G. The increase In myopia prevalence in young male Singapore adults from 1996-1997 to 2009-2010 *Invest Ophthalmol Vis Sci; 52: E-Abstract 2490* 2011.
13. Vitale S, Cotch MF, Sperduto R, Ellwein L. Costs of refractive correction of distance vision impairment in the United States, 1999-2002. *Ophthalmology* 2006;113:2163-2170.
14. Lim MC, Gazzard G, Sim EL, Tong L, Saw SM. Direct costs of myopia in Singapore. *Eye (Lond)* 2009;23:1086-1089.
15. Bar Dayan Y, Levin A, Morad Y, et al. The changing prevalence of myopia in young adults: a 13-year series of population-based prevalence surveys. *Invest Ophthalmol Vis Sci* 2005;46:2760-2765.
16. Wallman J, Winawer J. Homeostasis of eye growth and the question of myopia. *Neuron* 2004;43:447-468.
17. Wojciechowski R. Nature and nurture: the complex genetics of myopia and refractive error. *Clin Genet* 2011;79:301-320.
18. Morgan I, Rose K. How genetic is school myopia? *Prog Retin Eye Res* 2005;24:1-38.
19. Solouki AM, Verhoeven VJ, van Duijn CM, et al. A genome-wide association study identifies a susceptibility locus for refractive errors and myopia at 15q14. *Nat Genet* 2012;42:897-901.

20. Hysi PG, Young TL, Mackey DA, et al. A genome-wide association study for myopia and refractive error identifies a susceptibility locus at 15q25. *Nat Genet* 2010;42:902-905.
21. Li YJ, Goh L, Khor CC, et al. Genome-wide association studies reveal genetic variants in CTNND2 for high myopia in Singapore Chinese. *Ophthalmology* 2011;118:368-375.
22. Ip JM, Saw SM, Rose KA, et al. Role of near work in myopia: findings in a sample of Australian school children. *Invest Ophthalmol Vis Sci* 2008;49:2903-2910.
23. Wensor M, McCarty CA, Taylor HR. Prevalence and risk factors of myopia in Victoria, Australia. *Arch Ophthalmol* 1999;117:658-663.
24. Rose KA, Morgan IG, Smith W, Burlutsky G, Mitchell P, Saw SM. Myopia, lifestyle, and schooling in students of Chinese ethnicity in Singapore and Sydney. *Arch Ophthalmol* 2008;126:527-530.
25. Rose KA, Morgan IG, Ip J, et al. Outdoor activity reduces the prevalence of myopia in children. *Ophthalmology* 2008;115:1279-1285.
26. Rada JA, Shelton S, Norton TT. The sclera and myopia. *Exp Eye Res* 2006;82:185-200.
27. Wallman J, Turkel J, Trachtman J. Extreme myopia produced by modest change in early visual experience. *Science* 1978;201:1249-1251.
28. Wiesel TN, Raviola E. Myopia and eye enlargement after neonatal lid fusion in monkeys. *Nature* 1977;266:66-68.
29. Sherman SM, Norton TT, Casagrande VA. Myopia in the lid-sutured tree shrew (Tupaia glis). *Brain Res* 1977;124:154-157.
30. Howlett MH, McFadden SA. Form-deprivation myopia in the guinea pig (Cavia porcellus). *Vision Res* 2006;46:267-283.
31. Visscher PM, Hill WG, Wray NR. Heritability in the genomics era--concepts and misconceptions. *Nat Rev Genet* 2008;9:255-266.
32. Dirani M, Chamberlain M, Shekar SN, et al. Heritability of refractive error and ocular biometrics: the Genes in Myopia (GEM) twin study. *Invest Ophthalmol Vis Sci* 2006;47:4756-4761.
33. Chen YP, Hocking PM, Wang L, et al. Selective breeding for susceptibility to myopia reveals a gene-environment interaction. *Invest Ophthalmol Vis Sci* 2011;52:4003-4011.
34. Troilo D, Gottlieb MD, Wallman J. Visual deprivation causes myopia in chicks with optic nerve section. *Curr Eye Res* 1987;6:993-999.
35. Wildsoet C, Wallman J. Choroidal and scleral mechanisms of compensation for spectacle lenses in chicks. *Vision Res* 1995;35:1175-1194.
36. Wildsoet C. Neural pathways subserving negative lens-induced emmetropization in chicks--insights from selective lesions of the optic nerve and ciliary nerve. *Curr Eye Res* 2003;27:371-385.
37. Wallman J, Gottlieb MD, Rajaram V, Fugate-Wentzek LA. Local retinal regions control local eye growth and myopia. *Science* 1987;237:73-77.
38. Diether S, Schaeffel F. Local changes in eye growth induced by imposed local refractive error despite active accommodation. *Vision Res* 1997;37:659-668.
39. Stone RA, Khurana TS. Gene profiling in experimental models of eye growth: Clues to myopia pathogenesis. *Vision Res* 2010;50:2322-2333.

40. Rymer J, Wildsoet CF. The role of the retinal pigment epithelium in eye growth regulation and myopia: a review. *Vis Neurosci* 2005;22:251-261.
41. Nickla DL, Wallman J. The multifunctional choroid. *Prog Retin Eye Res* 2010;29:144-168.
42. Smith EL, 3rd, Ramamirtham R, Qiao-Grider Y, et al. Effects of foveal ablation on emmetropization and form-deprivation myopia. *Invest Ophthalmol Vis Sci* 2007;48:3914-3922.
43. Liu Y, Wildsoet C. The effect of two-zone concentric bifocal spectacle lenses on refractive error development and eye growth in young chicks. *Invest Ophthalmol Vis Sci* 2011;52:1078-1086.
44. Liu Y, Wildsoet C. The effective add inherent in 2-zone negative lenses inhibits eye growth in myopic young chicks. *Invest Ophthalmol Vis Sci* 2012;53:5085-5093.
45. Ho WC, Ng YF, Chu PH, et al. Impairment of retinal adaptive circuitry in the myopic eye. *Vision Res* 2011;51:367-375.
46. Ritchey ER, Zelinka C, Tang J, et al. Vision-guided ocular growth in a mutant chicken model with diminished visual acuity. *Exp Eye Res* 2012;102:59-69.
47. Fischer AJ, Morgan IG, Stell WK. Colchicine causes excessive ocular growth and myopia in chicks. *Vision Res* 1999;39:685-697.
48. Fischer AJ, Seltner RL, Stell WK. N-methyl-D-aspartate-induced excitotoxicity causes myopia in hatched chicks. *Can J Ophthalmol* 1997;32:373-377.
49. Mariani AP. Amacrine cells of the rhesus monkey retina. *J Comp Neurol* 1990;301:382-400.
50. Kolb H, Linberg KA, Fisher SK. Neurons of the human retina: a Golgi study. *J Comp Neurol* 1992;318:147-187.
51. Fischer AJ, McGuire JJ, Schaeffel F, Stell WK. Light- and focus-dependent expression of the transcription factor ZENK in the chick retina. *Nat Neurosci* 1999;2:706-712.
52. Wallman J. Retinal control of eye growth and refraction. In: Osborne NN, Chader GJ (eds), *Progress in Retinal Research.* New York: Pergamon Press; 1993:133-153.
53. Bitzer M, Schaeffel F. Defocus-induced changes in ZENK expression in the chicken retina. *Invest Ophthalmol Vis Sci* 2002;43:246-252.
54. Fischer AJ, Skorupa D, Schonberg DL, Walton NA. Characterization of glucagon-expressing neurons in the chicken retina. *J Comp Neurol* 2006;496:479-494.
55. Fischer AJ, Ritchey ER, Scott MA, Wynne A. Bullwhip neurons in the retina regulate the size and shape of the eye. *Dev Biol* 2008;317:196-212.
56. Hasegawa S, Terazono K, Nata K, Takada T, Yamamoto H, Okamoto H. Nucleotide sequence determination of chicken glucagon precursor cDNA. Chicken preproglucagon does not contain glucagon-like peptide II. *FEBS Lett* 1990;264:117-120.
57. Feldkaemper MP, Wang HY, Schaeffel F. Changes in retinal and choroidal gene expression during development of refractive errors in chicks. *Invest Ophthalmol Vis Sci* 2000;41:1623-1628.
58. Buck C, Schaeffel F, Simon P, Feldkaemper M. Effects of positive and negative lens treatment on retinal and choroidal glucagon and glucagon receptor mRNA levels in the chicken. *Invest Ophthalmol Vis Sci* 2004;45:402-409.

59. Ashby R, Kozulin P, Megaw PL, Morgan IG. Alterations in ZENK and glucagon RNA transcript expression during increased ocular growth in chickens. *Mol Vis* 2010;16:639-649.
60. Feldkaemper MP, Schaeffel F. Evidence for a potential role of glucagon during eye growth regulation in chicks. *Vis Neurosci* 2002;19:755-766.
61. Feldkaemper MP, Burkhardt E, Schaeffel F. Localization and regulation of glucagon receptors in the chick eye and preproglucagon and glucagon receptor expression in the mouse eye. *Exp Eye Res* 2004;79:321-329.
62. Vessey KA, Lencses KA, Rushforth DA, Hruby VJ, Stell WK. Glucagon receptor agonists and antagonists affect the growth of the chick eye: a role for glucagonergic regulation of emmetropization? *Invest Ophthalmol Vis Sci* 2005;46:3922-3931.
63. Zhu X, Wallman J. Opposite effects of glucagon and insulin on compensation for spectacle lenses in chicks. *Invest Ophthalmol Vis Sci* 2009;50:24-36.
64. Reis RA, Ventura AL, Kubrusly RC, de Mello MC, de Mello FG. Dopaminergic signaling in the developing retina. *Brain Res Rev* 2007;54:181-188.
65. Rohrer B, Stell WK. Localization of putative dopamine D2-like receptors in the chick retina, using in situ hybridization and immunocytochemistry. *Brain Res* 1995;695:110-116.
66. Dearry A, Burnside B. Stimulation of distinct D2 dopaminergic and alpha 2-adrenergic receptors induces light-adaptive pigment dispersion in teleost retinal pigment epithelium. *J Neurochem* 1988;51:1516-1523.
67. Bruinink A, Dawis S, Niemeyer G, Lichtensteiger W. Catecholaminergic binding sites in cat retina, pigment epithelium and choroid. *Exp Eye Res* 1986;43:147-151.
68. Nguyen-Legros J, Versaux-Botteri C, Vernier P. Dopamine receptor localization in the mammalian retina. *Mol Neurobiol* 1999;19:181-204.
69. Kebabian JW, Calne DB. Multiple receptors for dopamine. *Nature* 1979;277:93-96.
70. Vallone D, Picetti R, Borrelli E. Structure and function of dopamine receptors. *Neurosci Biobehav Rev* 2000;24:125-132.
71. Brandies R, Yehuda S. The possible role of retinal dopaminergic system in visual performance. *Neurosci Biobehav Rev* 2008;32:611-656.
72. Cohen Y, Peleg E, Belkin M, Polat U, Solomon AS. Ambient illuminance, retinal dopamine release and refractive development in chicks. *Exp Eye Res* 2012;103:33-40.
73. Megaw P, Morgan I, Boelen M. Vitreal dihydroxyphenylacetic acid (DOPAC) as an index of retinal dopamine release. *J Neurochem* 2001;76:1636-1644.
74. Stone RA, Lin T, Laties AM, Iuvone PM. Retinal dopamine and form-deprivation myopia. *Proc Natl Acad Sci U S A* 1989;86:704-706.
75. Megaw PL, Morgan IG, Boelen MK. Dopaminergic behaviour in chicken retina and the effect of form deprivation. *Aust N Z J Ophthalmol* 1997;25 Suppl 1:S76-78.
76. Ohngemach S, Hagel G, Schaeffel F. Concentrations of biogenic amines in fundal layers in chickens with normal visual experience, deprivation, and after reserpine application. *Vis Neurosci* 1997;14:493-505.
77. Guo SS, Sivak JG, Callender MG, Diehl-Jones B. Retinal dopamine and lens-induced refractive errors in chicks. *Curr Eye Res* 1995;14:385-389.
78. Luft WA, Iuvone PM, Stell WK. Spatial, temporal, and intensive determinants of dopamine release in the chick retina. *Vis Neurosci* 2004;21:627-635.

79. Rohrer B, Spira AW, Stell WK. Apomorphine blocks form-deprivation myopia in chickens by a dopamine D2-receptor mechanism acting in retina or pigmented epithelium. *Vis Neurosci* 1993;10:447-453.
80. McCarthy CS, Megaw P, Devadas M, Morgan IG. Dopaminergic agents affect the ability of brief periods of normal vision to prevent form-deprivation myopia. *Exp Eye Res* 2007;84:100-107.
81. Schmid KL, Wildsoet CF. Inhibitory effects of apomorphine and atropine and their combination on myopia in chicks. *Optom Vis Sci* 2004;81:137-147.
82. Nickla DL, Totonelly K. Dopamine antagonists and brief vision distinguish lens-induced- and form-deprivation-induced myopia. *Exp Eye Res* 2011;93:782-785.
83. Schaeffel F, Hagel G, Bartmann M, Kohler K, Zrenner E. 6-Hydroxy dopamine does not affect lens-induced refractive errors but suppresses deprivation myopia. *Vision Res* 1994;34:143-149.
84. Iuvone PM, Tigges M, Stone RA, Lambert S, Laties AM. Effects of apomorphine, a dopamine receptor agonist, on ocular refraction and axial elongation in a primate model of myopia. *Invest Ophthalmol Vis Sci* 1991;32:1674-1677.
85. Schaeffel F, Bartmann M, Hagel G, Zrenner E. Studies on the role of the retinal dopamine/melatonin system in experimental refractive errors in chickens. *Vision Res* 1995;35:1247-1264.
86. Hutchins JB. Acetylcholine as a neurotransmitter in the vertebrate retina. *Exp Eye Res* 1987;45:1-38.
87. Eckenstein F, Thoenen H. Production of specific antisera and monoclonal antibodies to choline acetyltransferase: characterization and use for identification of cholinergic neurons. *Embo J* 1982;1:363-368.
88. Voigt T. Cholinergic amacrine cells in the rat retina. *J Comp Neurol* 1986;248:19-35.
89. Millar T, Ishimoto I, Johnson CD, Epstein ML, Chubb IW, Morgan IG. Cholinergic and acetylcholinesterase-containing neurons of the chicken retina. *Neurosci Lett* 1985;61:311-316.
90. Spira AW, Millar TJ, Ishimoto I, et al. Localization of choline acetyltransferase-like immunoreactivity in the embryonic chick retina. *J Comp Neurol* 1987;260:526-538.
91. Baughman RW, Bader CR. Biochemical characterization and cellular localization of the cholinergic system in the chicken retina. *Brain Res* 1977;138:469-485.
92. Fukuda K, Kubo T, Akiba I, Maeda A, Mishina M, Numa S. Molecular distinction between muscarinic acetylcholine receptor subtypes. *Nature* 1987;327:623-625.
93. Nathanson NM. Molecular properties of the muscarinic acetylcholine receptor. *Annu Rev Neurosci* 1987;10:195-236.
94. Tietje KM, Nathanson NM. Embryonic chick heart expresses multiple muscarinic acetylcholine receptor subtypes. Isolation and characterization of a gene encoding a novel m2 muscarinic acetylcholine receptor with high affinity for pirenzepine. *J Biol Chem* 1991;266:17382-17387.
95. Tietje KM, Goldman PS, Nathanson NM. Cloning and functional analysis of a gene encoding a novel muscarinic acetylcholine receptor expressed in chick heart and brain. *J Biol Chem* 1990;265:2828-2834.
96. Gadbut AP, Galper JB. A novel M3 muscarinic acetylcholine receptor is expressed in chick atrium and ventricle. *J Biol Chem* 1994;269:25823-25829.

97. Creason S, Tietje KM, Nathanson NM. Isolation and functional characterization of the chick M5 muscarinic acetylcholine receptor gene. *J Neurochem* 2000;74:882-885.
98. Fischer AJ, McKinnon LA, Nathanson NM, Stell WK. Identification and localization of muscarinic acetylcholine receptors in the ocular tissues of the chick. *J Comp Neurol* 1998;392:273-284.
99. McKinnon LA, Nathanson NM. Tissue-specific regulation of muscarinic acetylcholine receptor expression during embryonic development. *J Biol Chem* 1995;270:20636-20642.
100. Pilar G, Nunez R, McLennan IS, Meriney SD. Muscarinic and nicotinic synaptic activation of the developing chicken iris. *J Neurosci* 1987;7:3813-3826.
101. Meriney SD, Pilar G. Cholinergic innervation of the smooth muscle cells in the choroid coat of the chick eye and its development. *J Neurosci* 1987;7:3827-3839.
102. McBrien NA, Jobling AI, Truong HT, Cottriall CL, Gentle A. Expression of muscarinic receptor subtypes in tree shrew ocular tissues and their regulation during the development of myopia. *Mol Vis* 2009;15:464-475.
103. Schmidt M, Humphrey MF, Wassle H. Action and localization of acetylcholine in the cat retina. *J Neurophysiol* 1987;58:997-1015.
104. Schmid K, Wildsoet C. Inhibitory effects of apomorphine and atropine and their combination on myopia in chicks. *Optom Vis Sci* 2004;81:137-147.
105. Stone RA, Lin T, Laties AM. Muscarinic antagonist effects on experimental chick myopia. *Exp Eye Res* 1991;52:755-758.
106. McBrien NA, Moghaddam HO, Reeder AP. Atropine reduces experimental myopia and eye enlargement via a nonaccommodative mechanism. *Invest Ophthalmol Vis Sci* 1993;34:205-215.
107. Cottriall CL, McBrien NA. The M1 muscarinic antagonist pirenzepine reduces myopia and eye enlargement in the tree shrew. *Invest Ophthalmol Vis Sci* 1996;37:1368-1379.
108. Cottriall CL, McBrien NA, Annies R, Leech EM. Prevention of form-deprivation myopia with pirenzepine: a study of drug delivery and distribution. *Ophthalmic Physiol Opt* 1999;19:327-335.
109. Luft WA, Ming Y, Stell WK. Variable effects of previously untested muscarinic receptor antagonists on experimental myopia. *Invest Ophthalmol Vis Sci* 2003;44:1330-1338.
110. McBrien NA, Cottriall CL, Annies R. Retinal acetylcholine content in normal and myopic eyes: a role in ocular growth control? *Vis Neurosci* 2001;18:571-580.
111. Pendrak K, Lin T, Stone RA. Ciliary ganglion choline acetyltransferase activity in avian macrophthalmos. *Exp Eye Res* 1995;60:237-243.
112. Fischer AJ, Miethke P, Morgan IG, Stell WK. Cholinergic amacrine cells are not required for the progression and atropine-mediated suppression of form-deprivation myopia. *Brain Res* 1998;794:48-60.
113. Lind GJ, Chew SJ, Marzani D, Wallman J. Muscarinic acetylcholine receptor antagonists inhibit chick scleral chondrocytes. *Invest Ophthalmol Vis Sci* 1998;39:2217-2231.
114. Schwahn HN, Kaymak H, Schaeffel F. Effects of atropine on refractive development, dopamine release, and slow retinal potentials in the chick. *Vis Neurosci* 2000;17:165-176.

115. Means AL, Gudas LJ. The roles of retinoids in vertebrate development. *Annu Rev Biochem* 1995;64:201-233.
116. Mangelsdorf DJ, Thummel C, Beato M, et al. The nuclear receptor superfamily: the second decade. *Cell* 1995;83:835-839.
117. Seko Y, Shimizu M, Tokoro T. Retinoic acid increases in the retina of the chick with form deprivation myopia. *Ophthalmic Res* 1998;30:361-367.
118. Mertz JR, Wallman J. Choroidal retinoic acid synthesis: a possible mediator between refractive error and compensatory eye growth. *Exp Eye Res* 2000;70:519-527.
119. Mertz JR, Howlett MHC, McFadden SA, Wallman J. Retinoic acid from both the retina and choroid influences eye growth. *Invest Ophthalmol Vis Sci (ARVO Suppl)* 1999;40:S849.
120. McFadden SA, Howlett MH, Mertz JR. Retinoic acid signals the direction of ocular elongation in the guinea pig eye. *Vision Res* 2004;44:643-653.
121. Mao JF, Liu SZ, Dou XQ. Retinoic acid metabolic change in retina and choroid of the guinea pig with lens-induced myopia. *Int J Ophthalmol* 2012;5:670-674.
122. Seko Y, Shimokawa H, Tokoro T. In vivo and in vitro association of retinoic acid with form-deprivation myopia in the chick. *Exp Eye Res* 1996;63:443-452.
123. Bitzer M, Feldkaemper M, Schaeffel F. Visually induced changes in components of the retinoic acid system in fundal layers of the chick. *Exp Eye Res* 2000;70:97-106.
124. Troilo D, Nickla DL, Mertz JR, Summers Rada JA. Change in the synthesis rates of ocular retinoic acid and scleral glycosaminoglycan during experimentally altered eye growth in marmosets. *Invest Ophthalmol Vis Sci* 2006;47:1768-1777.
125. Stone RA, Laties AM, Raviola E, Wiesel TN. Increase in retinal vasoactive intestinal polypeptide after eyelid fusion in primates. *Proc Natl Acad Sci U S A* 1988;85:257-260.
126. Seltner RL, Stell WK. The effect of vasoactive intestinal peptide on development of form deprivation myopia in the chick: a pharmacological and immunocytochemical study. *Vision Res* 1995;35:1265-1270.
127. Tkatchenko AV, Walsh PA, Tkatchenko TV, Gustincich S, Raviola E. Form deprivation modulates retinal neurogenesis in primate experimental myopia. *Proc Natl Acad Sci U S A* 2006;103:4681-4686.
128. Feldkaemper MP, Schaeffel F. Insulin inhibits compensation of plus lenses in chicks and stimulates myopia development *Invest Ophthalmol Vis Sci* 2007;48: E-Abstract 5924.
129. Zhu X, Chandrasekar D, Wallman J. Insulin has effects on chick eyes opposite to those of glucagon. *Invest Ophthalmol Vis Sci* 2007;48: E-Abstract 5925.
130. Rohrer B, Stell WK. Basic fibroblast growth factor (bFGF) and transforming growth factor beta (TGF-beta) act as stop and go signals to modulate postnatal ocular growth in the chick. *Exp Eye Res* 1994;58:553-561.
131. Simon P, Feldkaemper M, Bitzer M, Ohngemach S, Schaeffel F. Early transcriptional changes of retinal and choroidal TGFbeta-2, RALDH-2, and ZENK following imposed positive and negative defocus in chickens. *Mol Vis* 2004;10:588-597.
132. Ashby R, McCarthy CS, Maleszka R, Megaw P, Morgan IG. A muscarinic cholinergic antagonist and a dopamine agonist rapidly increase ZENK mRNA expression in the form-deprived chicken retina. *Exp Eye Res* 2007;85:15-22.

133. McGlinn AM, Baldwin DA, Tobias JW, Budak MT, Khurana TS, Stone RA. Form-deprivation myopia in chick induces limited changes in retinal gene expression. *Invest Ophthalmol Vis Sci* 2007;48:3430-3436.
134. Stone RA, McGlinn AM, Baldwin DA, Tobias JW, Iuvone PM, Khurana TS. Image defocus and altered retinal gene expression in chick: clues to the pathogenesis of ametropia. *Invest Ophthalmol Vis Sci* 2011;52:5765-5777.
135. Strauss O. The retinal pigment epithelium in visual function. *Physiol Rev* 2005;85:845-881.
136. Wimmers S, Karl MO, Strauss O. Ion channels in the RPE. *Prog Retin Eye Res* 2007;26:263-301.
137. Marmor M, Wolfensberger T. *The retinal pigment epithelium: function and disease*: Oxford University Press; 1998:745.
138. Buck C, Schaeffel F, Simon P, Feldkaemper M. Effects of positive and negative lens treatment on retinal and choroidal glucagon and glucagon receptor mRNA levels in the chicken. *Invest Ophthalmol Vis Sci* 2004;45:402-409.
139. Friedman Z, Hackett SF, Campochiaro PA. Human retinal pigment epithelial cells possess muscarinic receptors coupled to calcium mobilization. *Brain Res* 1988;446:11-16.
140. Zhang Y, Liu Y, Wildsoet CF. Bidirectional, optical sign-dependent regulation of BMP2 gene expression in chick retinal pigment epithelium. *Invest Ophthalmol Vis Sci* 2012;53:6072-6080.
141. Zhang Y, Liu Y, Ho Carol, Hammond D, CF. W. Differential expression of BMP7, TGF-β2, and noggin in chick RPE after imposed optical defocus *Invest Ophthalmol Vis Sci 53, E-Abstract 3458* 2012.
142. Lin T, Grimes PA, Stone RA. Expansion of the retinal pigment epithelium in experimental myopia. *Vision Res* 1993;33:1881-1885.
143. Zhang Y, Liu Y, Xu J, Nimri N, Wildsoet CF. Microarray analysis of RPE gene expression in chicks during long-term imposed hyperopic defocus. *Invest Ophthalmol Vis Sci* 2010;51: E-Abstract 3680.
144. Fleming PA, Harman AM, Beazley LD. Changing topography of the RPE resulting from experimentally induced rapid eye growth. *Vis Neurosci* 1997;14:449-461.
145. Harman AM, Hoskins R, Beazley LD. Experimental eye enlargement in mature animals changes the retinal pigment epithelium. *Vis Neurosci* 1999;16:619-628.
146. Rodgers RL. Glucagon and cyclic AMP: time to turn the page? *Curr Diabetes Rev* 2012;8:362-381.
147. Zhao P, Cladman W, Van Tol HH, Chidiac P. Fine-tuning of GPCR signals by intracellular G protein modulators. *Prog Mol Biol Transl Sci* 2013;115:421-453.
148. Koh SW, Chader GJ. Elevation of intracellular cyclic AMP and stimulation of adenylate cyclase activity by vasoactive intestinal peptide and glucagon in the retinal pigment epithelium. *J Neurochem* 1984;43:1522-1526.
149. Dong F, An JH, Ren YP, et al. [Expression of dopamine receptor D2 and adenosine receptor A2A in human retinal pigment epithelium]. *Zhonghua Yan Ke Za Zhi* 2007;43:1110-1113.
150. Dearry A, Falardeau P, Shores C, Caron MG. D2 dopamine receptors in the human retina: cloning of cDNA and localization of mRNA. *Cell Mol Neurobiol* 1991;11:437-453.

151. Zhang Y, Maminishkis A, Zhi C, et al. Apomorphine regulates TGF-β1 and TGF-β2 expression in human fetal retinal pigment epithelial cells. *Invest Ophthalmol Vis Sci* 2009;50: E-Abstract 3845.
152. Gallemore RP, Steinberg RH. Effects of dopamine on the chick retinal pigment epithelium. Membrane potentials and light-evoked responses. *Invest Ophthalmol Vis Sci* 1990;31:67-80.
153. Seko Y, Tanaka Y, Tokoro T. Apomorphine inhibits the growth-stimulating effect of retinal pigment epithelium on scleral cells in vitro. *Cell Biochem Funct* 1997;15:191-196.
154. Chua W-H, Balakrishnan V, Chan Y-H, et al. Atropine for the treatment of childhood myopia. *Ophthalmology* 2006;113:2285-2291.
155. Friedman Z, Hackett SF, Campochiaro PA. Human retinal pigment epithelial cells possess muscarinic receptors coupled to calcium mobilization. *Brain Res* 1988;446:11-16.
156. Osborne NN, FitzGibbon F, Schwartz G. Muscarinic acetylcholine receptor-mediated phosphoinositide turnover in cultured human retinal pigment epithelium cells. *Vision Res* 1991;31:1119-1127.
157. Salceda R. Muscarinic receptors binding in retinal pigment epithelium during rat development. *Neurochem Res* 1994;19:1207-1210.
158. de The H, Marchio A, Tiollais P, Dejean A. Differential expression and ligand regulation of the retinoic acid receptor alpha and beta genes. *Embo J* 1989;8:429-433.
159. Balmer JE, Blomhoff R. Gene expression regulation by retinoic acid. *J Lipid Res* 2002;43:1773-1808.
160. Waldbillig RJ, Arnold DR, Fletcher RT, Chader GJ. Insulin and IGF-I binding in developing chick neural retina and pigment epithelium: a characterization of binding and structural differences. *Exp Eye Res* 1991;53:13-22.
161. Zhang Z, Geller S, Su J, Flannery JG, Wildsoet CF. Effect of imposed defocus on the profile of gene expression in chick retinal pigment epithelium. *Invest Ophthalmol Vis Sc* 2007;48: E-Abstract 4417.
162. Koh SW. VIP stimulation of polarized macromolecule secretion in cultured chick embryonic retinal pigment epithelium. *Exp Cell Res* 1991;197:1-7.
163. Martin DM, Yee D, Feldman EL. Gene expression of the insulin-like growth factors and their receptors in cultured human retinal pigment epithelial cells. *Brain Res Mol Brain Res* 1992;12:181-186.
164. Takagi H, Yoshimura N, Tanihara H, Honda Y. Insulin-like growth factor-related genes, receptors, and binding proteins in cultured human retinal pigment epithelial cells. *Invest Ophthalmol Vis Sci* 1994;35:916-923.
165. Kvanta A. Expression and secretion of transforming growth factor-beta in transformed and nontransformed retinal pigment epithelial cells. *Ophthalmic Res* 1994;26:361-367.
166. Tanihara H, Yoshida M, Matsumoto M, Yoshimura N. Identification of transforming growth factor-beta expressed in cultured human retinal pigment epithelial cells. *Invest Ophthalmol Vis Sci* 1993;34:413-419.

167. Jacquemin E, Halley C, Alterio J, Laurent M, Courtois Y, Jeanny JC. Localization of acidic fibroblast growth factor (aFGF) mRNA in mouse and bovine retina by in situ hybridization. *Neurosci Lett* 1990;116:23-28.
168. Sternfeld MD, Robertson JE, Shipley GD, Tsai J, Rosenbaum JT. Cultured human retinal pigment epithelial cells express basic fibroblast growth factor and its receptor. *Curr Eye Res* 1989;8:1029-1037.
169. Alge-Priglinger CS, Kreutzer T, Obholzer K, et al. Oxidative stress-mediated induction of MMP-1 and MMP-3 in human RPE cells. *Invest Ophthalmol Vis Sci* 2009;50:5495-5503.
170. Alexander JP, Bradley JM, Gabourel JD, Acott TS. Expression of matrix metalloproteinases and inhibitor by human retinal pigment epithelium. *Invest Ophthalmol Vis Sci* 1990;31:2520-2528.
171. Zhang Y, Liu Y, Hammond D, Wildsoet CF. Possible roles of BMP2 and BMP4 in chick RPE in signaling the sign of defocus. *InInvest Ophthalmol Vis Sci* 2011;52:E-Abstract 6320.
172. De Stefano ME, Mugnaini E. Fine structure of the choroidal coat of the avian eye. Lymphatic vessels. *Invest Ophthalmol Vis Sci* 1997;38:1241-1260.
173. De Stefano ME, Mugnaini E. Fine structure of the choroidal coat of the avian eye. Vascularization, supporting tissue and innervation. *Anat Embryol (Berl)* 1997;195:393-418.
174. Pendrak K, Papastergiou GI, Lin T, Laties AM, Stone RA. Choroidal vascular permeability in visually regulated eye growth. *Exp Eye Res* 2000;70:629-637.
175. Junghans BM, Crewther SG, Liang H, Crewther DP. A role for choroidal lymphatics during recovery from form deprivation myopia? *Optom Vis Sci* 1999;76:796-803.
176. Hirata A, Negi A. Morphological changes of choriocapillaris in experimentally induced chick myopia. *Graefes Arch Clin Exp Ophthalmol* 1998;236:132-137.
177. Wallman J, Wildsoet C, Xu A, et al. Moving the retina: choroidal modulation of refractive state. *Vision Res* 1995;35:37-50.
178. Nickla DL. Transient increases in choroidal thickness are consistently associated with brief daily visual stimuli that inhibit ocular growth in chicks. *Exp Eye Res* 2007;84:951-959.
179. Zhu X, Park TW, Winawer J, Wallman J. In a matter of minutes, the eye can know which way to grow. *Invest Ophthalmol Vis Sci* 2005;46:2238-2241.
180. Kee CS, Marzani D, Wallman J. Differences in time course and visual requirements of ocular responses to lenses and diffusers. *Invest Ophthalmol Vis Sci* 2001;42:575-583.
181. Hu W, Criswell MH, Fong SL, et al. Differences in the temporal expression of regulatory growth factors during choroidal neovascular development. *Exp Eye Res* 2009;88:79-91.
182. Lambert V, Munaut C, Jost M, et al. Matrix metalloproteinase-9 contributes to choroidal neovascularization. *Am J Pathol* 2002;161:1247-1253.
183. Wang Y, Gillies C, Cone RE, O'Rourke J. Extravascular secretion of t-PA by the intact superfused choroid. *Invest Ophthalmol Vis Sci* 1995;36:1625-1632.
184. Lutty GA, Merges C, Threlkeld AB, Crone S, McLeod DS. Heterogeneity in localization of isoforms of TGF-beta in human retina, vitreous, and choroid. *Invest Ophthalmol Vis Sci* 1993;34:477-487.

185. Jobling AI, Wan R, Gentle A, Bui BV, McBrien NA. Retinal and choroidal TGF-beta in the tree shrew model of myopia: isoform expression, activation and effects on function. *Exp Eye Res* 2009;88:458-466.
186. Rada JA, Hollaway LR, Lam W, Li N, Napoli JL. Identification of RALDH2 as a visually regulated retinoic acid synthesizing enzyme in the chick choroid. *Invest Ophthalmol Vis Sci* 2012;53:1649-1662.
187. Dhillon B, Nickla D. The ocular growth inhibition effected by dopamine agonists and atropine is associated with transient increases in choroidal thickness in chicks. *Invest Ophthalmol Vis Sci E-Abstract 1732* 2008.
188. Nickla DL, Cheng AT. Atropine and apomorphine in emmetropization: evidence for inhibitory interactions on a common growth regulatory pathway. *Invest Ophthalmol Vis Sci E-Abstract 3848* 2009.
189. Marshall GE. Human scleral elastic system: an immunoelectron microscopic study. *Br J Ophthalmol* 1995;79:57-64.
190. Rada JA, Nickla DL, Troilo D. Decreased proteoglycan synthesis associated with form deprivation myopia in mature primate eyes. *Invest Ophthalmol Vis Sci* 2000;41:2050-2058.
191. Kang RN, Norton TT. Alteration of scleral morphology in tree shrews with induced myopia. *Invest Ophthalmol Vis Sci 34, S1209* 1993.
192. McBrien NA, Cornell LM, Gentle A. Structural and ultrastructural changes to the sclera in a mammalian model of high myopia. *Invest Ophthalmol Vis Sci* 2001;42:2179-2187.
193. Rada JA, Brenza HL. Increased latent gelatinase activity in the sclera of visually deprived chicks. *Invest Ophthalmol Vis Sci* 1995;36:1555-1565.
194. Norton TT, Rada JA. Reduced extracellular matrix in mammalian sclera with induced myopia. *Vision Res* 1995;35:1271-1281.
195. Gentle A, Liu Y, Martin JE, Conti GL, McBrien NA. Collagen gene expression and the altered accumulation of scleral collagen during the development of high myopia. *J Biol Chem* 2003;278:16587-16594.
196. Guggenheim JA, McBrien NA. Form-deprivation myopia induces activation of scleral matrix metalloproteinase-2 in tree shrew. *Invest Ophthalmol Vis Sci* 1996;37:1380-1395.
197. Siegwart JT, Jr., Norton TT. The time course of changes in mRNA levels in tree shrew sclera during induced myopia and recovery. *Invest Ophthalmol Vis Sci* 2002;43:2067-2075.
198. Gao H, Frost MR, Siegwart JT, Jr., Norton TT. Patterns of mRNA and protein expression during minus-lens compensation and recovery in tree shrew sclera. *Mol Vis* 2011;17:903-919.
199. Gentle A, McBrien NA. Retinoscleral control of scleral remodelling in refractive development: a role for endogenous FGF-2? *Cytokine* 2002;18:344-348.
200. Phillips JR, Khalaj M, McBrien NA. Induced myopia associated with increased scleral creep in chick and tree shrew eyes. *Invest Ophthalmol Vis Sci* 2000;41:2028-2034.
201. Siegwart JT, Jr., Norton TT. Regulation of the mechanical properties of tree shrew sclera by the visual environment. *Vision Res* 1999;39:387-407.
202. Gottlieb MD, Joshi HB, Nickla DL. Scleral changes in chicks with form-deprivation myopia. *Curr Eye Res* 1990;9:1157-1165.

203. Kusakari T, Sato T, Tokoro T. Regional scleral changes in form-deprivation myopia in chicks. *Exp Eye Res* 1997;64:465-476.
204. Christensen AM, Wallman J. Evidence that increased scleral growth underlies visual deprivation myopia in chicks. *Invest Ophthalmol Vis Sci* 1991;32:2143-2150.
205. Rada JA, Thoft RA, Hassell JR. Increased aggrecan (cartilage proteoglycan) production in the sclera of myopic chicks. *Dev Biol* 1991;147:303-312.
206. Seko Y, Tanaka Y, Tokoro T. Influence of bFGF as a potent growth stimulator and TGF-beta as a growth regulator on scleral chondrocytes and scleral fibroblasts in vitro. *Ophthalmic Res* 1995;27:144-152.
207. Hu J, Cui D, Yang X, et al. Bone morphogenetic protein-2: a potential regulator in scleral remodeling. *Mol Vis* 2008;14:2373-2380.
208. Wang Q, Zhao G, Xing S, Zhang L, Yang X. Role of bone morphogenetic proteins in form-deprivation myopia sclera. *Mol Vis* 2011;17:647-657.
209. Vincenti MP, White LA, Schroen DJ, Benbow U, Brinckerhoff CE. Regulating expression of the gene for matrix metalloproteinase-1 (collagenase): mechanisms that control enzyme activity, transcription, and mRNA stability. *Crit Rev Eukaryot Gene Expr* 1996;6:391-411.
210. Liu Q, Wu J, Wang X, Zeng J. Changes in muscarinic acetylcholine receptor expression in form deprivation myopia in guinea pigs. *Mol Vis* 2007;13:1234-1244.
211. Gwiazda J. Treatment options for myopia. *Optom Vis Sci* 2009;86:624-628.
212. Tong L, Wong EH, Chan YH, Balakrishnan V. A multiple regression approach to study optical components of myopia in Singapore school children. *Ophthalmic Physiol Opt* 2002;22:32-37.
213. Saw SM, Carkeet A, Chia KS, Stone RA, Tan DT. Component dependent risk factors for ocular parameters in Singapore Chinese children. *Ophthalmology* 2002;109:2065-2071.
214. Mutti DO, Mitchell GL, Moeschberger ML, Jones LA, Zadnik K. Parental myopia, near work, school achievement, and children's refractive error. *Invest Ophthalmol Vis Sci* 2002;43:3633-3640.
215. Jones LA, Sinnott LT, Mutti DO, Mitchell GL, Moeschberger ML, Zadnik K. Parental history of myopia, sports and outdoor activities, and future myopia. *Invest Ophthalmol Vis Sci* 2007;48:3524-3532.
216. Tse DY, To CH. Graded competing regional myopic and hyperopic defocus produce summated emmetropization set points in chick. *Invest Ophthalmol Vis Sci* 2011;52:8056-8062.
217. Sankaridurg P, Holden B, Smith E, 3rd, et al. Decrease in rate of myopia progression with a contact lens designed to reduce relative peripheral hyperopia: one-year results. *Invest Ophthalmol Vis Sci* 2011;52:9362-9367.
218. Anstice NS, Phillips JR. Effect of dual-focus soft contact lens wear on axial myopia progression in children. *Ophthalmology* 2011;118:1152-1161.
219. Cho P, Cheung SW. Retardation of myopia in Orthokeratology (ROMIO) study: a 2-year randomized clinical trial. *Invest Ophthalmol Vis Sci* 2012;53:7077-7085.
220. Song YY, Wang H, Wang BS, Qi H, Rong ZX, Chen HZ. Atropine in ameliorating the progression of myopia in children with mild to moderate myopia: a meta-analysis of controlled clinical trials. *J Ocul Pharmacol Ther* 2011;27:361-368.

221. Lee JJ, Fang PC, Yang IH, et al. Prevention of myopia progression with 0.05% atropine solution. *J Ocul Pharmacol Ther* 2006;22:41-46.
222. Chia A, Chua WH, Cheung YB, et al. Atropine for the treatment of childhood myopia: safety and efficacy of 0.5%, 0.1%, and 0.01% doses (Atropine for the Treatment of Myopia 2). *Ophthalmology* 2012;119:347-354.
223. Ward B, Tarutta EP, Mayer MJ. The efficacy and safety of posterior pole buckles in the control of progressive high myopia. *Eye* 2009;Ahead of print. doi: 10.1038/eye.2008.1433.
224. Su J, Wall ST, Healy KE, Wildsoet CF. Scleral reinforcement through host tissue integration with biomimetic enzymatically degradable semi-interpenetrating polymer network. *Tissue Eng Part A* 2010;16:905-916.
225. Gharbiya M, Cruciani F, Parisi F, Cuozzo G, Altimari S, Abdolrahimzadeh S. Long-term results of intravitreal bevacizumab for choroidal neovascularisation in pathological myopia. *Br J Ophthalmol* 2012;96:1068-1072.
226. Irving EL, Sivak JG, Callender MG. Refractive plasticity of the developing chick eye. *Ophthalmic Physiol Opt* 1992;12:448-456.
227. Papastergiou GI, Schmid GF, Laties AM, Pendrak K, Lin T, Stone RA. Induction of axial eye elongation and myopic refractive shift in one-year-old chickens. *Vision Res* 1998;38:1883-1888.
228. Kocur I, Resnikoff S. New challenges for VISION 2020. *Ophthalmic Epidemiol* 2005;12:291-292.
229. Goldschmidt E. Refraction in the newborn. *Acta Ophthalmol (Copenh)* 1969;47:570-578.
230. Graham MV, Gray OP. Refraction of premature babies' eyes. *Br Med J* 1963;1:1452-1454.
231. Deng L, Gwiazda J. Birth season, photoperiod, and infancy refraction. *Optom Vis Sci* 2011;88:383-387.
232. Saw SM, Tong L, Chua WH, et al. Incidence and progression of myopia in Singaporean school children. *Invest Ophthalmol Vis Sci* 2005;46:51-57.
233. McBrien NA, Norton TT. The development of experimental myopia and ocular component dimensions in monocularly lid-sutured tree shrews (Tupaia belangeri). *Vision Res* 1992;32:843-852.
234. Smith EL, 3rd, Hung LF. The role of optical defocus in regulating refractive development in infant monkeys. *Vision Res* 1999;39:1415-1435.
235. Wagner DO, Sieber C, Bhushan R, Borgermann JH, Graf D, Knaus P. BMPs: from bone to body morphogenetic proteins. *Sci Signal* 2010;3:mr1.
236. Chen D, Zhao M, Mundy GR. Bone morphogenetic proteins. *Growth Factors* 2004;22:233-241.
237. Plas DT, Dhande OS, Lopez JE, et al. Bone morphogenetic proteins, eye patterning, and retinocollicular map formation in the mouse. *J Neurosci* 2008;28:7057-7067.
238. Hogan BL. Bmps: multifunctional regulators of mammalian embryonic development. *Harvey Lect* 1996;92:83-98.
239. Derynck R, Miyazono K. *The TGF-β family*. Cold Spring Harbor, New York: : Cold Spring Harbor Laboratory Press 2008:1-149.
240. Bandyopadhyay A, Yadav PS, Prashar P. BMP signaling in development and diseases: A pharmacological perspective. *Biochem Pharmacol* 2013.

241. Belecky-Adams T, Adler R. Developmental expression patterns of bone morphogenetic proteins, receptors, and binding proteins in the chick retina. *J Comp Neurol* 2001;430:562-572.
242. Sakuta H, Takahashi H, Shintani T, Etani K, Aoshima A, Noda M. Role of bone morphogenic protein 2 in retinal patterning and retinotectal projection. *J Neurosci* 2006;26:10868-10878.
243. Mathura JR, Jr., Jafari N, Chang JT, et al. Bone morphogenetic proteins-2 and -4: negative growth regulators in adult retinal pigmented epithelium. *Invest Ophthalmol Vis Sci* 2000;41:592-600.
244. Fischer AJ, Schmidt M, Omar G, Reh TA. BMP4 and CNTF are neuroprotective and suppress damage-induced proliferation of Muller glia in the retina. *Mol Cell Neurosci* 2004;27:531-542.
245. Lyons KM, Hogan BL, Robertson EJ. Colocalization of BMP 7 and BMP 2 RNAs suggests that these factors cooperatively mediate tissue interactions during murine development. *Mech Dev* 1995;50:71-83.
246. Muller F, Rohrer H, Vogel-Hopker A. Bone morphogenetic proteins specify the retinal pigment epithelium in the chick embryo. *Development* 2007;134:3483-3493.
247. Xu J, Zhu D, Sonoda S, et al. Over-expression of BMP4 inhibits experimental choroidal neovascularization by modulating VEGF and MMP-9. *Angiogenesis* 2012;15:213-227.
248. Dudley AT, Lyons KM, Robertson EJ. A requirement for bone morphogenetic protein-7 during development of the mammalian kidney and eye. *Genes Dev* 1995;9:2795-2807.
249. Bakrania P, Efthymiou M, Klein JC, et al. Mutations in BMP4 cause eye, brain, and digit developmental anomalies: overlap between the BMP4 and hedgehog signaling pathways. *Am J Hum Genet* 2008;82:304-319.
250. Hillger F, Herr G, Rudolph R, Schwarz E. Biophysical comparison of BMP-2, ProBMP-2, and the free pro-peptide reveals stabilization of the pro-peptide by the mature growth factor. *J Biol Chem* 2005;280:14974-14980.
251. Israel DI, Nove J, Kerns KM, Moutsatsos IK, Kaufman RJ. Expression and characterization of bone morphogenetic protein-2 in Chinese hamster ovary cells. *Growth Factors* 1992;7:139-150.
252. Wang EA, Rosen V, D'Alessandro JS, et al. Recombinant human bone morphogenetic protein induces bone formation. *Proc Natl Acad Sci U S A* 1990;87:2220-2224.
253. Scheufler C, Sebald W, Hulsmeyer M. Crystal structure of human bone morphogenetic protein-2 at 2.7 A resolution. *J Mol Biol* 1999;287:103-115.
254. Mueller TD, Nickel J. Promiscuity and specificity in BMP receptor activation. *FEBS Lett* 2012;586:1846-1859.
255. Felin JE, Mayo JL, Loos TJ, et al. Nuclear variants of bone morphogenetic proteins. *BMC Cell Biol* 2010;11:20.
256. Cui Y, Hackenmiller R, Berg L, et al. The activity and signaling range of mature BMP-4 is regulated by sequential cleavage at two sites within the prodomain of the precursor. *Genes Dev* 2001;15:2797-2802.
257. Klosch B, Furst W, Kneidinger R, et al. Expression and purification of biologically active rat bone morphogenetic protein-4 produced as inclusion bodies in recombinant Escherichia coli. *Biotechnol Lett* 2005;27:1559-1564.

258. Nelsen SM, Christian JL. Site-specific cleavage of BMP4 by furin, PC6, and PC7. *J Biol Chem* 2009;284:27157-27166.
259. Bessa PC, Cerqueira MT, Rada T, et al. Expression, purification and osteogenic bioactivity of recombinant human BMP-4, -9, -10, -11 and -14. *Protein Expr Purif* 2009;63:89-94.
260. Monroe DG, Jin DF, Sanders MM. Estrogen opposes the apoptotic effects of bone morphogenetic protein 7 on tissue remodeling. *Mol Cell Biol* 2000;20:4626-4634.
261. Urist MR. Bone: formation by autoinduction. *Science* 1965;150:893-899.
262. Wozney JM, Rosen V, Celeste AJ, et al. Novel regulators of bone formation: molecular clones and activities. *Science* 1988;242:1528-1534.
263. Wordinger RJ, Clark AF. Bone morphogenetic proteins and their receptors in the eye. *Exp Biol Med (Maywood)* 2007;232:979-992.
264. Tominaga T, Abe H, Ueda O, et al. Activation of bone morphogenetic protein 4 signaling leads to glomerulosclerosis that mimics diabetic nephropathy. *J Biol Chem* 2011;286:20109-20116.
265. Trousse F, Esteve P, Bovolenta P. Bmp4 mediates apoptotic cell death in the developing chick eye. *J Neurosci* 2001;21:1292-1301.
266. Behesti H, Holt JK, Sowden JC. The level of BMP4 signaling is critical for the regulation of distinct T-box gene expression domains and growth along the dorso-ventral axis of the optic cup. *BMC Dev Biol* 2006;6:62.
267. Cui W, Bryant MR, Sweet PM, McDonnell PJ. Changes in gene expression in response to mechanical strain in human scleral fibroblasts. *Exp Eye Res* 2004;78:275-284.
268. Sehgal R, Andres DJ, Adler R, Belecky-Adams TL. Bone morphogenetic protein 7 increases chick photoreceptor outer segment initiation. *Invest Ophthalmol Vis Sci* 2006;47:3625-3634.
269. Shen W, Finnegan S, Lein P, Sullivan S, Slaughter M, Higgins D. Bone morphogenetic proteins regulate ionotropic glutamate receptors in human retina. *Eur J Neurosci* 2004;20:2031-2037.
270. Francis PH, Richardson MK, Brickell PM, Tickle C. Bone morphogenetic proteins and a signalling pathway that controls patterning in the developing chick limb. *Development* 1994;120:209-218.
271. Rogers MB, Rosen V, Wozney JM, Gudas LJ. Bone morphogenetic proteins-2 and -4 are involved in the retinoic acid-induced differentiation of embryonal carcinoma cells. *Mol Biol Cell* 1992;3:189-196.
272. Abrams KL, Xu J, Nativelle-Serpentini C, Dabirshahsahebi S, Rogers MB. An evolutionary and molecular analysis of Bmp2 expression. *J Biol Chem* 2004;279:15916-15928.
273. Helvering LM, Sharp RL, Ou X, Geiser AG. Regulation of the promoters for the human bone morphogenetic protein 2 and 4 genes. *Gene* 2000;256:123-138.
274. Reddi AH. Morphogenetic messages are in the extracellular matrix: biotechnology from bench to bedside. *Biochem Soc Trans* 2000;28:345-349.
275. Goldman DC, Donley N, Christian JL. Genetic interaction between Bmp2 and Bmp4 reveals shared functions during multiple aspects of mouse organogenesis. *Mech Dev* 2009;126:117-127.
276. Kawabata M, Imamura T, Miyazono K. Signal transduction by bone morphogenetic proteins. *Cytokine Growth Factor Rev* 1998;9:49-61.

277. Chalazonitis A, D'Autreaux F, Guha U, et al. Bone morphogenetic protein-2 and -4 limit the number of enteric neurons but promote development of a TrkC-expressing neurotrophin-3-dependent subset. *J Neurosci* 2004;24:4266-4282.
278. Bartmann M, Schaeffel F, Hagel G, Zrenner E. Constant light affects retinal dopamine levels and blocks deprivation myopia but not lens-induced refractive errors in chickens. *Vis Neurosci* 1994;11:199-208.
279. Ohngemach S, Buck C, Simon P, Schaeffel F, Feldkaemper M. Temporal changes of novel transcripts in the chicken retina following imposed defocus. *Mol Vis* 2004;10:1019-1027.
280. Schippert R, Brand C, Schaeffel F, Feldkaemper MP. Changes in scleral MMP-2, TIMP-2 and TGFbeta-2 mRNA expression after imposed myopic and hyperopic defocus in chickens. *Exp Eye Res* 2006;82:710-719.
281. Stone RA, Liu J, Sugimoto R, Capehart C, Zhu X, Pendrak K. GABA, experimental myopia, and ocular growth in chick. *Invest Ophthalmol Vis Sci* 2003;44:3933-3946.
282. Xu J, Liu Y, Wildsoet CF. The effect of optic nerve section on the yoked inhibition by atropine of lens-induced myopia in chicks *Invest Ophthalmol Vis Sci* 2010;51: E-Abstract 3677.
283. Verhoeven VJ, Hysi PG, Wojciechowski R, et al. Genome-wide meta-analyses of multiancestry cohorts identify multiple new susceptibility loci for refractive error and myopia. *Nat Genet* 2013;45:314-318.
284. Veth KN, Willer JR, Collery RF, et al. Mutations in zebrafish lrp2 result in adult-onset ocular pathogenesis that models myopia and other risk factors for glaucoma. *PLoS Genet* 2011;7:e1001310.
285. Hornbeak DM, Young TL. Myopia genetics: a review of current research and emerging trends. *Curr Opin Ophthalmol* 2009;20:356-362.
286. Jacobi FK, Zrenner E, Broghammer M, Pusch CM. A genetic perspective on myopia. *Cell Mol Life Sci* 2005;62:800-808.
287. Cohen SY. Anti-VEGF drugs as the 2009 first-line therapy for choroidal neovascularization in pathologic myopia. *Retina* 2009;29:1062-1066.
288. Ip JM, Huynh SC, Robaei D, et al. Ethnic differences in the impact of parental myopia: findings from a population-based study of 12-year-old Australian children. *Invest Ophthalmol Vis Sci* 2007;48:2520-2528.
289. Woo WW, Lim KA, Yang H, et al. Refractive errors in medical students in Singapore. *Singapore Med J* 2004;45:470-474.
290. Matsumura H, Hirai H. Prevalence of myopia and refractive changes in students from 3 to 17 years of age. *Surv Ophthalmol* 1999;44 Suppl 1:S109-115.
291. Saw SM, Gazzard G, Koh D, et al. Prevalence rates of refractive errors in Sumatra, Indonesia. *Invest Ophthalmol Vis Sci* 2002;43:3174-3180.
292. Wildsoet CF. Active emmetropization--evidence for its existence and ramifications for clinical practice. *Ophthalmic Physiol Opt* 1997;17:279-290.
293. Watanabe D, Takagi H, Suzuma K, Oh H, Ohashi H, Honda Y. Expression of connective tissue growth factor and its potential role in choroidal neovascularization. *Retina* 2005;25:911-918.
294. McLeod DS, Grebe R, Bhutto I, Merges C, Baba T, Lutty GA. Relationship between RPE and choriocapillaris in age-related macular degeneration. *Invest Ophthalmol Vis Sci* 2009;50:4982-4991.

295. Witmer AN, Vrensen GF, Van Noorden CJ, Schlingemann RO. Vascular endothelial growth factors and angiogenesis in eye disease. *Prog Retin Eye Res* 2003;22:1-29.
296. Lipshutz RJ, Fodor SP, Gingeras TR, Lockhart DJ. High density synthetic oligonucleotide arrays. *Nat Genet* 1999;21:20-24.
297. Brand C, Schaeffel F, Feldkaemper MP. A microarray analysis of retinal transcripts that are controlled by image contrast in mice. *Mol Vis* 2007;13:920-932.
298. Schippert R, Schaeffel F, Feldkaemper MP. Microarray analysis of retinal gene expression in chicks during imposed myopic defocus. *Mol Vis* 2008;14:1589-1599.
299. Shelton L, Troilo D, Lerner MR, Gusev Y, Brackett DJ, Rada JS. Microarray analysis of choroid/RPE gene expression in marmoset eyes undergoing changes in ocular growth and refraction. *Mol Vis* 2008;14:1465-1479.
300. Becker C, Hammerle-Fickinger A, Riedmaier I, Pfaffl MW. mRNA and microRNA quality control for RT-qPCR analysis. *Methods* 2010;50:237-243.
301. Schroeder A, Mueller O, Stocker S, et al. The RIN: an RNA integrity number for assigning integrity values to RNA measurements. *BMC Mol Biol* 2006;7:3.
302. Raman T, O'Connor TP, Hackett NR, et al. Quality control in microarray assessment of gene expression in human airway epithelium. *BMC Genomics* 2009;10:493.
303. R Development Core Team. *R: A language and environment for statistical computing*. Vienna, Austria. <**Error! Hyperlink reference not valid.** R Foundation for Statistical Computing; 2009.
304. Gentleman RC, Carey VJ, Bates DM, et al. Bioconductor: open software development for computational biology and bioinformatics. *Genome Biol* 2004;5:R80.
305. Gautier L, Cope L, Bolstad BM, Irizarry RA. affy--analysis of Affymetrix GeneChip data at the probe level. *Bioinformatics* 2004;20:307-315.
306. Irizarry RA, Hobbs B, Collin F, et al. Exploration, normalization, and summaries of high density oligonucleotide array probe level data. *Biostatistics* 2003;4:249-264.
307. Irizarry RA, Bolstad BM, Collin F, Cope LM, Hobbs B, Speed TP. Summaries of Affymetrix GeneChip probe level data. *Nucleic Acids Res* 2003;31:e15.
308. Kauffmann A, Gentleman R, Huber W. arrayQualityMetrics--a bioconductor package for quality assessment of microarray data. *Bioinformatics* 2009;25:415-416.
309. Cope LM, Irizarry RA, Jaffee HA, Wu Z, Speed TP. A benchmark for Affymetrix GeneChip expression measures. *Bioinformatics* 2004;20:323-331.
310. Liu G, Loraine AE, Shigeta R, et al. NetAffx: Affymetrix probesets and annotations. *Nucleic Acids Res* 2003;31:82-86.
311. Huang da W, Sherman BT, Lempicki RA. Systematic and integrative analysis of large gene lists using DAVID bioinformatics resources. *Nat Protoc* 2009;4:44-57.
312. Saeed AI, Bhagabati NK, Braisted JC, et al. TM4 microarray software suite. *Methods Enzymol* 2006;411:134-193.
313. Saeed AI, Sharov V, White J, et al. TM4: a free, open-source system for microarray data management and analysis. *Biotechniques* 2003;34:374-378.
314. Li M, Reilly C. Assessing the quality of hybridized RNA in Affymetrix GeneChips using linear regression. *J Biomol Tech* 2008;19:122-128.
315. Luyten FP, Cunningham NS, Ma S, et al. Purification and partial amino acid sequence of osteogenin, a protein initiating bone differentiation. *J Biol Chem* 1989;264:13377-13380.

316. Chubinskaya S, Hurtig M, Rueger DC. OP-1/BMP-7 in cartilage repair. *Int Orthop* 2007;31:773-781.
317. Christiansen JH, Coles EG, Wilkinson DG. Molecular control of neural crest formation, migration and differentiation. *Curr Opin Cell Biol* 2000;12:719-724.
318. Thomadakis G, Ramoshebi LN, Crooks J, Rueger DC, Ripamonti U. Immunolocalization of Bone Morphogenetic Protein-2 and -3 and Osteogenic Protein-1 during murine tooth root morphogenesis and in other craniofacial structures. *Eur J Oral Sci* 1999;107:368-377.
319. Xu J, He S, Spee C, Ryan SJ, Hinton DR. TNF-{alpha} Induced MMP-9 Expression is Regulated by BMP-4 in Choroidal Neovascularization *Invest Ophthalmol Vis Sci* 2010;51: E-Abstract 4100.
320. Wozney JM. The bone morphogenetic protein family and osteogenesis. *Mol Reprod Dev* 1992;32:160-167.
321. Groppe J, Greenwald J, Wiater E, et al. Structural basis of BMP signalling inhibition by the cystine knot protein Noggin. *Nature* 2002;420:636-642.
322. Adler R, Belecky-Adams TL. The role of bone morphogenetic proteins in the differentiation of the ventral optic cup. *Development* 2002;129:3161-3171.
323. Zimmerman LB, De Jesus-Escobar JM, Harland RM. The Spemann organizer signal noggin binds and inactivates bone morphogenetic protein 4. *Cell* 1996;86:599-606.
324. Wu XB, Li Y, Schneider A, et al. Impaired osteoblastic differentiation, reduced bone formation, and severe osteoporosis in noggin-overexpressing mice. *J Clin Invest* 2003;112:924-934.
325. Devlin RD, Du Z, Pereira RC, et al. Skeletal overexpression of noggin results in osteopenia and reduced bone formation. *Endocrinology* 2003;144:1972-1978.
326. Brunet LJ, McMahon JA, McMahon AP, Harland RM. Noggin, cartilage morphogenesis, and joint formation in the mammalian skeleton. *Science* 1998;280:1455-1457.
327. Yamada Y, Nezu J, Shimane M, Hirata Y. Molecular cloning of a novel vascular endothelial growth factor, VEGF-D. *Genomics* 1997;42:483-488.
328. Marconcini L, Marchio S, Morbidelli L, et al. c-fos-induced growth factor/vascular endothelial growth factor D induces angiogenesis in vivo and in vitro. *Proc Natl Acad Sci U S A* 1999;96:9671-9676.
329. Risau W. Mechanisms of angiogenesis. *Nature* 1997;386:671-674.
330. Stacker SA, Caesar C, Baldwin ME, et al. VEGF-D promotes the metastatic spread of tumor cells via the lymphatics. *Nat Med* 2001;7:186-191.
331. Takahashi H, Shibuya M. The vascular endothelial growth factor (VEGF)/VEGF receptor system and its role under physiological and pathological conditions. *Clin Sci (Lond)* 2005;109:227-241.
332. Pe'er J, Folberg R, Itin A, Gnessin H, Hemo I, Keshet E. Upregulated expression of vascular endothelial growth factor in proliferative diabetic retinopathy. *Br J Ophthalmol* 1996;80:241-245.
333. Hera R, Keramidas M, Peoc'h M, Mouillon M, Romanet JP, Feige JJ. Expression of VEGF and angiopoietins in subfoveal membranes from patients with age-related macular degeneration. *Am J Ophthalmol* 2005;139:589-596.
334. Gerber HP, Vu TH, Ryan AM, Kowalski J, Werb Z, Ferrara N. VEGF couples hypertrophic cartilage remodeling, ossification and angiogenesis during endochondral bone formation. *Nat Med* 1999;5:623-628.

335. Achen MG, Jeltsch M, Kukk E, et al. Vascular endothelial growth factor D (VEGF-D) is a ligand for the tyrosine kinases VEGF receptor 2 (Flk1) and VEGF receptor 3 (Flt4). *Proc Natl Acad Sci U S A* 1998;95:548-553.
336. Blaauwgeers HG, Holtkamp GM, Rutten H, et al. Polarized vascular endothelial growth factor secretion by human retinal pigment epithelium and localization of vascular endothelial growth factor receptors on the inner choriocapillaris. Evidence for a trophic paracrine relation. *Am J Pathol* 1999;155:421-428.
337. Kim I, Ryan AM, Rohan R, et al. Constitutive expression of VEGF, VEGFR-1, and VEGFR-2 in normal eyes. *Invest Ophthalmol Vis Sci* 1999;40:2115-2121.
338. Fitzgerald ME, Wildsoet CF, Reiner A. Temporal relationship of choroidal blood flow and thickness changes during recovery from form deprivation myopia in chicks. *Exp Eye Res* 2002;74:561-570.
339. Troilo D, Nickla DL, Wildsoet CF. Choroidal thickness changes during altered eye growth and refractive state in a primate. *Invest Ophthalmol Vis Sci* 2000;41:1249-1258.
340. Siegwart JT, Jr., Norton TT. The susceptible period for deprivation-induced myopia in tree shrew. *Vision Res* 1998;38:3505-3515.
341. Orlandini M, Marconcini L, Ferruzzi R, Oliviero S. Identification of a c-fos-induced gene that is related to the platelet-derived growth factor/vascular endothelial growth factor family. *Proc Natl Acad Sci U S A* 1996;93:11675-11680.
342. Parrales A, Palma-Nicolas JP, Lopez E, Lopez-Colome AM. Thrombin stimulates RPE cell proliferation by promoting c-Fos-mediated cyclin D1 expression. *J Cell Physiol* 2010;222:302-312.
343. Sagar SM, Sharp FR. Light induces a Fos-like nuclear antigen in retinal neurons. *Brain Res Mol Brain Res* 1990;7:17-21.
344. Betsholtz C. Biology of platelet-derived growth factors in development. *Birth Defects Res C Embryo Today* 2003;69:272-285.
345. Andrae J, Gallini R, Betsholtz C. Role of platelet-derived growth factors in physiology and medicine. *Genes Dev* 2008;22:1276-1312.
346. Robbins SG, Mixon RN, Wilson DJ, et al. Platelet-derived growth factor ligands and receptors immunolocalized in proliferative retinal diseases. *Invest Ophthalmol Vis Sci* 1994;35:3649-3663.
347. Yoshida M, Tanihara H, Yoshimura N. Platelet-derived growth factor gene expression in cultured human retinal pigment epithelial cells. *Biochem Biophys Res Commun* 1992;189:66-71.
348. Li R, Maminishkis A, Wang FE, Miller SS. PDGF-C and -D induced proliferation/migration of human RPE is abolished by inflammatory cytokines. *Invest Ophthalmol Vis Sci* 2007;48:5722-5732.
349. Campochiaro PA, Hackett SF, Vinores SA, et al. Platelet-derived growth factor is an autocrine growth stimulator in retinal pigmented epithelial cells. *J Cell Sci* 1994;107 (Pt 9):2459-2469.
350. Campochiaro PA, Sugg R, Grotendorst G, Hjelmeland LM. Retinal pigment epithelial cells produce PDGF-like proteins and secrete them into their media. *Exp Eye Res* 1989;49:217-227.

351. Nagineni CN, Kutty V, Detrick B, Hooks JJ. Expression of PDGF and their receptors in human retinal pigment epithelial cells and fibroblasts: regulation by TGF-beta. *J Cell Physiol* 2005;203:35-43.
352. Heller LC, Li Y, Abrams KL, Rogers MB. Transcriptional regulation of the Bmp2 gene. Retinoic acid induction in F9 embryonal carcinoma cells and Saccharomyces cerevisiae. *J Biol Chem* 1999;274:1394-1400.
353. Golz S, Lantin C, Mey J. Retinoic acid-dependent regulation of BMP4 and Tbx5 in the embryonic chick retina. *Neuroreport* 2004;15:2751-2755.
354. Van den Wijngaard A, Pijpers MA, Joosten PH, Roelofs JM, Van zoelen EJ, Olijve W. Functional characterization of two promoters in the human bone morphogenetic protein-4 gene. *J Bone Miner Res* 1999;14:1432-1441.
355. Dorai H, Shepard A, Ozkaynak E, et al. The 5' flanking region of the human bone morphogenetic protein-7 gene. *Biochem Biophys Res Commun* 2001;282:823-831.
356. Grimsrud CD, Rosier RN, Puzas JE, et al. Bone morphogenetic protein-7 in growth-plate chondrocytes: regulation by retinoic acid is dependent on the stage of chondrocyte maturation. *J Orthop Res* 1998;16:247-255.
357. Trelles RD, Leon JR, Kawakami Y, Simoes S, Izpisua Belmonte JC. Expression of the chick vascular endothelial growth factor D gene during limb development. *Mech Dev* 2002;116:239-242.
358. Kaetzel DM. Transcription of the platelet-derived growth factor A-chain gene. *Cytokine Growth Factor Rev* 2003;14:427-446.
359. Morgan I, Kucharski R, Krongkaew N, Firth SI, Megaw P, Maleszka R. Screening for differential gene expression during the development of form-deprivation myopia in the chicken. *Optom Vis Sci* 2004;81:148-155.
360. Dolle P, Ruberte E, Leroy P, Morriss-Kay G, Chambon P. Retinoic acid receptors and cellular retinoid binding proteins. I. A systematic study of their differential pattern of transcription during mouse organogenesis. *Development* 1990;110:1133-1151.
361. Pavan B, Dalpiaz A, Biondi C, et al. An RPE cell line as a useful in vitro model for studying retinoic acid receptor beta: expression and affinity. *Biosci Rep* 2008;28:327-334.
362. Sun H, Gilbert DJ, Copeland NG, Jenkins NA, Nathans J. Peropsin, a novel visual pigment-like protein located in the apical microvilli of the retinal pigment epithelium. *Proc Natl Acad Sci U S A* 1997;94:9893-9898.
363. Bailey MJ, Cassone VM. Opsin photoisomerases in the chick retina and pineal gland: characterization, localization, and circadian regulation. *Invest Ophthalmol Vis Sci* 2004;45:769-775.
364. Koyanagi M, Terakita A, Kubokawa K, Shichida Y. Amphioxus homologs of Go-coupled rhodopsin and peropsin having 11-cis- and all-trans-retinals as their chromophores. *FEBS Lett* 2002;531:525-528.
365. Liang H, Crewther DP, Crewther SG, Barila AM. A role for photoreceptor outer segments in the induction of deprivation myopia. *Vision Res* 1995;35:1217-1225.
366. Crewther DP. The role of photoreceptors in the control of refractive state. *Prog Retin Eye Res* 2000;19:421-457.
367. Maminishkis A, Chen S, Jalickee S, et al. Confluent monolayers of cultured human fetal retinal pigment epithelium exhibit morphology and physiology of native tissue. *Invest Ophthalmol Vis Sci* 2006;47:3612-3624.

368. Shi G, Maminishkis A, Banzon T, et al. Control of chemokine gradients by the retinal pigment epithelium. *Invest Ophthalmol Vis Sci* 2008;49:4620-4630.
369. Li R, Maminishkis A, Banzon T, et al. IFN{gamma} regulates retinal pigment epithelial fluid transport. *Am J Physiol Cell Physiol* 2009;297:C1452-1465.
370. Seko Y, Shimokawa H, Tokoro T. Expression of bFGF and TGF-beta 2 in experimental myopia in chicks. *Invest Ophthalmol Vis Sci* 1995;36:1183-1187.
371. Jobling AI, Nguyen M, Gentle A, McBrien NA. Isoform-specific changes in scleral transforming growth factor-beta expression and the regulation of collagen synthesis during myopia progression. *J Biol Chem* 2004;279:18121-18126.
372. Honda S, Fujii S, Sekiya Y, Yamamoto M. Retinal control on the axial length mediated by transforming growth factor-beta in chick eye. *Invest Ophthalmol Vis Sci* 1996;37:2519-2526.
373. Kishi H, Kuroda E, Mishima HK, Yamashita U. Role of TGF-beta in the retinoic acid-induced inhibition of proliferation and melanin synthesis in chick retinal pigment epithelial cells in vitro. *Cell Biol Int* 2001;25:1125-1129.
374. Nagineni CN, Cherukuri KS, Kutty V, Detrick B, Hooks JJ. Interferon-gamma differentially regulates TGF-beta1 and TGF-beta2 expression in human retinal pigment epithelial cells through JAK-STAT pathway. *J Cell Physiol* 2007;210:192-200.
375. Pfeffer BA, Flanders KC, Guerin CJ, Danielpour D, Anderson DH. Transforming growth factor beta 2 is the predominant isoform in the neural retina, retinal pigment epithelium-choroid and vitreous of the monkey eye. *Exp Eye Res* 1994;59:323-333.
376. Sarkar DK, Chaturvedi K, Oomizu S, Boyadjieva NI, Chen CP. Dopamine, dopamine D2 receptor short isoform, transforming growth factor (TGF)-beta1, and TGF-beta type II receptor interact to inhibit the growth of pituitary lactotropes. *Endocrinology* 2005;146:4179-4188.
377. Pastorcic M, De A, Boyadjieva N, Vale W, Sarkar DK. Reduction in the expression and action of transforming growth factor beta 1 on lactotropes during estrogen-induced tumorigenesis in the anterior pituitary. *Cancer Res* 1995;55:4892-4898.
378. Boundy VA, Luedtke RR, Artymyshyn RP, Filtz TM, Molinoff PB. Development of polyclonal anti-D2 dopamine receptor antibodies using sequence-specific peptides. *Mol Pharmacol* 1993;43:666-676.
379. Kebabian JW, Petzold GL, Greengard P. Dopamine-sensitive adenylate cyclase in caudate nucleus of rat brain, and its similarity to the "dopamine receptor". *Proc Natl Acad Sci U S A* 1972;69:2145-2149.
380. Creese I, Sibley DR, Hamblin MW, Leff SE. The classification of dopamine receptors: relationship to radioligand binding. *Annu Rev Neurosci* 1983;6:43-71.
381. Li R, Wen R, Banzon T, Maminishkis A, Miller SS. Neurotrophic factors affect RPE physiology. *Invest Ophthalmol Vis Sci* 2010;51:E-Abstract 470.
382. Ma W, Zhao L, Fontainhas AM, Fariss RN, Wong WT. Microglia in the mouse retina alter the structure and function of retinal pigmented epithelial cells: a potential cellular interaction relevant to AMD. *PLoS One* 2009;4:e7945.
383. Beier M, Franke A, Paunel-Gorgulu AN, Scheerer N, Dunker N. Transforming growth factor beta mediates apoptosis in the ganglion cell layer during all programmed cell death periods of the developing murine retina. *Neurosci Res* 2006;56:193-203.

384. Hocking JC, Hehr CL, Chang RY, Johnston J, McFarlane S. TGFbeta ligands promote the initiation of retinal ganglion cell dendrites in vitro and in vivo. *Mol Cell Neurosci* 2008;37:247-260.
385. Friedman Z, Hackett SF, Campochiaro PA. Characterization of adenylate cyclase in human retinal pigment epithelial cells in vitro. *Exp Eye Res* 1987;44:471-479.
386. Jobling AI, Gentle A, Metlapally R, McGowan BJ, McBrien NA. Regulation of scleral cell contraction by transforming growth factor-beta and stress: competing roles in myopic eye growth. *J Biol Chem* 2009;284:2072-2079.
387. Connor TB, Jr., Roberts AB, Sporn MB, et al. Correlation of fibrosis and transforming growth factor-beta type 2 levels in the eye. *J Clin Invest* 1989;83:1661-1666.
388. Lyons RM, Keski-Oja J, Moses HL. Proteolytic activation of latent transforming growth factor-beta from fibroblast-conditioned medium. *J Cell Biol* 1988;106:1659-1665.
389. Yu Q, Stamenkovic I. Cell surface-localized matrix metalloproteinase-9 proteolytically activates TGF-beta and promotes tumor invasion and angiogenesis. *Genes Dev* 2000;14:163-176.
390. Schultz-Cherry S, Murphy-Ullrich JE. Thrombospondin causes activation of latent transforming growth factor-beta secreted by endothelial cells by a novel mechanism. *J Cell Biol* 1993;122:923-932.
391. Munger JS, Huang X, Kawakatsu H, et al. The integrin alpha v beta 6 binds and activates latent TGF beta 1: a mechanism for regulating pulmonary inflammation and fibrosis. *Cell* 1999;96:319-328.
392. Tan J, Deng ZH, Liu SZ, Wang JT, Huang C. TGF-beta2 in human retinal pigment epithelial cells: expression and secretion regulated by cholinergic signals in vitro. *Curr Eye Res* 2010;35:37-44.
393. Liu NP, Fitzgibbon F, Nash M, Osborne NN. Epidermal growth factor potentiates the transmitter-induced stimulation of C-AMP and inositol phosphates in human pigment epithelial cells in culture. *Exp Eye Res* 1992;55:489-497.
394. Strunnikova NV, Maminishkis A, Barb JJ, et al. Transcriptome analysis and molecular signature of human retinal pigment epithelium. *Hum Mol Genet* 2010;19:2468-2486.
395. Solouki AM, Verhoeven VJ, van Duijn CM, et al. A genome-wide association study identifies a susceptibility locus for refractive errors and myopia at 15q14. *Nat Genet* 2010;42:897-901.